VTT PUBLICATIONS 722

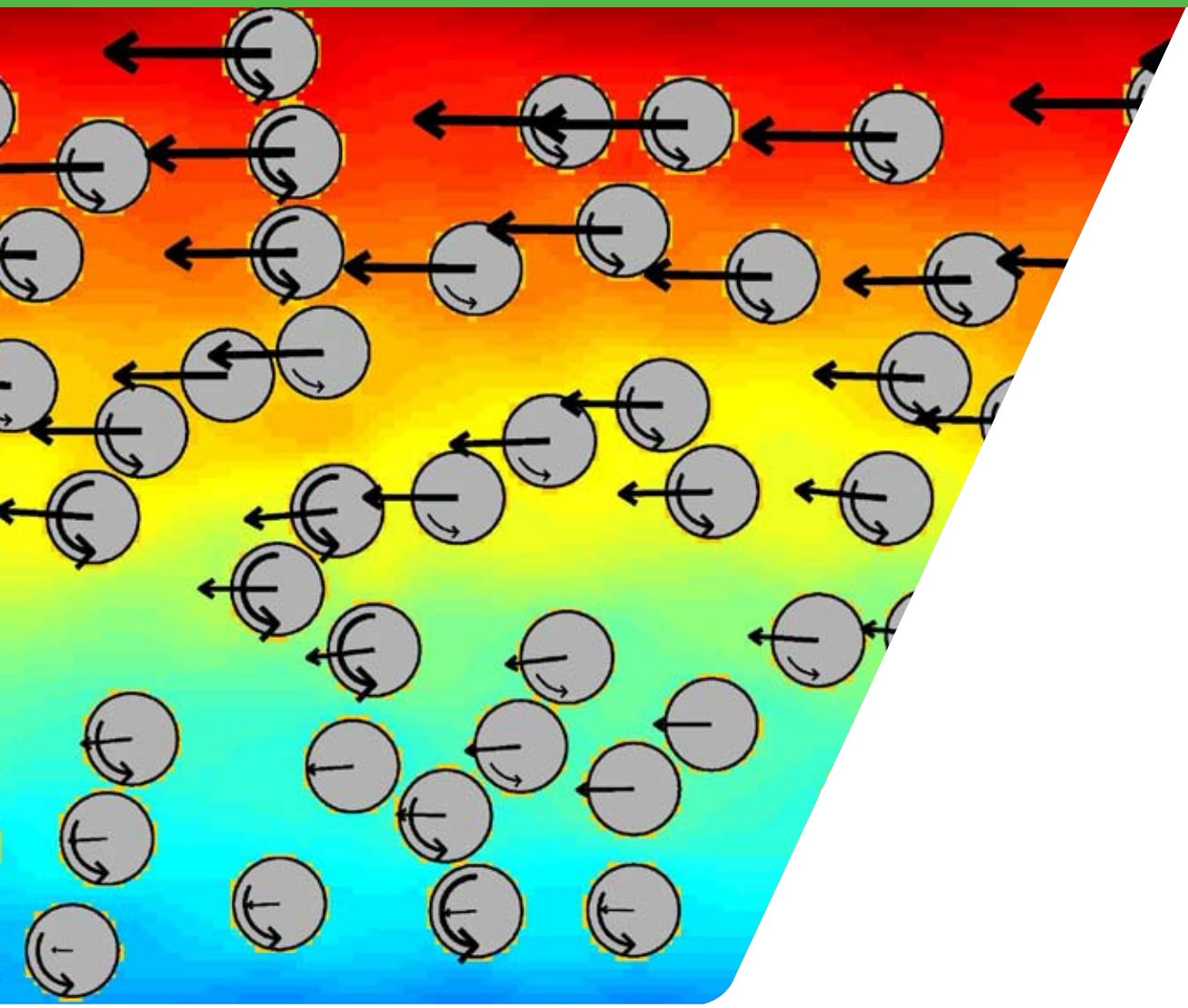

Kai Hiltunen, Ari Jäsberg, Sirpa Kallio, Hannu Karema,
Markku Kataja, Antti Koponen, Mikko Manninen &
Veikko Taivassalo

Multiphase Flow Dynamics

Theory and Numerics

VTT PUBLICATIONS 722

Multiphase Flow Dynamics

Theory and Numerics

Kai Hiltunen, Ari Jäsberg, Sirpa Kallio, Hannu Karema,
Markku Kataja, Antti Koponen,
Mikko Manninen & Veikko Taivassalo

ISBN 978-951-38-7365-3 (soft back ed.)
ISSN 1235-0621 (soft back ed.)

ISBN 978-951-38-7366-0 (URL: http://www.vtt.fi/publications/index.jsp)
ISSN 1455-0849 (URL: http://www.vtt.fi/publications/index.jsp)

JULKAISIJA – UTGIVARE – PUBLISHER

VTT, Vuorimiehentie 3, PL 1000, 02044 VTT
puh. vaihde 020 722 111, faksi 020 722 4374

VTT, Bergsmansvägen 3, PB 1000, 02044 VTT
tel. växel 020 722 111, fax 020 722 4374

VTT Technical Research Centre of Finland, Vuorimiehentie 3, P.O. Box 1000, FI-02044 VTT, Finland
phone internat. +358 20 722 111, fax + 358 20 722 4374

Edita Prima Oy, Helsinki 2009

Kai Hiltunen, Ari Jäsberg, Sirpa Kallio, Hannu Karema, Markku Kataja, Antti Koponen, Mikko Manninen & Veikko Taivassalo. Multiphase Flow Dynamics. Theory and Numerics [Monifaasivirtausten dynamiikka. Teoriaa ja numeriikkaa]. Espoo 2009. VTT Publications 722. 113 p. + app. 4 p.

Keywords multiphase flows, volume averaging, ensemble averaging, mixture models, multifluid finite volume method, multifluid finite element method, particle tracking, the lattice-BGK model

Abstract

The purpose of this work is to review the present status of both theoretical and numerical research of multiphase flow dynamics and to make the results of that fundamental research more readily available for students and for those working with practical problems involving multiphase flow. Flows that appear in many of the common industrial processes are intrinsically multiphase flows – *e.g.* flows of gas-particle suspensions, liquid-particle suspensions, and liquid-fiber suspensions, as well as bubbly flows, liquid-liquid flows, and the flow through porous medium. In the first part of this publication we give a comprehensive review of the theory of multiphase flows accounting for several alternative approaches. The second part is devoted to numerical methods for solving multiphase flow equations.

Kai Hiltunen, Ari Jäsberg, Sirpa Kallio, Hannu Karema, Markku Kataja, Antti Koponen, Mikko Manninen & Veikko Taivassalo. Multiphase Flow Dynamics. Theory and Numerics [Monifaasivirtausten dynamiikka. Teoriaa ja numeriikkaa]. Espoo 2009. VTT Publications 722. 113 s. + liitt. 4 s.

Avainsanat multiphase flows, volume averaging, ensemble averaging, mixture models, multifluid finite volume method, multifluid finite element method, particle tracking, the lattice-BGK model

Tiivistelmä

Työssä tarkastellaan monifaasivirtausten teoreettisen ja numeerisen tutkimuksen nykytilaa, ja muodostetaan tuon perustutkimuksen tuloksista selkeä kokonaisuus opiskelijoiden ja käytännön virtausongelmien kanssa työskentelevien käyttöön. Monissa teollisissa prosesseissa esiintyvät virtaukset ovat olennaisesti monifaasivirtauksia – esimerkiksi kaasu-partikkeli-, neste-partikkeli- ja neste-kuitususpensioiden virtaukset, sekä kuplavirtaukset, neste-neste-virtaukset ja virtaus huokoisen aineen läpi. Julkaisun ensimmäisessä osassa tarkastellaan kattavasti monifaasivirtausten teoriaa ja esitetään useita vaihtoehtoisia lähestymistapoja. Toisessa osassa käydään läpi monifaasivirtauksia kuvaavien yhtälöiden numeerisia ratkaisumenetelmiä.

Preface

This monograph was originally compiled within the project "Dynamics of Multiphase Flows" which was a part of the Finnish national Computational Fluid Dynamics Technology Programme 1995–1999. The purpose of this work is to review the present status of both theoretical and numerical research of multiphase flow dynamics and to make the results of that fundamental research more readily available for students and for those working with practical problems involving multiphase flow. Indeed, flows that appear in many of the common industrial processes are intrinsically multiphase flows. For example, gas-particle suspensions or liquid-particle suspensions appear in combustion processes, pneumatic conveyors, separators and in numerous processes within chemical industry, while flows of liquid-fiber suspensions are essential in paper and pulp industry. Bubbly flows may be found in evaporators, cooling systems and cavitation processes, while liquid-liquid flows frequently appear in oil extraction. A specific category of multiphase flows is the flow through porous medium which is important in filtration and precipitation processes and especially in numerous geophysical applications within civil and petroleum engineering.

The advanced technology associated with these flows has great economical value. Nevertheless, our basic knowledge and understanding of these processes is often quite limited as, in general, is our capability of solving these flows. In this respect, the condition within multiphase flow problems is very much different from the conventional single phase flows. At present, relatively reliable models exist and versatile commercial computer programs are available and capable of solving even large scale industrial problems of single phase flows. Advanced commercial computer codes now include features which also facilitate numerical simulation of multiphase flows. In most cases, however, a realistic numerical solution of practical multiphase flows requires, not only a powerful computer and an effective code, but deep understanding of the physical content and of the nature of the equations that are being solved as well as of the underlying dynamics of the microscopic processes that govern the observed behaviour of the flow.

In the first part of this monograph we give a comprehensive review of the theory of multiphase flows accounting for several alternative approaches. We also give general quidelines for solving the 'closure problem', which involves,

e.g., characterising the interactions between different phases and thereby deriving the final closed set of equations for the particular multiphase flow under consideration. The second part is devoted to numerical methods for solving those equations.

Contents

1. Equations of multiphase flow

1.1 Introduction

A multiphase fluid is composed of two or more distinct components or 'phases' which themselves may be fluids or solids, and has the characteristic properties of a fluid. Within the dicipline of multiphase flow dynamics the present status is quite different from that of the single phase flows. The theoretical background of the single phase flows is well established (the crux of the theory being the Navier-Stokes equation) and apparently the only outstanding practical problem that still remains unsolved is turbulence, or perhaps more generally, problems associated with flow stability. While it is rather straightforward to derive the equations of the conservation of mass, momentum and energy for an arbitrary mixture, no general counterpart of the Navier-Stokes equation for multiphase flows have been found. Using a proper averaging procedure it is however quite possible to derive a set of "equations of multiphase flows" which in principle correctly describes the dynamics of any multiphase system and is subject only to very general assumptions (see section 1.2 below). The drawback is that this set of equations invariably includes more unknown variables than independent equations, and can thus not be solved. In order to close this set of equations, additional system dependent costitutive relations and material laws are needed. Considering the many forms of industrial multiphase flows, such as flow in a fluidized bed, bubbly flow in nuclear reactors, gas-particle flow in combustion reactors and fiber suspension flows within pulp and paper industry, it seems virtually impossible to infer constitutive laws that would correctly describe interactions and material properties of the various phases involved, and that would be common even for these few systems. Furthermore, even in a laminar flow of, *e.g.*, liquid-particle suspensions, the presence of particles induces fluctuating motion of both particles and fluid. Analogously to the Reynolds stresses that arise from time averaging the turbulent motion of a single phase fluid, averaging over this "pseudo-turbulent" motion in multiphase systems leads to additional correlation terms that are unknown

a priori. For genuinely turbulent multiphase flows, the dynamics of the turbulence and the interaction between various phases are problems that presumably will elude general and practical solution for decades to come.

A direct consequence of the complexity and diversity of these flows is that the dicipline of multiphase fluid dynamics is and may long remain a prominently experimental branch of fluid mechanics. Preliminary small scale model testing followed by a trial and error stage with the full scale system is still the only conceivable solution for many practical engineering problems involving multiphase flows. Inferring the necessary constitutive relations from measured data and verifying the final results are of vital importance also within those approaches for which theoretical modeling and subsequent numerical solution is considered feasible.

In general, a multiphase fluid may be a relatively homogeneous mixture of its components, or it may be manifestly inhomogeneous in macroscopic scales. While much of the general flow dynamics covered by the present monograph can be applied to both types of multiphase fluids, we shall mainly ignore here macroscopically inhomogeneous flows such as stratified flow and plug flow of liquid and gas in a partially filled tube. In what follows we thus restrict ourselves to flows of macroscopically homogeneous multiphase fluids. In modeling such flows, several alternative approaches can be taken. Perhaps the most frequently used method is to treat the multicomponent mixture, *e.g.*, a liquid-particle suspension, effectively as a single fluid with rheological properties that may depend on local particle concentration. This approach may be used in cases where the velocities of various phases are nearly equal and when the effect of the interactions between the phases can be adequately described by means of rheological variables such as viscosity. The advantage of these 'homogeneous models' is that numerical solution may be attempted utilizing conventional single fluid algorithms and effective commercial programs. In some cases the method can be improved by adding a separate particle tracking feature or an additional particle transport mechanism superposed on the mean flow. Although various traditional methods based on a single fluid approach may be sufficient for predicting gross features of certain special cases of also multiphase flows, it has become increasingly clear, that in numerous cases of practical interest, an adequate description requires recognition of the underlying multiphase character of the system.

Genuine models for multiphase flows have been developed mainly following two different approaches. Within the 'Eulerian approach' all phases are treated formally as fluids which obey normal one phase equations of motion in the unobservable 'mesoscopic' level (*e.g*, in the size scale of suspended particles) — with appropriate boundary conditions specified at phase boundaries. The macroscopic flow equations are derived from these mesoscopic equations using an averaging procedure of some kind. This averaging procedure can be carried out in several alternative ways such as time averaging

[Ish75, Dre83], volume averaging [Ish75, Dre83, Soo90, Dre71, DS71, Nig79] and ensemble averaging [Ish75, Dre83, Buy71, Hwa89, JL90]. Various combinations of these basic methods can also been considered [Ish75]. Irrespective of the method used, the averaging procedure leads to equations of the same generic form, namely the form of the original phasial equations with a few extra terms. These extra terms include the interactions (change of mass, momentum *etc.*) at phase boundaries and terms analogous to the ordinary Reynold's stresses in the turbulent single phase flow equations. Each averaging procedure may however provide a slightly different view in the physical interpretation of these additional terms and, consequently, may suggest different approach for solving the closure problem that is invariably associated with the solution of these equations. The manner in which the various possible interaction mechanisms are naturally divided between these additional terms, may also depend on the averaging procedure being used.

The advantage of the Eulerian method is its generality: in principle it can be applied to any multiphase system, irrespective of the number and nature of the phases. A drawback of the straightforward Eulerian approach is that it often leads to a very complicated set of flow equations and closure relations. In some cases, however, it is possible to use a simplified formulation of the full Eulerian approach, namely 'mixture model' (or 'algebraic slip model'). The mixture model may be applicable, *e.g.*, for a relatively homogeneous suspension of one or more species of dispersed phase that closely follow the motion of the continuous carrier fluid. For such a system the mixture model includes the continuity equation and the momentum equations for the mixture, and the continuity equations for each dispersed phase. The slip velocities between the continuous phase and the dispersed phases are inferred from approximate algebraic balance equations. This reduces the computational effort considerably, especially when several dispersed phases are considered.

Another common approach is the so called 'Lagrangian method' which is mainly restricted to particulate suspensions. Within that approach only the fluid phase is treated as continuous while the motion of the discontinuous particulate phase is obtained by integrating the equation of motion of individual particles along their trajectories. (In practical applications a "particle" may represent a single physical particle or a group of particles.)

In this chapter we review the theoretical basis of multiphase flow dynamics. We first derive the basic equations of multiphase flows within the Eulerian approach using both volume averaging and ensemble averaging, and discuss the guiding principles for solving the closure problem within the Eulerian scheme. We then consider the basic formalism and applicability of the mixture model and the Lagrangian multiphase model. Finally, we give a few practical examples of possible closure relations.

1.2 Volume averaging

1.2.1 Equations

In this section we shall derive the 'equations of multiphase flow' using the volume averaging method. To this end, we first define appropriate volume averaged dynamic flow quantities and then derive the required flow equations for those variables by averaging the corresponding phasial equations [Ish75, Dre83, Soo90, Dre71, DS71, Nig79]. While ensemble averaging may appear as the most elegant approach from the theoretical point of view, volume averaging provides perhaps the most intuitive and straightforward interpretation of the dynamic quantities and interaction terms involved. Volume averaging also illustrates the potential problems and intricacies that are common to all averaging methods within Eulerian approach.

Volume averaging is based on the assumption that a length scale L_c exists such that $l \ll L_c \ll L$, where L is the 'macroscopic' length scale of the system and l is a length scale that we shall call 'mesoscopic' in what follows. The mesoscopic length scale is associated with the distribution of the various phases within the mixture. (The 'microscopic' length scale would then be the molecular scale.)

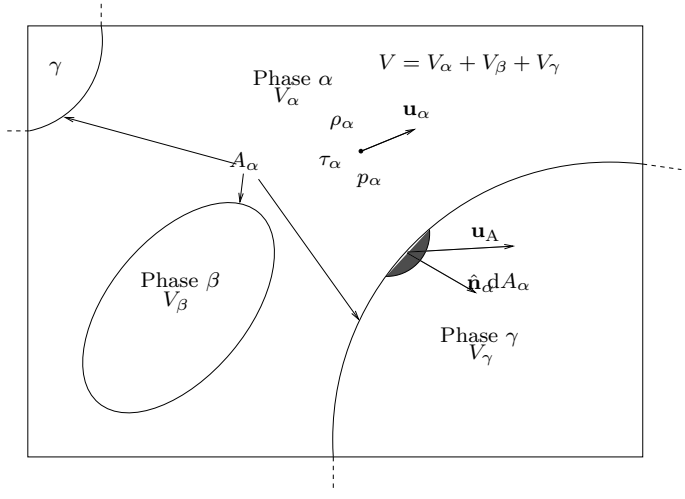

Figure 1.1: Averaging volume V including three phases α, β, and γ.

To begin with, we consider a representative averaging volume $V \sim L_c^3$ which contains distinct domains of each phase such that $V = \sum_\alpha V_\alpha$ where V_α is the volume occupied by phase α within V (see Fig. 1.1). We assume that for each phase α the usual fluid mechanical equations for mass, momentum and energy conservation are valid at any interior point of V_α,

namely

$$\frac{\partial}{\partial t}\rho_\alpha + \nabla\cdot(\rho_\alpha \mathbf{u}_\alpha) = 0 \tag{1.1}$$

$$\frac{\partial}{\partial t}(\rho_\alpha \mathbf{u}_\alpha) + \nabla\cdot(\rho_\alpha \mathbf{u}_\alpha \mathbf{u}_\alpha) = -\nabla p_\alpha + \nabla\cdot\tau_\alpha + \mathbf{F}_\alpha \tag{1.2}$$

$$\frac{\partial}{\partial t}(\rho_\alpha E_\alpha) + \nabla\cdot(\rho_\alpha \mathbf{u}_\alpha E_\alpha) = \tag{1.3}$$
$$-\nabla\cdot(\mathbf{u}_\alpha p_\alpha) + \nabla\cdot(\mathbf{u}_\alpha\cdot\tau_\alpha) + \mathbf{u}_\alpha\cdot\mathbf{F}_\alpha - \nabla\cdot\mathbf{J}_{q\alpha} + J_{E\alpha}.$$

Here,

$$\begin{aligned}
\rho_\alpha &= \text{density of pure phase } \alpha\\
\mathbf{u}_\alpha &= \text{flow velocity}\\
p_\alpha &= \text{pressure}\\
\tau_\alpha &= \text{deviatoric stress tensor}\\
E_\alpha &= \text{total energy per unit mass}\\
\mathbf{F}_\alpha &= \text{external force density}\\
\mathbf{J}_{q\alpha} &= \text{heat flux into phase } \alpha\\
J_{E\alpha} &= \text{heat source density.}
\end{aligned}$$

Eqns. (1.1) through (1.3) are assumed to be valid both for laminar and for turbulent flow. These equations are valid even if one of the phases is not actually a fluid but consists, *e.g.*, of solid particles suspended in a fluid. In that case the stress tensor τ_α contains viscous stresses for the fluid and elastic deviatoric stresses for the particles. However, the concept of 'pressure' may not always be very useful for a solid material. In such cases it may be preferable to use the total stress tensor $\sigma_\alpha = -p_\alpha \mathbb{1} + \tau_\alpha$ instead, whence $-\nabla p_\alpha + \nabla\cdot\tau_\alpha = \nabla\cdot\sigma_\alpha$.

Similarly to single phase flows, the energy equation (1.3) is necessary only in the presence of heat transfer. For simplicity, we shall from now on neglect the energy equation and consider only mass and momentum equations. For derivation of the energy equation for multiphase flows, see Refs. [Soo90] and [Hwa89].

Eqns. (1.1) and (1.2) for phase α are subject to the following boundary conditions at the interface $A_{\alpha\gamma}$ between phase α and any other phase γ inside volume V (see Fig. 1.2) [Soo90].

$$\rho_\alpha(\mathbf{u}_\alpha - \mathbf{u}_\mathrm{A})\cdot\hat{\mathbf{n}}_\alpha + \rho_\gamma(\mathbf{u}_\gamma - \mathbf{u}_\mathrm{A})\cdot\hat{\mathbf{n}}_\gamma = 0 \tag{1.4}$$

$$\rho_\alpha \mathbf{u}_\alpha(\mathbf{u}_\alpha - \mathbf{u}_\mathrm{A})\cdot\hat{\mathbf{n}}_\alpha + \rho_\gamma \mathbf{u}_\gamma(\mathbf{u}_\gamma - \mathbf{u}_\mathrm{A})\cdot\hat{\mathbf{n}}_\gamma = \tag{1.5}$$
$$(-p_\alpha\mathbb{1} + \tau_\alpha)\cdot\hat{\mathbf{n}}_\alpha + (-p_\gamma\mathbb{1} + \tau_\gamma)\cdot\hat{\mathbf{n}}_\gamma - \nabla_\mathrm{A}\sigma_{\alpha\gamma} + \frac{2\sigma_{\alpha\gamma}}{|\mathbf{R}_\mathrm{A}|}\hat{\mathbf{R}}_\mathrm{A},$$

where

$$\hat{\mathbf{n}}_\alpha = \text{unit outward normal vector of phase } \alpha$$

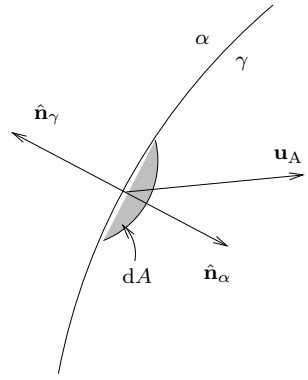

Figure 1.2: A portion of the interface between phases α and γ.

$$
\begin{aligned}
\mathbf{u}_\mathrm{A} &= \text{velocity of the interface} \\
\hat{\mathbf{R}}_\mathrm{A} &= \mathbf{R}_\mathrm{A}/|\mathbf{R}_\mathrm{A}| \\
\mathbf{R}_\mathrm{A} &= \text{inerface curvature radius vector} \\
\sigma_{\alpha\gamma} &= \text{interface surface tension} \\
\nabla_\mathrm{A} &= \nabla - \hat{\mathbf{R}}_\mathrm{A} \cdot \nabla = \text{surface gradient operator} \\
\mathbb{1} &= \text{second rank unit tensor}
\end{aligned}
$$

The interface $A_\alpha = \bigcup_\gamma A_{\alpha\gamma}$ may, however, have a very complicated shape which depends on time and which actually should be solved simultaneously with the flow equations. Therefore, it is usually not possible to apply the boundary conditions (1.4) and (1.5) and to solve the mesoscopic equations (1.1) and (1.2) in the usual manner. This is the basic reason why we have to resort to averaged equations, in general.

For any quantity q_α (scalar, vector or tensor) defined in phase α we define the following averages [Ish75, Hwa89]

$$\langle q_\alpha \rangle = \frac{1}{V} \int_{V_\alpha} q_\alpha \, dV \tag{1.6}$$

$$\tilde{q}_\alpha = \frac{1}{V_\alpha} \int_{V_\alpha} q_\alpha \, dV = \frac{1}{\phi_\alpha} \langle q_\alpha \rangle \tag{1.7}$$

$$\bar{q}_\alpha = \frac{\int_{V_\alpha} \rho_\alpha q_\alpha \, dV}{\int_{V_\alpha} \rho_\alpha \, dV} = \frac{\langle \rho_\alpha q_\alpha \rangle}{\phi_\alpha \tilde{\rho}_\alpha}, \tag{1.8}$$

where

$$\phi_\alpha = V_\alpha / V. \tag{1.9}$$

is the volume fraction of phase α and is subject to the constraint that

$$\sum_\alpha \phi_\alpha = 1. \tag{1.10}$$

The quantities defined by Eqns. (1.6), (1.7) and (1.8) are called the partial average, the intrinsic or phasic average and the Favré or mass weighted average of q_α, respectively. At this point we leave until later the decision of which particular average of each flow quantity we should choose to appear as the final dynamic quantity of the averaged theory.

In order to derive the governing equations for the averaged quantities defined above, we wish to apply averaging to equations (1.1) and (1.2). To this end, we notice that the following rules apply to the partial averages (and to the other two averages),

$$\langle f + g \rangle = \langle f \rangle + \langle g \rangle \tag{1.11}$$

$$\langle \langle f \rangle g \rangle = \langle f \rangle \langle g \rangle \tag{1.12}$$

$$\langle C \rangle = C \text{ for constant } C. \tag{1.13}$$

It is also rather straightforward to show that the following rules hold for partial averages of various derivatives of q_α [Soo90],

$$\langle \nabla q_\alpha \rangle = \nabla \langle q_\alpha \rangle + \frac{1}{V} \int_{A_\alpha} q_\alpha \hat{\mathbf{n}}_\alpha \, dA \tag{1.14}$$

$$\langle \nabla \cdot \mathbf{q}_\alpha \rangle = \nabla \cdot \langle \mathbf{q}_\alpha \rangle + \frac{1}{V} \int_{A_\alpha} \mathbf{q}_\alpha \cdot \hat{\mathbf{n}}_\alpha \, dA \tag{1.15}$$

$$\langle \frac{\partial}{\partial t} q_\alpha \rangle = \frac{\partial}{\partial t} \langle q_\alpha \rangle - \frac{1}{V} \int_{A_\alpha} q_\alpha \mathbf{u}_\mathrm{A} \cdot \hat{\mathbf{n}}_\alpha \, dA. \tag{1.16}$$

For later purposes, it is also useful to define the phase indicator function Θ_α such that

$$\Theta_\alpha(\mathbf{r}, t) = \begin{cases} 1, & \mathbf{r} \in \text{phase } \alpha \text{ at time } t \\ 0, & \text{otherwise.} \end{cases} \tag{1.17}$$

Using Eqns. (1.6) and (1.14) with $q_\alpha = \Theta_\alpha$, it is straightforward to see that

$$\langle \Theta_\alpha \rangle = \phi_\alpha, \tag{1.18}$$

and that

$$\frac{1}{V} \int_{A_\alpha} \hat{\mathbf{n}}_\alpha \, dA = -\nabla \phi_\alpha. \tag{1.19}$$

Applying partial averaging on both sides of Eqns. (1.1) and (1.2) and using Eqns. (1.11)-(1.16) the following equations are obtained

$$\frac{\partial}{\partial t} \langle \rho_\alpha \rangle + \nabla \cdot \langle \rho_\alpha \mathbf{u}_\alpha \rangle = \Gamma_\alpha \tag{1.20}$$

$$\frac{\partial}{\partial t} \langle \rho_\alpha \mathbf{u}_\alpha \rangle + \nabla \cdot \langle \rho_\alpha \mathbf{u}_\alpha \mathbf{u}_\alpha \rangle = -\nabla \langle p_\alpha \rangle + \nabla \cdot \langle \tau_\alpha \rangle + \langle \mathbf{F}_\alpha \rangle + \mathbf{M}_\alpha, \tag{1.21}$$

where the so called 'transfer integrals' Γ_α and $\mathbf{M}_\alpha$ are defined by

$$\Gamma_\alpha = -\frac{1}{V}\int_{A_\alpha} \rho_\alpha(\mathbf{u}_\alpha - \mathbf{u}_\mathrm{A})\cdot\hat{\mathbf{n}}_\alpha\, dA \tag{1.22}$$

$$\mathbf{M}_\alpha = \frac{1}{V}\int_{A_\alpha} (-p_\alpha \mathbb{1} + \tau_\alpha)\cdot\hat{\mathbf{n}}_\alpha\, dA - \frac{1}{V}\int_{A_\alpha} \rho_\alpha \mathbf{u}_\alpha(\mathbf{u}_\alpha - \mathbf{u}_\mathrm{A})\cdot\hat{\mathbf{n}}_\alpha\, dA. \tag{1.23}$$

The flow equations as given by Eqns. (1.20) and (1.21) are not yet in a closed form amenable for solution. Firstly, the properties of each pure phase are not specified at this point. Secondly, the transfer integrals (1.22) and (1.23), which include the interactions (mass and momentum transfer) between phases, are still given in terms of integrals of the original mesoscopic quantities over the unknown phase boundaries. The additional constitutive relations, which are required to specify the material properties and to relate the transfer integrals with the proper averaged quantities, are discussed in more detail below. Thirdly, averages of various products of original variables that appear on the left side of the equations are independent of each other. Even if all the necessary constitutive relations are assumed to be known, we still have more independent variables than equations for each phase. In order to reduce the number of independent variables, we must express averages of these products in terms of products of suitable averages. This can be done in several alternative ways which may lead to slightly different results. Here we shall use Favré averaging for velocity and, depending on which is more convenient, either partial or intrinsic averaging for density and pressure. Defining the velocity fluctuation $\delta\mathbf{u}_\alpha$ by

$$\mathbf{u}_\alpha = \bar{\mathbf{u}}_\alpha + \delta\mathbf{u}_\alpha, \tag{1.24}$$

it is easy to see that the averages of products that appear in Eqns. (1.20) and (1.21) can be written as

$$\langle\rho_\alpha\mathbf{u}_\alpha\rangle = \langle\rho_\alpha\rangle\bar{\mathbf{u}}_\alpha = \phi_\alpha\tilde{\rho}_\alpha\bar{\mathbf{u}}_\alpha \tag{1.25}$$

$$\langle\rho_\alpha\mathbf{u}_\alpha\mathbf{u}_\alpha\rangle = \langle\rho_\alpha\rangle\bar{\mathbf{u}}_\alpha\bar{\mathbf{u}}_\alpha + \langle\rho_\alpha\delta\mathbf{u}_\alpha\delta\mathbf{u}_\alpha\rangle = \phi_\alpha\tilde{\rho}_\alpha\bar{\mathbf{u}}_\alpha\bar{\mathbf{u}}_\alpha + \langle\rho_\alpha\delta\mathbf{u}_\alpha\delta\mathbf{u}_\alpha\rangle \tag{1.26}$$

The averaged equations now acquire the form

$$\frac{\partial}{\partial t}(\phi_\alpha\tilde{\rho}_\alpha) + \nabla\cdot(\phi_\alpha\tilde{\rho}_\alpha\bar{\mathbf{u}}_\alpha) = \Gamma_\alpha \tag{1.27}$$

$$\frac{\partial}{\partial t}(\phi_\alpha\tilde{\rho}_\alpha\bar{\mathbf{u}}_\alpha) + \nabla\cdot(\phi_\alpha\tilde{\rho}_\alpha\bar{\mathbf{u}}_\alpha\bar{\mathbf{u}}_\alpha) = -\nabla(\phi_\alpha\tilde{p}_\alpha) + \nabla\cdot\langle\tau_\alpha\rangle + \phi_\alpha\tilde{\mathbf{F}}_\alpha + \mathbf{M}_\alpha + \nabla\cdot\langle\tau_{\delta\alpha}\rangle, \tag{1.28}$$

where

$$\langle \tau_{\delta\alpha} \rangle = -\langle \rho_\alpha \delta \mathbf{u}_\alpha \delta \mathbf{u}_\alpha \rangle. \tag{1.29}$$

This tensor is sometimes called a pseudo-turbulent stress tensor since it is analogous to the usual Reynolds stress tensor of turbulent one phase flow. Notice however, that tensor $\langle \tau_{\delta\alpha} \rangle$ is defined here as a volume average instead of a time average as the usual Reynolds stress. It also contains momentum fluxes that arise both from the turbulent fluctuations of the mesoscopic flow and from the fluctuations of the velocity of phase α due to the presence of other phases. Consequently, tensor $\langle \tau_{\delta\alpha} \rangle$ does not necessarily vanish even if the mesoscopic flow is laminar.

Integrating the mesoscopic boundary conditions (1.4) and (1.5) over the interphase $A_{\alpha\gamma}$, summing over α and γ and using definitions (1.22) and (1.23), we find that

$$\sum_\alpha \Gamma_\alpha = 0 \tag{1.30}$$

$$\sum_\alpha \mathbf{M}_\alpha = -\frac{1}{2V} \sum_{\substack{\alpha,\gamma \\ \alpha \neq \gamma}} \int_{A_{\alpha\gamma}} (-\nabla_{\mathrm{A}} \sigma_{\alpha\gamma} + \frac{2\sigma_{\alpha\gamma}}{|\mathbf{R}_{\mathrm{A}}|} \hat{\mathbf{R}}_{\mathrm{A}}) dA. \tag{1.31}$$

Eqn. (1.30) ensures conservation of the total mass of the mixture, while the right side of Eqn. (1.31) gives rise to surface effects such as 'capillary' pressure differences between various phases.

Eqns. (1.27) and (1.28) together with constraints (1.10), (1.30) and (1.31) are the most general averaged equations of multiphase flow (with no heat transfer), which can be derived without reference to the particular properties of the system (other than the general continuum assumptions).

The basic dynamical variables of the averaged theory can be taken to be the three components of the mass-averaged velocities $\bar{\mathbf{u}}_\alpha$ and the volume fractions ϕ_α (or, alternatively, the averaged densities $\langle \rho_\alpha \rangle$). Provided that all the other variables and terms that appear in Eqns. (1.27) and (1.28) can be related to these basic variables using definitions (1.6) through (1.8), constraints (1.10), (1.30) and (1.31) and constitutive relations, we thus have a closed set of four unknown variables and four independent equations for each phase α.

1.2.2 Constitutive relations

Eqns. (1.27) and (1.28) are, in principle, exact equations for the averaged quantities. So far, they do not contain much information about the dynamics of the particular system to be described. That information must be provided by a set of system dependent constitutive relations which specify the material properties of each phase, the interactions between different phases and the (pseudo)turbulent stresses of each phase in the presence of other phases.

These relations finally render the set of equations in a closed form where solution is feasible.

At this point we do not attempt to elaborate in detail the possible strategies for attaining the constitutive relations in specific cases, but simply state the basic principles that should be followed in inferring such relations. The unknown terms that appear in the averaged equations (1.27) and (1.28), such as the transfer integrals and stress terms that still contain mesoscopic quantities, should be replaced by new terms which

- depend only on the averaged dynamic quantities (and their derivatives),
- have the same physical content, tensorial form and dimension as the original terms,
- have the same symmetry properties as the original terms (isotropy, frame indifference *etc.*),
- include the effects of all the physical processes or mechanisms that are considered to be important in the system to be described.

Typically, constitutive relations are given in a form where these new terms include free parameters which are supposed to be determined experimentally. For more detailed discussion of the constitutive relations and constitutive principles, see Refs. [DALJ90, Dre83, DLJ79, Dre76, Hwa89, HS89, HS91, BS78, Buy92a, Buy92b].

In some cases constitutive laws can readily be derived from the properties of the mixture, or from the properties of the pure phase. For example, the incompressibility of the pure phase α implies the constitutive relation $\tilde{\rho}_\alpha$=constant. Similarly, the equation of state $p_\alpha = C\rho_\alpha$, where C=constant for the pure phase, implies $\tilde{p}_\alpha = C\tilde{\rho}_\alpha$. In most cases, however, the constitutive relations must be either extracted from experiments, derived analytically under suitable simplifying assumptions, or postulated.

Including a given physical mechanism in the model by imposing proper constitutive relations is not always straightforward even if adequate experimental and theoretical information is available. In particular, making specific assumptions concerning one of the unknown quantities may induce constraints on other terms. For example, the transfer integrals Γ_α and $\mathbf{M}_\alpha$ contain the effect of exchange of mass and momentum between the phases. According to Eqn. (1.22), the quantity Γ_α gives the rate of mass transfer per unit volume through the phase boundary A_α into phase α from the other phases. In a reactive mixture, where phase α is changed into phase γ, the mass transfer term Γ_α might be given in terms of the experimental rate of the chemical reaction $\alpha \to \gamma$, correlated to the volume fractions ϕ_α and ϕ_γ, and to the temperature of the mixture T. Similarly, the quantity $\mathbf{M}_\alpha$ gives the rate of momentum transfer per unit volume into phase α through the

phase boundary A_α. The second integral on the right side of Eqn. (1.23) contains the transfer of momentum carried by the mass exchanged between phases. It is obvious that this part of the momentum transfer integral $\mathbf{M}_\alpha$ must be consistently correlated with the mass transfer integral Γ_α. Similarly, the first integral on the right side of Eqn. (1.23) contains the change of momentum of phase α due to stresses imposed on the phase boundary by the other phases. Physically, this term contains forces such as buoyancy which may be correlated to average pressures and gradients of volume fractions, and viscous drag which might be correlated to volume fractions and average velocity differences. For instance in a liquid-particle suspension, the average stress inside solid particles depends on the hydrodynamic forces acting on the surface of the particles. The choice of, *e.g.*, drag force correlation between fluid and particles should therefore influence the choice of the stress correlation for the particulate phase. While this particular problem can be solved exactly for some idealized cases [DALJ90], there seems to be no general solution available.

Perhaps the most intricate term which is to be correlated to the averaged quantities through constitutive relations is the tensor $\langle \tau_{\delta\alpha} \rangle$ given by Eqn. (1.29). It contains the momentum transfer inside phase α which arises from the genuine turbulence of phase α and from the velocity fluctuations due to presence of other phases, and which are present also in the case that the flow is laminar in the mesoscopic scale. Moreover, the truly turbulent fluctuations of phase α may be substantially modulated by the other phases. Bearing in mind the intricacies that are encountered in modeling turbulence in single phase flows, it is evident that inferring realistic constitutive relations for tensor $\langle \tau_{\delta\alpha} \rangle$ remains as a considerable challenge. It may, however, be attempted, *e.g.*, for fluid-particle suspensions by generalising the corresponding models for single phase flows, such as turbulence energy dissipation models, large-eddy simulations or direct numerical simulations. A recent review on the topic is given by Crowe, Troutt and Chung in Ref. [CTC96].

In the remaining part of this section we shall shortly discuss a few particular cases where additional simplifying assumptions can be made, namely liquid-particle suspension, bubbly flow and multifluid flow. These examples emphasize further the circumstance that no general set of equations exists that, as such, would be valid and readily solvable for an arbitrary multiphase flow, or even for an arbitrary two-phase flow. Instead, the flow equations appropriate for each particular system should be derived separately starting from the general (but unclosed) set of equations given in section 1.2 and utilizing all the specific assumptions and approximations that are plausible for that system (or class of systems). We notice, however, that the assumptions made here concerning, *e.g.*, bubbly flow may not be generally valid for all such flows. Nor are they the only possible extra assumptions that can be made, but should be taken merely as examples of the kind of hypotheses

that are reasonable owing to the nature of that category of systems. Detailed examples of more complete closure relations will be given in section 1.6.

In chapter 2 (see section 2.5) we shall briefly discuss novel numerical methods that can be used to infer constitutive relations by means of direct numerical simulation in a mesoscopic level.

Liquid-particle suspension

Consider a binary system of solid particles suspended in a Newtonian liquid. We denote the continuous fluid phase by subscript f and the dispersed particle phase by subscript d. We assume that both phases are incompressible, that the suspension is non-reactive, *i.e.*, there is no mass transfer between the two phases, and that surface tension between solid and liquid is negligible. Both the densities $\tilde{\rho}_\mathrm{f}$ and $\tilde{\rho}_\mathrm{d}$ are thus constants, and

$$\Gamma_\mathrm{f} = \Gamma_\mathrm{d} = 0 \tag{1.32}$$

$$\mathbf{M}_\mathrm{f} + \mathbf{M}_\mathrm{d} = 0. \tag{1.33}$$

The mutual momentum transfer integral can now be written as

$$\begin{aligned} \mathbf{M} \equiv \mathbf{M}_\mathrm{f} = -\mathbf{M}_\mathrm{d} &= \frac{1}{V}\int_{A_\mathrm{f}} (-p_\mathrm{f}\mathbb{1} + \tau_\mathrm{f})\cdot\hat{\mathbf{n}}_\mathrm{f}\, dA \\ &= -\frac{1}{V}\int_{A} (-p_\mathrm{f}\mathbb{1} + \tau_\mathrm{f})\cdot\hat{\mathbf{n}}\, dA, \end{aligned} \tag{1.34}$$

where $A = A_\mathrm{f} = A_\mathrm{d}$ and $\hat{\mathbf{n}} = \hat{\mathbf{n}}_\mathrm{d} = -\hat{\mathbf{n}}_\mathrm{f}$. Introducing the fluid pressure fluctuation by $\delta p_\mathrm{f} = p_\mathrm{f} - \tilde{p}_\mathrm{f}$ and using Eqn. (1.19), the momentum transfer integral can be cast in the form

$$\mathbf{M} = \tilde{p}_\mathrm{f}\,\nabla\phi + \mathbf{D}, \tag{1.35}$$

where

$$\mathbf{D} = -\frac{1}{V}\int_{A} (-\delta p_\mathrm{f}\mathbb{1} + \tau_\mathrm{f})\cdot\hat{\mathbf{n}}\, dA, \tag{1.36}$$

and $\phi = \phi_\mathrm{f}$. The averaged flow equations can now be written in the final form as

$$\frac{\partial}{\partial t}\phi + \nabla\cdot(\phi\bar{\mathbf{u}}_\mathrm{f}) = 0 \tag{1.37}$$

$$\frac{\partial}{\partial t}(1-\phi) + \nabla\cdot((1-\phi)\bar{\mathbf{u}}_\mathrm{d}) = 0 \tag{1.38}$$

$$\begin{aligned} \tilde{\rho}_\mathrm{f}[\frac{\partial}{\partial t}(\phi\bar{\mathbf{u}}_\mathrm{f}) + \nabla\cdot(\phi\bar{\mathbf{u}}_\mathrm{f}\bar{\mathbf{u}}_\mathrm{f})] &= -\phi\nabla\tilde{p}_\mathrm{f} + \nabla\cdot\langle\tau_\mathrm{f}\rangle + \phi\tilde{\mathbf{F}}_\mathrm{f} \\ &\quad +\mathbf{D} + \nabla\cdot\langle\tau_{\delta\mathrm{f}}\rangle \end{aligned} \tag{1.39}$$

$$\begin{aligned} \tilde{\rho}_\mathrm{d}[\frac{\partial}{\partial t}((1-\phi)\bar{\mathbf{u}}_\mathrm{d}) + \nabla\cdot((1-\phi)\bar{\mathbf{u}}_\mathrm{d}\bar{\mathbf{u}}_\mathrm{d})] &= +\nabla\cdot\langle\sigma_\mathrm{d}\rangle + (1-\phi)\tilde{\mathbf{F}}_\mathrm{d} \\ &\quad -\mathbf{D} - \tilde{p}_\mathrm{f}\,\nabla\phi + \nabla\cdot\langle\tau_{\delta\mathrm{d}}\rangle, \end{aligned} \tag{1.40}$$

where $\langle \tau_\mathrm{f} \rangle$ is the averaged viscous stress tensor of the fluid, and $\langle \sigma_\mathrm{d} \rangle$ is the averaged total stress tensor of the dispersed phase. An example of more complete constitutive relations for a dilute liquid-particle suspension is given in section 1.6.1.

Bubbly flow with mass transfer

If the dispersed phase consists of small gas bubbles instead of solid particles, the overall structure of the system still remains similar to the liquid-particle suspension discussed in the previous section. A few things will change, however. Firstly, the dispersed phase is not incompressible. Instead, the intrinsic density $\tilde{\rho}_\mathrm{d}$ depends on pressure $\tilde{p}_\mathrm{d}$ and temperature T as given by the equation of state of the gas,

$$\tilde{\rho}_\mathrm{d} = \tilde{\rho}_\mathrm{d}(\tilde{p}_\mathrm{d}, T). \tag{1.41}$$

Secondly, mass transfer between the phases generally occur. The gas phase usually consists of several gaseous components including the vapor of the liquid. The mass transfer may take place as evaporation of the liquid or dissolution of the gas at the surface of the bubbles. Instead of Eqn. (1.32) we now have

$$\Gamma_\mathrm{f} = -\Gamma_\mathrm{d} = \Gamma, \tag{1.42}$$

where the mass transfer rate Γ is a measurable quantity which may depend on the pressure, on the temperature and on the prevailing vapor content of the gas *etc.* In this case, also the second term on the right side of Eqn. (1.23), which includes the momentum carried by the mass exchanged, is non-zero. This term can be related to the mass transfer rate Γ by defining the average velocity $\bar{\mathbf{u}}_\mathrm{m}$ at the phase interface by the equation

$$\frac{1}{V}\int_{A_\mathrm{d}} \rho_\mathrm{d}\mathbf{u}_\mathrm{d}(\mathbf{u}_\mathrm{d} - \mathbf{u}_\mathrm{A}) \cdot \hat{\mathbf{n}}_\mathrm{d}\, dA = \bar{\mathbf{u}}_\mathrm{m}\Gamma. \tag{1.43}$$

At this stage, velocity $\bar{\mathbf{u}}_\mathrm{m}$ is of course unknown and must be modeled separately. A natural first choice would be that $\bar{\mathbf{u}}_\mathrm{m}$ is the mass averaged velocity of the mixture, *i.e.*,

$$\bar{\mathbf{u}}_\mathrm{m} = \frac{\phi\tilde{\rho}_\mathrm{f}\bar{\mathbf{u}}_\mathrm{f} + (1-\phi)\tilde{\rho}_\mathrm{d}\bar{\mathbf{u}}_\mathrm{d}}{\phi\tilde{\rho}_\mathrm{f} + (1-\phi)\tilde{\rho}_\mathrm{d}}. \tag{1.44}$$

Thirdly, surface tension between the phases may be important. For small bubbles one may ignore the surface gradient term $-\nabla_\mathrm{A}\sigma_\mathrm{df}$ in Eqn. (1.31). Assuming that $2\sigma_\mathrm{df}/|\mathbf{R}_\mathrm{A}| = \tilde{p}_\mathrm{d} - \tilde{p}_\mathrm{f}$ (capillary pressure) it is straightforward to see that, instead of Eqn. (1.33), we now have

$$\mathbf{M}_\mathrm{f} + \mathbf{M}_\mathrm{d} = -(\tilde{p}_\mathrm{d} - \tilde{p}_\mathrm{f})\nabla\phi. \tag{1.45}$$

Following the analysis given by Eqns. (1.34) through (1.35) we can now verify that

$$\mathbf{M}_\mathrm{f} = \tilde{p}_\mathrm{f}\,\nabla\phi + \mathbf{D} + \bar{\mathbf{u}}_\mathrm{m}\Gamma_\mathrm{d} \tag{1.46}$$

$$\mathbf{M}_\mathrm{d} = \tilde{p}_\mathrm{d}\,\nabla(1-\phi) - \mathbf{D} - \bar{\mathbf{u}}_\mathrm{m}\Gamma_\mathrm{d}, \tag{1.47}$$

where the quantity $\mathbf{D}$ is still given by Eqn. (1.36). The flow equations for bubbly flow with small bubbles may thus be given in the form

$$\tilde{\rho}_\mathrm{f}\frac{\partial}{\partial t}\phi + \tilde{\rho}_\mathrm{f}\nabla\cdot(\phi\bar{\mathbf{u}}_\mathrm{f}) = \Gamma \tag{1.48}$$

$$\frac{\partial}{\partial t}[(1-\phi)\tilde{\rho}_\mathrm{d}] + \nabla\cdot[(1-\phi)\tilde{\rho}_\mathrm{d}\bar{\mathbf{u}}_\mathrm{d}] = -\Gamma \tag{1.49}$$

$$\tilde{\rho}_\mathrm{f}[\frac{\partial}{\partial t}(\phi\bar{\mathbf{u}}_\mathrm{f}) + \nabla\cdot(\phi\bar{\mathbf{u}}_\mathrm{f}\bar{\mathbf{u}}_\mathrm{f})] = -\phi\nabla\tilde{p}_\mathrm{f} + \nabla\cdot\langle\tau_\mathrm{f}\rangle \tag{1.50}$$
$$+\phi\tilde{\mathbf{F}}_\mathrm{f} + \mathbf{D} + \bar{\mathbf{u}}_\mathrm{m}\Gamma_\mathrm{d} + \nabla\cdot\langle\tau_{\delta\mathrm{f}}\rangle$$

$$\frac{\partial}{\partial t}[(1-\phi)\tilde{\rho}_\mathrm{d}\bar{\mathbf{u}}_\mathrm{d}] + \nabla\cdot[(1-\phi)\tilde{\rho}_\mathrm{d}\bar{\mathbf{u}}_\mathrm{d}\bar{\mathbf{u}}_\mathrm{d}] = -(1-\phi)\nabla\tilde{p}_\mathrm{d} + \nabla\cdot\langle\tau_\mathrm{d}\rangle \tag{1.51}$$
$$+(1-\phi)\tilde{\mathbf{F}}_\mathrm{d} - \mathbf{D} - \bar{\mathbf{u}}_\mathrm{m}\Gamma_\mathrm{d} + \nabla\cdot\langle\tau_{\delta\mathrm{d}}\rangle.$$

Multifluid system

As a final example, we consider a system which consists of several continuous or discontinuous fluid phases under the simplifying assumptions that there is no mass transfer between the phases and that the surface tension can be neglected for each pair of phases. It thus follows that

$$\Gamma_\alpha = 0 \qquad \text{for all phases } \alpha \tag{1.52}$$

$$\sum_\alpha \mathbf{M}_\alpha = 0. \tag{1.53}$$

Analogously to Eqn. (1.35) we can decompose the momentum transfer integrals as

$$\mathbf{M}_\alpha = \tilde{p}_\alpha\,\nabla\phi_\alpha + \mathbf{D}_\alpha, \tag{1.54}$$

where

$$\mathbf{D}_\alpha = \frac{1}{V}\int_{A_\alpha}(-\delta p_\alpha \mathbb{1} + \tau_\alpha)\cdot\hat{\mathbf{n}}_\alpha\,dA. \tag{1.55}$$

In the special case where the system is at complete rest, the phases must share the same pressure (this follows from Eqn. (1.5) in the case that $\sigma_{\alpha\gamma} = 0$). We shall assume here that this is approximately true also in the general case where flow is present. We thus have that $\tilde{p}_\alpha \approx \tilde{p}$, where $\tilde{p}$ is the common pressure of all phases. Since $\nabla(\sum_\alpha \phi_\alpha) = 0$, it follows from Eqns. (1.53) and (1.54) that

$$\sum_\alpha \mathbf{D}_\alpha = 0. \tag{1.56}$$

For the present multifluid system, Eqns. (1.27) and (1.28) can now be written in the form

$$\frac{\partial}{\partial t}(\phi_\alpha \tilde{\rho}_\alpha) + \nabla \cdot (\phi_\alpha \tilde{\rho}_\alpha \bar{\mathbf{u}}_\alpha) = 0 \tag{1.57}$$

$$\frac{\partial}{\partial t}(\phi_\alpha \tilde{\rho}_\alpha \bar{\mathbf{u}}_\alpha) + \nabla \cdot (\phi_\alpha \tilde{\rho}_\alpha \bar{\mathbf{u}}_\alpha \bar{\mathbf{u}}_\alpha) = -\phi_\alpha \nabla \tilde{p} + \nabla \cdot \langle \tau_\alpha \rangle + \phi_\alpha \tilde{\mathbf{F}}_\alpha + \mathbf{D}_\alpha + \nabla \cdot \langle \tau_{\delta\alpha} \rangle. \tag{1.58}$$

These equations will be further considered in chapter 2 where various methods for numerical solution of multiphase flows are discussed.

The apparent restriction to a single common pressure $\tilde{p}$ of phases in Eqns. (1.58) is not actually a severe limitation of generality. If for any reason the pressure varies between phases, it is always possible to define $\tilde{p}$ as an appropriate average of the phasial pressures $\tilde{p}_\alpha$ and to include the effect of the deviatoric part $\tilde{p}_\alpha - \tilde{p}$ in the other terms on the right side of Eqn. (1.58) such as in $\nabla \cdot \langle \tau_\alpha \rangle$ or in $\mathbf{D}_\alpha$.

1.3 Ensemble averaging

In the previous section we derived the equations of multiphase flow (ignoring the energy equation) using volume averaging. In this section we shall repeat the derivation using a different approach, namely ensemble averaging [Ish75, Dre83, Buy71, Hwa89, JL90]. As we shall see, the resulting general equations are formally identical to those derived in the previous section, Eqns. (1.27) and (1.28). While ensemble averaging, of all the averaging methods that are commonly used within the Eulerian approach, appears as the most elegant one, mathematical charm alone would not be a sufficient cause for duplicating our efforts at this point. As discussed in section 1.2.2 however, the major problem within multiphase fluid dynamics is not derivation of the conservation equations, but the closure of the equations. Ensemble averaging, as the standard averaging method of also the modern statistical physics, provides a different view in the physical interpretation of the interaction terms and of the Reynolds stresses and may thereby provide a different approach for solving the closure problem.

Conceptually, ensemble averaging is achieved by repeating the measurement at a fixed time and position for a large number of systems with identical macroscopic properties and boundary conditions, and finding the mean value of the results. Although the properties and the boundary conditions are unchanged at the macroscopic level for each system, they differ at the mesoscopic level. This leads to a scatter of the observed values. We denote the collection of these macroscopically identical systems by C (the ensemble) and its individual member by μ. If $f(\mathbf{r}, t; \mu)$ is any quantity observed

for a system μ at point $\mathbf{r}$ and time t, its ensemble average $\langle f \rangle$ is defined by

$$\langle f \rangle(\mathbf{r}, t) = \int_C f(\mathbf{r}, t; \mu)\, dm(\mu), \tag{1.59}$$

where the measure $dm(\mu)$ is the probability of observing system μ within C. If all the necessary derivatives of f exist, it follows from the linearity of the ensemble averaging that

$$\langle \frac{\partial}{\partial t} f \rangle = \frac{\partial}{\partial t} \langle f \rangle \tag{1.60}$$

$$\langle \nabla f \rangle = \nabla \langle f \rangle. \tag{1.61}$$

Notice that Eqns. (1.60) and (1.61) do not include any additional interfacial terms, in contrast to Eqns. (1.14) through (1.16) for volume averaging. The difference lies in the different definitions of variables and averages. The observable quantity f itself is not associated to any particular phase of the system. For example if f is density, then $f(\mathbf{r}, t; \mu)$ is the local value of the density of the phase that happens to occupy point $\mathbf{r}$ at time t. Also the ensemble average is calculated without paying any attention to the phase that occupies the point at which the average is calculated. The volume average of a quantity defined for a certain phase is, on the other hand, calculated only over the part of the total averaging volume occupied by that particular phase, which gives rise to the surface integrals.

The partial average of f in phase α is defined by

$$\langle \Theta_\alpha f \rangle, \tag{1.62}$$

where Θ_α is the phase indicator function defined by Eqn. (1.17). Considering the phase indicator function as a generalized function (distribution), it can be shown that it satisfies the equation

$$\frac{D^s \Theta_\alpha}{Dt} \equiv \frac{\partial}{\partial t} \Theta_\alpha + \mathbf{u}_\mathrm{A} \cdot \nabla \Theta_\alpha = 0, \tag{1.63}$$

To see this, consider

$$\begin{aligned} &\int_{\mathbb{R}^3 \times \mathbb{R}} \left(\frac{\partial}{\partial t} \Theta_\alpha + \mathbf{u}_\mathrm{A} \cdot \nabla \Theta_\alpha \right) \psi \, dV dt \\ &= - \int_{\mathbb{R}^3 \times \mathbb{R}} \Theta_\alpha \left(\frac{\partial}{\partial t} \psi + \nabla \cdot (\psi \mathbf{u}_\mathrm{A}) \right) dV dt \\ &= - \int_{-\infty}^{\infty} \left(\int_{V_\alpha} \left(\frac{\partial}{\partial t} \psi + \nabla \cdot (\psi \mathbf{u}_\mathrm{A}) \right) dV \right) dt \\ &= - \int_{-\infty}^{\infty} \left(\frac{d}{dt} \int_{V_\alpha(t)} \psi \, dV \right) dt \\ &= 0, \end{aligned} \tag{1.64}$$

where $\mathbf{u}_\mathrm{A}$ is the velocity of the phase interface, $V_\alpha(t)$ is the volume occupied by phase α at time t, and ψ is a test function, which is sufficiently smooth and has a compact support both in V and t. In order that the second line makes sense we must extend $\mathbf{u}_\mathrm{A}$ smoothly through phase α. It is now easy to show that

$$\begin{aligned}
\langle \Theta_\alpha \nabla f \rangle &= \nabla \langle \Theta_\alpha f \rangle - \langle f \nabla \Theta_\alpha \rangle && (1.65)\\
\langle \Theta_\alpha \nabla \cdot f \rangle &= \nabla \cdot \langle \Theta_\alpha f \rangle - \langle f \cdot \nabla \Theta_\alpha \rangle && (1.66)\\
\langle \Theta_\alpha \frac{\partial}{\partial t} f \rangle &= \frac{\partial}{\partial t} \langle \Theta_\alpha f \rangle - \langle f \frac{\partial}{\partial t} \Theta_\alpha \rangle && (1.67)\\
&= \frac{\partial}{\partial t} \langle \Theta_\alpha f \rangle + \langle f \mathbf{u}_\mathrm{A} \cdot \nabla \Theta_\alpha \rangle,
\end{aligned}$$

where on the last line we have utilized Eqn. (1.63). The gradient of the phase indicator function is non-zero only at the phase interfaces, which leads to the conclusion that Eqns. (1.65) through (1.67) are counterparts of Eqns. (1.14) through (1.16) and, in particular, that the second terms on the right side of Eqns. (1.65) through (1.67) are counterparts of the surface integrals in Eqns. (1.14) through (1.16).

We assume that inside each phase, the normal fluid mechanical equations for mass and momentum are valid, namely

$$\begin{aligned}
\frac{\partial}{\partial t} \rho + \nabla \cdot (\rho \mathbf{u}) &= 0 && (1.68)\\
\frac{\partial}{\partial t} (\rho \mathbf{u}) + \nabla \cdot (\rho \mathbf{u}\mathbf{u}) &= \nabla \cdot \sigma + \mathbf{F}. && (1.69)
\end{aligned}$$

where $\rho, \mathbf{u}, \tau$ and $\mathbf{F}$ are local density, flow velocity, stress tensor and external force density, respectively. In what follows, we do not consider the energy equation. The hydrodynamic quantities that appear in Eqns. (1.68) and (1.69) are assumed to be well behaving within each phase but can have discontinuities at phase interfaces. Multiplying Eqns. (1.68) and (1.69) by Θ_α, performing ensemble averaging and using Eqns. (1.65) and (1.67), we get

$$\begin{aligned}
\frac{\partial}{\partial t} \langle \Theta_\alpha \rho \rangle + \nabla \cdot \langle \Theta_\alpha \rho \mathbf{u} \rangle &= \langle \rho (\mathbf{u} - \mathbf{u}_\mathrm{A}) \cdot \nabla \boldsymbol{\Theta}_\alpha \rangle && (1.70)\\
\frac{\partial}{\partial t} \langle \Theta_\alpha \rho \mathbf{u} \rangle + \nabla \cdot \langle \Theta_\alpha \rho \mathbf{u}\mathbf{u} \rangle &= \nabla \cdot \langle \Theta_\alpha \sigma \rangle + \langle \Theta_\alpha \mathbf{F} \rangle && (1.71)\\
&\quad + \langle (\rho \mathbf{u} (\mathbf{u} - \mathbf{u}_\mathrm{A}) - \sigma) \cdot \nabla \Theta_\alpha \rangle.
\end{aligned}$$

In analogy with Eqns. (1.7) and (1.8) we define the intrinsic and Favré averages of any quantity f as

$$\begin{aligned}
\tilde{f}_\alpha &= \langle \Theta_\alpha f \rangle / \langle \Theta_\alpha \rangle = \langle \Theta_\alpha f \rangle / \phi_\alpha && (1.72)\\
\bar{f}_\alpha &= \langle \Theta_\alpha \rho f \rangle / \langle \Theta_\alpha \rho \rangle = \langle \Theta_\alpha \rho f \rangle / (\phi_\alpha \tilde{\rho}_\alpha), && (1.73)
\end{aligned}$$

respectively. Here,

$$\phi_\alpha = \langle \Theta_\alpha \rangle, \tag{1.74}$$

which we call the 'volume fraction' of phase α following the common convention even though 'statistical fraction' might be a more proper term.

In order to approach a closed set of equations we again use Favré averaged velocity $\bar{\mathbf{u}}_\alpha$ and the velocity fluctuation $\delta\mathbf{u}_\alpha$ defined for phase α as

$$\bar{\mathbf{u}}_\alpha = \langle \Theta_\alpha \rho \mathbf{u} \rangle / (\phi_\alpha \tilde{\rho}_\alpha) \tag{1.75}$$

$$\delta\mathbf{u}_\alpha = \mathbf{u} - \bar{\mathbf{u}}_\alpha. \tag{1.76}$$

With these conventions the momentum flux term in Eqn. (1.71) can be rewritten as

$$\langle \Theta_\alpha \rho \mathbf{u}\mathbf{u} \rangle = \phi_\alpha \tilde{\rho}_\alpha \bar{\mathbf{u}}_\alpha \bar{\mathbf{u}}_\alpha - \tau_{\delta\alpha}, \tag{1.77}$$

where the Reynolds stress tensor $\tau_{\delta\alpha}$ is defined by

$$\tau_{\delta\alpha} = -\langle \Theta_\alpha \rho \delta\mathbf{u}_\alpha \delta\mathbf{u}_\alpha \rangle. \tag{1.78}$$

Using Eqns. (1.74) through (1.77), the averaged equations (1.70) and (1.71) finally acquire the form

$$\frac{\partial}{\partial t}(\phi_\alpha \tilde{\rho}_\alpha) + \nabla \cdot (\phi_\alpha \tilde{\rho}_\alpha \bar{\mathbf{u}}_\alpha) = \Gamma_\alpha \tag{1.79}$$

$$\begin{aligned} &\frac{\partial}{\partial t}(\phi_\alpha \tilde{\rho}_\alpha \mathbf{u}_\alpha) + \nabla \cdot (\phi_\alpha \tilde{\rho}_\alpha \bar{\mathbf{u}}_\alpha \bar{\mathbf{u}}_\alpha) \\ &\quad = \nabla \cdot (\phi_\alpha \tilde{\sigma}_\alpha + \tau_{\delta\alpha}) + (\phi_\alpha \tilde{\mathbf{F}}_\alpha) + \mathbf{M}_\alpha, \end{aligned} \tag{1.80}$$

where the quantities Γ_α and $\mathbf{M}_\alpha$ are defined by

$$\Gamma_\alpha = \langle \rho(\mathbf{u} - \mathbf{u}_\mathrm{A}) \cdot \nabla \Theta_\alpha \rangle \tag{1.81}$$

$$\mathbf{M}_\alpha = \langle (\rho \mathbf{u}(\mathbf{u} - \mathbf{u}_\mathrm{A}) - \sigma) \cdot \nabla \Theta_\alpha \rangle. \tag{1.82}$$

These terms are the analogues of the transfer integrals that appear in the corresponding volume averaged equations (1.22) and (1.23). They include the rate of mass and momentum transfer between the phases.

As stated before, the general averaged equations obtained using ensemble averaging are formally identical with those derived within the volume averaging scheme in section 1.2. All the terms that appear in the ensemble averaged equations have analogous physical content with the corresponding term in the volume averaged equations. The only difference is that the different formal definitions of terms such as $\tau_{\delta\alpha}$, Γ_α and $\mathbf{M}_\alpha$ within these two approaches may offer different ways of relating these quantities with the basic averaged variables ϕ_α, $\tilde{\rho}_\alpha$, $\tilde{p}_\alpha$, $\bar{\mathbf{u}}_\alpha$, *etc.*, and thereby solving the closure problem for a given system.

1.4 Mixture models

The mixture model (or algebraic slip model) is a simplified formulation of the multiphase flow equations. We consider a suspension of a dispersed phase (particles, drops, or bubbles) in a continuous fluid (liquid or gas). If the dispersed phase follows closely the fluid motion (small particles), it seems natural to write the balance equations for the mixture of the dispersed and continuous phases and take the relative motion of the phases into account as a correction. The mixture model consists then of the continuity and momentum equations for the mixture and the continuity equations for the individual dispersed phases. The slip velocity between the dispersed and continuous phases is taken into account by introducing corresponding convection terms in the continuity equations.

The essential character of the mixture model is that only one set of velocity components is solved from the differential equations for momentum conservation. The velocities of the dispersed phases are inferred from approximate algebraic balance equations. This reduces the computational effort considerably, especially when several dispersed phases need to be considered.

The mixture model equations are derived in the literature applying various approaches [Ish75, Ung93, Gid94]. The form of the equations also varies depending on the application. Ishii [Ish75] derives the mixture equations from a general balance equation. In this section, we derive the mixture model equations from the original multiphase equations. This approach is transparent and the required simplifications are clearly shown. Furthermore, the applicability of the model can be explicitly analysed.

Continuity equation for the mixture

From the continuity equation for phase α (1.27), we obtain by summing over all phases

$$\frac{\partial}{\partial t}\sum_{\alpha=1}^{n}(\phi_\alpha\tilde{\rho}_\alpha) + \nabla\cdot\sum_{\alpha=1}^{n}(\phi_\alpha\tilde{\rho}_\alpha\bar{\mathbf{u}}_\alpha) = \sum_{\alpha=1}^{n}\Gamma_\alpha \tag{1.83}$$

The right hand side of Eqn. (1.83) vanishes due to the conservation of the total mass, Eqn. (1.30), and we obtain the continuity equation of the mixture

$$\frac{\partial}{\partial t}(\rho_\mathrm{m}) + \nabla\cdot(\rho_\mathrm{m}\bar{\mathbf{u}}_\mathrm{m}) = 0 \tag{1.84}$$

Here the mixture density and the mixture velocity are defined as

$$\rho_\mathrm{m} = \sum_{\alpha=1}^{n}\phi_\alpha\tilde{\rho}_\alpha \tag{1.85}$$

$$\bar{\mathbf{u}}_\mathrm{m} = \frac{1}{\rho_\mathrm{m}}\sum_{\alpha=1}^{n}\phi_\alpha\tilde{\rho}_\alpha\bar{\mathbf{u}}_\alpha = \sum_{\alpha=1}^{n}c_\alpha\bar{\mathbf{u}}_\alpha \tag{1.86}$$

The mixture velocity $\bar{\mathbf{u}}_\mathrm{m}$ represents the velocity of the mass center. Notice that ρ_m varies although the component densities are constant. The mass fraction of phase α is defined as

$$c_\alpha = \frac{\phi_\alpha \tilde{\rho}_\alpha}{\rho_\mathrm{m}} \tag{1.87}$$

Eqn. (1.84) has the same form as the continuity equation for single phase flow.

Momentum equation for the mixture

The momentum equation for the mixture follows from the phase momentum equations (1.28) by summing over all phases

$$\begin{aligned} \frac{\partial}{\partial t}\sum_{\alpha=1}^{n}\phi_\alpha\tilde{\rho}_\alpha\bar{\mathbf{u}}_\alpha \quad &+ \quad \nabla\cdot\sum_{\alpha=1}^{n}\phi_\alpha\tilde{\rho}_\alpha\bar{\mathbf{u}}_\alpha\bar{\mathbf{u}}_\alpha \\ &= \quad -\sum_{\alpha=1}^{n}\nabla(\phi_\alpha\tilde{p}_\alpha) + \nabla\cdot\sum_{\alpha=1}^{n}\phi_\alpha(\tilde{\tau}_\alpha + \tilde{\tau}_{\delta\alpha}) \\ &\quad + \sum_{\alpha=1}^{n}\phi_\alpha\tilde{\mathbf{F}}_\alpha + \sum_{\alpha=1}^{n}\mathbf{M}_\alpha. \end{aligned} \tag{1.88}$$

Here, the stress terms have been written in terms of intrinsic averages of the stress tensors using Eqn. (1.7). Using the definitions (1.85) and (1.86) of the mixture density ρ_m and the mixture velocity $\bar{\mathbf{u}}_\mathrm{m}$, the second term of (1.88) can be rewritten as

$$\nabla\cdot\sum_{\alpha=1}^{n}\phi_\alpha\tilde{\rho}_\alpha\bar{\mathbf{u}}_\alpha\bar{\mathbf{u}}_\alpha = \nabla\cdot(\rho_\mathrm{m}\bar{\mathbf{u}}_\mathrm{m}\bar{\mathbf{u}}_\mathrm{m}) + \nabla\cdot\sum_{\alpha=1}^{n}\phi_\alpha\tilde{\rho}_\alpha\bar{\mathbf{u}}_{\mathrm{m}\alpha}\bar{\mathbf{u}}_{\mathrm{m}\alpha} \tag{1.89}$$

where $\bar{\mathbf{u}}_{\mathrm{m}\alpha}$ is the diffusion velocity, *i.e.*, the velocity of phase α relative to the center of the mixture mass

$$\bar{\mathbf{u}}_{\mathrm{m}\alpha} = \bar{\mathbf{u}}_\alpha - \bar{\mathbf{u}}_\mathrm{m} \tag{1.90}$$

In terms of the mixture variables, the momentum equation takes the form

$$\begin{aligned} \frac{\partial}{\partial t}(\rho_\mathrm{m}\bar{\mathbf{u}}_\mathrm{m}) + \nabla\cdot(\rho_\mathrm{m}\bar{\mathbf{u}}_\mathrm{m}\bar{\mathbf{u}}_\mathrm{m}) \quad &= \quad -\nabla p_\mathrm{m} + \nabla\cdot(\langle\tau_\mathrm{m}\rangle + \langle\tau_{\delta\mathrm{m}}\rangle) + \nabla\cdot\langle\tau_{\mathrm{D}\mathrm{m}}\rangle \\ &\quad + \mathbf{F}_\mathrm{m} + \mathbf{M}_\mathrm{m} \end{aligned} \tag{1.91}$$

The three stress tensors are defined as

$$\langle\tau_\mathrm{m}\rangle = -\sum_{\alpha=1}^{n}\phi_\alpha\tilde{\tau}_\alpha \tag{1.92}$$

$$\langle \tau_{\delta \mathrm{m}} \rangle = -\sum_{\alpha=1}^{n} \phi_\alpha \langle \tilde{\rho}_\alpha \delta \mathbf{u}_\alpha \delta \mathbf{u}_\alpha \rangle \tag{1.93}$$

$$\langle \tau_{\mathrm{Dm}} \rangle = -\sum_{\alpha=1}^{n} \phi_\alpha \tilde{\rho}_\alpha \bar{\mathbf{u}}_{\mathrm{m}\alpha} \bar{\mathbf{u}}_{\mathrm{m}\alpha} \tag{1.94}$$

and represent the average viscous stress, turbulent stress, and diffusion stress due to the phase slip, respectively. In Eqn. (1.91), the pressure of the mixture is defined by the relation

$$p_{\mathrm{m}} = \sum_{\alpha=1}^{n} \phi_\alpha \tilde{p}_\alpha \tag{1.95}$$

In practice, the phase pressures are often taken to be equal, *i.e.*, $\tilde{p}_\alpha = p_{\mathrm{m}}$. Accordingly, the last term on the right hand side of (1.91), $\mathbf{M}_m$, comprises only the influence of the surface tension force on the mixture and depends on the geometry of the interface. The other additional term in (1.91) compared to the one phase momentum equation is the diffusion stress term $\nabla \cdot \tau_{\mathrm{Dm}}$ representing the momentum transfer due to the relative motions.

Continuity equation for a phase

We return to consider an individual phase. Using the definition of the diffusion velocity (1.90) to eliminate the phase velocity in the continuity equation (1.27) gives

$$\frac{\partial}{\partial t}(\phi_\alpha \tilde{\rho}_\alpha) + \nabla \cdot (\phi_\alpha \tilde{\rho}_\alpha \bar{\mathbf{u}}_{\mathrm{m}}) = \Gamma_\alpha - \nabla \cdot (\phi_\alpha \tilde{\rho}_\alpha \bar{\mathbf{u}}_{\mathrm{m}\alpha}) \tag{1.96}$$

If the phase densities are constants and phase changes do not occur, the continuity equation reduces to

$$\frac{\partial}{\partial t}\phi_\alpha + \nabla \cdot (\phi_\alpha \bar{\mathbf{u}}_{\mathrm{m}}) = -\nabla \cdot (\phi_\alpha \bar{\mathbf{u}}_{\mathrm{m}\alpha}) \tag{1.97}$$

The term on the right hand side represents the diffusion of the particles due to the phase slip.

Diffusion velocity

In the mixture model, the momentum equations for the dispersed phases are not solved and therefore a closure model has to be derived for the diffusion velocities. The balance equation for calculating the relative velocity can be rigorously derived by combining the momentum equations for the dispersed phase and the mixture. In the following, we consider one dispersed particulate phase, p, for simplicity. Using Eqn. (1.54) for $\mathbf{M}_p$ and the continuity equation, the momentum equation of the dispersed phase p (1.28) can be

rewritten as follows (here gravity is used for external force , *i.e.*, $\tilde{\mathbf{F}}_\alpha = \tilde{\rho}_\alpha \mathbf{g}$, $\mathbf{F}_\mathrm{m} = \rho_\mathrm{m}\mathbf{g}$)

$$\begin{aligned}\phi_\mathrm{p}\tilde{\rho}_\mathrm{p}\frac{\partial}{\partial t}\bar{\mathbf{u}}_\mathrm{p} + \phi_\mathrm{p}\tilde{\rho}_\mathrm{p}(\bar{\mathbf{u}}_\mathrm{p}\cdot\nabla)\bar{\mathbf{u}}_\mathrm{p} &= -\phi_\mathrm{p}\nabla(\tilde{p}_\mathrm{p}) + \nabla\cdot[\phi_\mathrm{p}(\tilde{\tau}_\mathrm{p} + \tilde{\tau}_{\delta\mathrm{p}})] \\ &\quad + \phi_\mathrm{p}\tilde{\rho}_\mathrm{p}\mathbf{g} + \mathrm{D}_\mathrm{p} \qquad (1.98)\end{aligned}$$

The corresponding equation for the mixture is

$$\rho_\mathrm{m}\frac{\partial}{\partial t}\bar{\mathbf{u}}_\mathrm{m} + \rho_\mathrm{m}(\bar{\mathbf{u}}_\mathrm{m}\cdot\nabla)\bar{\mathbf{u}}_\mathrm{m} = -\nabla p_\mathrm{m} + \nabla\cdot(\tau_\mathrm{m} + \tau_{\delta\mathrm{m}} + \tau_{D\mathrm{m}}) + \rho_\mathrm{m}\mathbf{g} \quad (1.99)$$

Here we have neglected the surface tension forces and therefore $\mathbf{M}_\mathrm{m} = 0$. Assuming that the phase pressures are equal, *i.e.*, $p_\mathrm{m} = \tilde{p}_\mathrm{p}$, we can eliminate the pressure gradient from (1.98) and (1.99). As a result we obtain an equation for $\mathbf{D}_\mathrm{p}$

$$\begin{aligned}\mathbf{D}_\mathrm{p} &= \phi_\mathrm{p}\left(\tilde{\rho}_\mathrm{p}\frac{\partial}{\partial t}\bar{\mathbf{u}}_\mathrm{mp} + (\tilde{\rho}_\mathrm{p} - \rho_\mathrm{m})\frac{\partial}{\partial t}\bar{\mathbf{u}}_\mathrm{m}\right) \\ &\quad + \phi_\mathrm{p}[\tilde{\rho}_\mathrm{p}(\bar{\mathbf{u}}_\mathrm{p}\cdot\nabla)\bar{\mathbf{u}}_\mathrm{p} - \rho_\mathrm{m}(\bar{\mathbf{u}}_\mathrm{m}\cdot\nabla)\bar{\mathbf{u}}_\mathrm{m}] \\ &\quad - \nabla\cdot[\phi_\mathrm{p}(\tilde{\tau}_\mathrm{p} + \tilde{\tau}_{\delta\mathrm{p}})] + \phi_\mathrm{p}\nabla\cdot(\tau_\mathrm{m} + \tau_{\delta\mathrm{m}} + \tau_{\mathrm{D}\mathrm{m}}) \\ &\quad - \phi_\mathrm{p}\left(\tilde{\rho}_\mathrm{p} - \rho_\mathrm{m}\right)\mathbf{g} \qquad (1.100)\end{aligned}$$

In (1.100) we have utilized the definition (1.90) for the diffusion velocity $\bar{\mathbf{u}}_\mathrm{mp}$. Next, we will make several approximations to simplify Eqn. (1.100). Using the local equilibrium approximation, we drop from the first term the time derivative of $\bar{\mathbf{u}}_\mathrm{mp}$. In the second term, we approximate

$$(\bar{\mathbf{u}}_\mathrm{p}\cdot\nabla)\bar{\mathbf{u}}_\mathrm{p} \approx (\bar{\mathbf{u}}_\mathrm{m}\cdot\nabla)\bar{\mathbf{u}}_\mathrm{m} \quad (1.101)$$

The viscous and diffusion stresses are omitted as small compared to the leading terms. The turbulent stress cannot be neglected if we wish to keep the turbulent diffusion of the dispersed phase in the model. However, all turbulent effects are omitted for the moment. In that case, the final simplified equilibrium equation for $\mathbf{D}_\mathrm{p}$ is

$$\mathbf{D}_\mathrm{p} = \phi_\mathrm{p}(\tilde{\rho}_\mathrm{p} - \rho_\mathrm{m})\left[\mathbf{g} - (\bar{\mathbf{u}}_\mathrm{m}\cdot\nabla)\bar{\mathbf{u}}_\mathrm{m} - \frac{\partial}{\partial t}\bar{\mathbf{u}}_\mathrm{m}\right]. \quad (1.102)$$

Since $\mathbf{D}_\mathrm{p}$ is a function of the slip velocity $\bar{\mathbf{u}}_\mathrm{cp} = \bar{\mathbf{u}}_\mathrm{p} - \bar{\mathbf{u}}_\mathrm{c}$, Eqn. (1.102) is an algebraic formula for the diffusion velocity

$$\bar{\mathbf{u}}_\mathrm{mp} = (1 - c_\mathrm{p})\bar{\mathbf{u}}_\mathrm{cp} \quad (1.103)$$

The mixture model consists of Eqns. (1.84), (1.91), (1.96), and (1.102) together with constitutive equations for the viscous and turbulent stresses.

Validity of the mixture model

The terms omitted in arriving to Eqn. (1.102) from Eqn. (1.100) (except turbulence terms) can be rewritten in the following form

$$\phi_\mathrm{p}\tilde{\rho}_\mathrm{p}\left[\frac{\partial}{\partial t}\bar{\mathbf{u}}_\mathrm{mp}+(\bar{\mathbf{u}}_\mathrm{mp}\cdot\nabla)\bar{\mathbf{u}}_\mathrm{mp}\right]+\phi_\mathrm{p}\tilde{\rho}_\mathrm{p}[(\bar{\mathbf{u}}_\mathrm{m}\cdot\nabla)\bar{\mathbf{u}}_\mathrm{mp}+(\bar{\mathbf{u}}_\mathrm{mp}\cdot\nabla)\bar{\mathbf{u}}_\mathrm{m}]$$
$$+\phi_\mathrm{p}\nabla\cdot(\tau_\mathrm{m}+\tau_\mathrm{Dm})-\nabla\cdot(\phi_\mathrm{p}\tilde{\tau}_\mathrm{p}) \qquad (1.104)$$

The local equilibrium approximation requires that the particles are rapidly accelerated to the terminal velocity. This corresponds to setting the first term in (1.104) equal to zero. Consider first a constant body force, like gravitation. A criterion for neglecting the acceleration is related to the relaxation time of a particle, t_p. In the Stokes regime t_p is given by

$$t_\mathrm{p}=\frac{\tilde{\rho}_\mathrm{p}d_\mathrm{p}^2}{18\mu_\mathrm{m}}, \qquad Re_\mathrm{p}<1 \qquad (1.105)$$

and in the Newton regime (constant C_D) by

$$t_\mathrm{p}=\frac{4\tilde{\rho}_\mathrm{p}d_\mathrm{p}}{3\tilde{\rho}_\mathrm{c}C_D u_t}, \qquad Re_\mathrm{p}>1000 \qquad (1.106)$$

where u_t is the terminal velocity. Within the time t_p, the particle travels the distance $l_\mathrm{p}=t_\mathrm{p}u_t/e$, which characterizes the length scale of the acceleration. If the density ratio $\tilde{\rho}_\mathrm{p}/\tilde{\rho}_\mathrm{c}$ is small, the virtual mass and Basset terms in the equation of motion cannot be neglected. The Basset term in particular effectively increases the relaxation time. The true length scale l'_p of the particle acceleration can be an order of magnitude larger than l_p [MTK96]. An appropriate requirement for the local equilibrium is thus $l'_\mathrm{p}<<L$, where L is a typical dimension of the system.

The second term in (1.104) corresponds, in rotational motion, the Coriolis force. The radial particle velocity caused by the centrifugal acceleration causes in turn a tangential acceleration. To the first order, the second term in (1.104) is proportional to $\bar{u}_{\mathrm{m}\varphi}\bar{u}_\mathrm{cp}/r$, which has to be compared with the leading term $\bar{u}^2_{\mathrm{m}\varphi}/r$ (r is the radius of curvature). Neglecting the second term thus requires simply that

$$\frac{\bar{u}_\mathrm{cp}}{\bar{u}_{\mathrm{m}\varphi}}<<1 \qquad (1.107)$$

In the Stokes regime, this condition can be expressed as

$$d_\mathrm{p}<<\sqrt{\frac{18\mu_\mathrm{c}}{\omega(\tilde{\rho}_\mathrm{p}-\tilde{\rho}_\mathrm{c})}}, \qquad (1.108)$$

where ω is the angular velocity of the rotation.

In the last two terms of Eqn. (1.104), the viscous stresses can obviously be regarded as small compared to the leading terms, except possibly inside a boundary layer. The diffusion stress can be neglected within the approximation of local equilibrium.

In the above analysis, we assumed that the suspension is homogeneous in small spatial scales. If this is not the case and dense clusters of particles are formed, the mixture model is usually not applicable. Clustering in a scale comparable to the length scale of turbulent fluctuations is typical for small particles ($d_\mathrm{p} < 200\mu$m) in gases. The clustering can lead to a substantial decrease in the effective drag coefficient. Consequently, the particle relaxation time becomes large and the local equilibrium approximation is not valid. Although the mixture model is in principle valid for small particles ($d_\mathrm{p} < 50\mu$m) in gases, it can be used only for dilute suspensions with solids to gas mass ratio below 1.

1.5 Particle tracking models

Historically Lagrangian tracking models were first introduced in very dilute flows of particulate suspensions[BH79], characteristic e.g. for electrostatic precipitators. In these flows, the dispersed phase number density is low enough such that the flow is dominated by the continuous carrier phase. Mathematically the delineation between dilute and dense particulate flows is established by the hydrodynamic response (or relaxation) time of the particle t_p and the mean time between successive collisions between the particles t_c. In a dilute flow $t_\mathrm{p}/t_\mathrm{c} < 1$. The particle then has enough time to respond to the surrounding fluid field before the next collision, and the motion of the particle is primarily controlled by the fluid flow. This assumption allows separation of the solution for the two phases. Within the most simple approach to particle tracking one first solves the flow of the carrier fluid without taking particles into consideration. Next, particles are released at desired positions in the solution domain. The trajectories of the particles are then found by integrating an appropriate force balance equation (see section 1.5.1) for each particle. Particle patches instead of single particles may also be used at this point in order to reduce computational effort. This type of approach is also known as *one-way coupling* as the information is mainly transfered from the carrier phase to the dispersed phase and not in the opposite direction.

In flows frequently found, *e.g.*, in pneumatic conveying, the number density of the particulate phase is relatively high such that the presence of particles affects the flow of the carrier phase while the collisions between particles can still be ignored. Then, *two-way coupling* is said to prevail since information is transfered from the carrier phase to dispersed phase and vice versa. Lagrangian particle tracking method can be used to solve also this

type of flow through an appropriate iterative procedure. The principle of numerical solution for one-way coupled systems and for two-way coupled systems is illustrated in Fig. 2.5.

In dense particulate flows, such as those found in fluidized beds, we have that $t_p/t_c > 1$, whereby the motion of a particle is significantly affected also by interactions with other particles. These flows represent the case of *four-way coupling* where information is also transfered between particles, and are often solved using Eulerian multiphase models.

As stated above, particle tracking method includes first solving the usual single-phase flow equations with proper boundary conditions for the carrier phase, and then an initial value problem for an ordinary differential equation separately for each particle. (For flows with two-way coupling, this procedure must be iterated.) In many cases particle tracking method leads to a marked simplification as compared to the continuum Eulerian method which requires the solution of a boundary value problem for coupled partial differential equations, (Eqns. (1.27) and (1.28)), for both phases. Fundamental difficulties associated with the closure of Eulerian multiphase models may also be avoided within the Lagrangian approach. Although the particle tracking method is conceptually simple, it is not always quite straightforward in practice. Firstly, the equation of motion of an individual particle in the surrounding fluid, discussed in the next section, may be quite complicated. Secondly, turbulent flow poses a problem also within particle tracking method. In particular, the modification of fluid turbulence due to presence of the dispersed phase still lacks models with adequate theoretical justification [Cro93].

Provided that an adequate equation of motion of the particle is given, the particle tracking method is in general readily applicable in laminar flows and in cases where only the mean trajectories of particles in a turbulent flow are of interest. If, however, dispersion of particles in a turbulent flow is considered, additional modeling is needed in order to relate the dispersion rate of particles with the statistical characteristics of turbulence of the carrier fluid. That topic is discussed in section 1.5.2.

1.5.1 Equation of motion for a single particle

The basic equation that describes the motion of a sphere settling in a quiescent fluid due to gravity is the well-known equation by Basset [Bas88], Boussinesq [Bou03] and Oseen [Ose27] (BBO). The original BBO equation was based on the assumption that the Reynolds number of the particle is low enough for the disturbance field produced by the motion of the sphere to be governed by the unsteady Stokes equation. Later, Tchen extended the

BBO equation to an unsteady and non-uniform flow as follows [Tch47]

$$\begin{aligned} m_{\mathrm{p}}\frac{\mathrm{d}\mathbf{v}}{\mathrm{d}t} &= \overbrace{6\pi r_{\mathrm{p}}\mu_{\mathrm{f}}(\mathbf{u}-\mathbf{v})}^{\mathrm{I}} - \overbrace{\frac{m_{\mathrm{f}}}{\rho_{\mathrm{f}}}\nabla p}^{\mathrm{II}} + \overbrace{\frac{m_{\mathrm{f}}}{2}\frac{\mathrm{d}}{\mathrm{d}t}(\mathbf{u}-\mathbf{v})}^{\mathrm{III}} \\ &+ \overbrace{6r_{\mathrm{p}}^2\sqrt{\pi\mu_{\mathrm{f}}\rho_{\mathrm{f}}}\int_{t_0}^{t}\frac{\frac{\mathrm{d}}{\mathrm{d}\tau}\{\mathbf{u}(\mathbf{y}(\tau),\tau)-\mathbf{v}(\tau)\}}{\sqrt{t-\tau}}\,\mathrm{d}\tau}^{\mathrm{IV}} \\ &+ \overbrace{(m_{\mathrm{p}}-m_{\mathrm{f}})\mathbf{g}}^{\mathrm{V}}. \end{aligned} \tag{1.109}$$

Here, r_{p} is the radius of the particle, m_{p} and m_{f} are the mass of the particle and the mass of a fluid sphere of radius r_{p}, ρ_{f} and μ_{f} are the density and the dynamic viscosity of the fluid, $\mathbf{v}(t)$ is the velocity vector of the particle instantaneously centred at $\mathbf{y}(t)$ and $\mathbf{u}(\mathbf{y}(t),t)$ is the Eulerian velocity vector of the fluid at position $\mathbf{y}(t)$. It should be noted that $\mathbf{u}$ represents the fluid velocity at the mass centre of the particle as if the particle would not create any disturbance field. The convective derivative following the motion of the particle is given by

$$\frac{\mathrm{d}}{\mathrm{d}t} = \left(\frac{\partial}{\partial t} + v_j\frac{\partial}{\partial x_j}\right)_{\mathbf{y}(t)}. \tag{1.110}$$

The numbered terms in Eqn. (1.109) are the Stokes drag force (I), the force by fluid pressure gradient (II), the force by added mass (III), the Basset history term (IV) and the buoyancy term (V). Notice, that hydrostatic pressure component is not included in the pressure p, but is taken into account in the buoyancy term V in Eqn. (1.109).

Several authors have pointed out inconsistencies in Eqn. (1.109) [Lum57, Buy66, Ril71]. Maxey and Riley [MR83] were the first to derive the equation of motion of a small particle rationally from basic principles. They formulated the problem for the motion of a rigid Stokes sphere in a nonuniform flow field following the approach of Riley [Ril71] for the undisturbed flow. The disturbance field caused by the sphere was calculated generalizing the results of Basset [Bas88] and extending the work of Burgers [Bur38]. The equation of motion given by Maxey and Riley is

$$\begin{aligned} m_{\mathrm{p}}\frac{\mathrm{d}\mathbf{v}}{\mathrm{d}t} &= (m_{\mathrm{p}}-m_{\mathrm{f}})\mathbf{g} + m_{\mathrm{f}}\frac{\mathrm{d}\mathbf{u}}{\mathrm{d}t} - \frac{m_{\mathrm{f}}}{2}\frac{\mathrm{d}}{\mathrm{d}t}(\mathbf{v}-\mathbf{u}-\frac{r_{\mathrm{p}}^2}{10}\nabla^2\mathbf{u}) \\ &- 6\pi r_{\mathrm{p}}\mu_{\mathrm{f}}(\mathbf{v}-\mathbf{u}-\frac{r_{\mathrm{p}}^2}{6}\nabla^2\mathbf{u}) \\ &- 6r_{\mathrm{p}}^2\sqrt{\pi\mu_{\mathrm{f}}\rho_{\mathrm{f}}}\int_{t_0}^{t}\frac{\frac{\mathrm{d}}{\mathrm{d}\tau}(\mathbf{v}-\mathbf{u}-\frac{r_{\mathrm{p}}^2}{6}\nabla^2\mathbf{u})}{\sqrt{t-\tau}}\,\mathrm{d}\tau. \end{aligned} \tag{1.111}$$

The initial conditions are that the sphere is introduced at $t = t_0$ and that there is no disturbance flow prior to this.

By comparing Eqn. (1.111) with the BBO equation, Eqn. (1.109), it is seen that the Stokes drag, the added mass and the Basset history terms have been modified by the inclusion of terms containing the Laplacian of the fluid velocity. These modifications thus include the effects of velocity curvature on the drag force of a particle at low Reynolds numbers, *i.e.*, Faxen relations [Fax22]. Other modifications of the BBO equation than those discussed above can be found in the literature (see, *e.g.*, [Aut83, Buy66]).

In many practical cases, the most important terms on the right side of the BBO equation or of Eqn. (1.111) are the gravity term and the Stokes drag term. Especially for rapidly accelerating or oscillating flows also the other terms may become important, however. In order to select an appropriate form of the equation, it is thus important to estimate the magnitude of all the force terms in each particular case. In most applications, the Basset history term is ignored either as insignificant, or due to excessive numerical complications brought about by the integral included in this term.

It can be shown that for a laminar time dependent flow (and for the mean field of a turbulent flow), Eqn. (1.111) is valid provided that [MR83]

$$\frac{r_\mathrm{p}}{L} \ll 1, \quad \frac{r_\mathrm{p} W}{\nu_\mathrm{f}} \ll 1 \quad \text{and} \quad \frac{r_\mathrm{p}^2}{\nu_\mathrm{f}} \frac{U}{L} \ll 1, \tag{1.112}$$

where L is the characteristic length scale of the system, W is the characteristic relative velocity $(\mathbf{v} - \mathbf{u})$ and U/L is the scale of fluid velocity gradient for undisturbed flow.

For a turbulent flow there is no single set of scales but a continuous spectrum of velocity and length scales. The large scale energetic motions may be characterized by the integral turbulent length scale L_t and by the rms velocity $u_\mathrm{rms} = \sqrt{\overline{\delta u^2}}$. The dissipative small scale motions are described by the Kolmogorov microscales of length and velocity

$$\eta_\mathrm{k} = \left(\frac{\nu_\mathrm{f}^3}{\epsilon} \right)^{1/4} \quad \text{and} \quad v_\mathrm{k} = (\nu_\mathrm{f} \epsilon)^{1/4} \,, \tag{1.113}$$

respectively. Here, ϵ denotes the dissipation rate of turbulent energy. These two limiting scales are related by

$$\frac{\eta_\mathrm{k}}{L_\mathrm{t}} = \mathcal{O}\left\{ \mathrm{Re}_\lambda^{-1/2} \right\} \quad \text{and} \quad \frac{v_\mathrm{k}}{u_\mathrm{rms}} = \mathcal{O}\left\{ \mathrm{Re}_\lambda^{-3/2} \right\} \,, \tag{1.114}$$

where Re_λ is the Reynolds number defined by the Taylor microscale λ, i.e. $Re_\lambda = u_\mathrm{rms} \lambda / \nu_\mathrm{f}$ [TL72]. The steepest velocity gradients are found at the dissipative scales. The appropriate scale of the velocity gradient is thus given by $v_\mathrm{k}/\eta_\mathrm{k}$, or equivalently by u_rms/λ. For a turbulent field the conditions of validity of Eqn. (1.111) are thus given by

$$\frac{r_\mathrm{p}}{\eta_\mathrm{k}} \ll 1, \quad \frac{r_\mathrm{p} W}{\nu_\mathrm{f}} = \mathcal{O}\left\{ \frac{r_\mathrm{p}}{\eta_\mathrm{k}} \frac{W}{v_\mathrm{k}} \right\} \ll 1 \quad \text{and} \quad \frac{r_\mathrm{p}^2}{\nu_\mathrm{f}} \frac{v_\mathrm{k}}{\eta_\mathrm{k}} = \mathcal{O}\left\{ \frac{r_\mathrm{p}^2}{\eta_\mathrm{k}^2} \right\} \ll 1 \,. \tag{1.115}$$

These conditions are usually much more restrictive than the conditions given by Eqn. (1.112) for the mean velocity field of a turbulent flow, and for a laminar flow.

Provided that the conditions given by Eqn. (1.115) are fulfilled, the path of an individual particle in a turbulent flow can in principle be solved using the preferred form of Eqn. (1.111) (or of Eqn. (1.109)). However, this straightforward approach is not feasible, in general, since the full turbulent flow field $\mathbf{u}$ of the carrier fluid is not known. Instead, we may assume that the mean (time averaged) velocity $\bar{\mathbf{u}}$ and the necessary *statistical* properties of the turbulence are known (as given by measurements or by an appropriate turbulence model). The particle tracking method then involves first solving the mean velocity of the particle $\bar{\mathbf{v}}$ at a given instant of time t using Eqn. (1.111) where the turbulent fluid velocity field $\mathbf{u}$ is replaced by the mean velocity $\bar{\mathbf{u}} = \mathbf{u} - \delta\mathbf{u}$ (and $\delta\mathbf{u}$ is the turbulent velocity fluctuation). The displacement of the particle due to the mean flow during a short time interval Δt is given by $\Delta\bar{\mathbf{y}} = \bar{\mathbf{v}}\Delta t$. An additional stochastic displacement $\delta\mathbf{y}$ due to turbulent dispersion must then be added to yield the total displacement $\Delta\bar{\mathbf{y}} + \delta\mathbf{y}$ of the particle at time interval Δt. The path of the particle during a finite time is found by iterating this process through subseqent short time intervals. The pathline of an individual particle thus consists of a smooth contribution from the mean flow, a possible drift due to gravity or other external forces, and of a twisted random walk contribution due to turbulence. When applied to a large number of particles, this approach leads to a convection-diffusion type of behaviour of the dispersed phase.

If conditions of *one-way coupling* prevail the location of the particle can be found by the described integration process with the knowledge of the existing fluid field, available by preceding solution of fluid phase. For conditions of *two-way coupling* this field is known just after solving the particle trajectory changing the process inherently to coupled and nonlinear. Therefore, alternating iterative solution of fluid and dispersed phases until convergence is necessary.

Calculation of the dispersive displacement yet requires additional modeling to find the propability distribution for the random variable $\delta\mathbf{y}$. This can be done making use of Eqn. (1.111) and assuming only the necessary spectral characteristics of the fluid turbulence to be known. Specific particle dispersion models are discussed further in the next section.

1.5.2 Particle dispersion

The most important property in characterizing the response of particles to the fluid flow is their hydrodynamic response time t_p. For a rigid sphere in Stokes flow ($Re_\mathrm{p} < 1$), t_p is given as

$$t_\mathrm{p} = \frac{\rho_\mathrm{p} d_\mathrm{p}^2}{18\mu_\mathrm{f}}, \tag{1.116}$$

where ρ_p is the density of particles, d_p the diameter and μ_f the fluid dynamic viscosity. This characteristic time is related to the particle inertia and form drag. Above the Stokes regime, t_p depends on the particle Reynolds number Re_p defined in terms of the relative velocity between the particle and the fluid $\mathbf{u}_{\mathrm{f}p}$

$$Re_\mathrm{p} = \frac{\rho_\mathrm{f} d_\mathrm{p}(\mathbf{u}-\mathbf{v})}{\mu_\mathrm{f}} = \frac{\rho_\mathrm{f} d_\mathrm{p}\mathbf{u}_{\mathrm{f}p}}{\mu_\mathrm{f}}. \tag{1.117}$$

Thus, for $Re_\mathrm{p} > 1$ t_p is defined as

$$t_\mathrm{p} = \frac{4\rho_\mathrm{p} d_\mathrm{p}}{3\rho_\mathrm{f} C_D \mathbf{u}_{\mathrm{f}p}}, \tag{1.118}$$

where $C_D = C_D(Re_\mathrm{p})$ is the drag coefficient of the particle. As the particle is transported by the mean flow and dispersed by the turbulence, scales for both of them are required. The mean flow can be scaled by a mean characteristic velocity U and a characteristic length scale L. The Stokes number, defined by

$$St = \frac{t_\mathrm{p} U}{L}, \tag{1.119}$$

gives the ratio of the hydrodynamic response time to the time scale of the mean flow. It thus indicates how well the particle can respond to the mean flow.

To describe the dispersion by the turbulence both Lagrangian and Eulerian scales of turbulence are required as the dispersion of small neutrally buoyant particles is governed by the Lagrangian scales and the dispersion of large heavy particles is dominated by the Eulerian scales. For Eulerian integral time scales, a scale related to the frame moving with the mean flow $\mathrm{T}_{\mathrm{m}E}$ and a scale determined with a fixed frame $\mathrm{T}_{\mathrm{f}E}$ exist. The former can be measured and the latter can then be calculated but no device exist for the direct measurement of Lagrangian integral scales T_L. The response of the particles to turbulence is commonly expressed by a Stokes number in which $\mathrm{T}_{\mathrm{m}E}$ is used as the fluid time scale

$$St = \frac{t_\mathrm{p}}{\mathrm{T}_{\mathrm{m}E}}. \tag{1.120}$$

The importance of the Stokes number and the above parameters can be demonstrated by expressing the equation of motion of a single particle Eqn. (1.109) in non-dimensional form

$$\frac{\mathrm{d}\mathbf{v}^+}{\mathrm{d}t^+} = \frac{(\mathbf{u}^+ - \mathbf{v}^+)f}{St} - \frac{\gamma\delta_{i3}}{St}. \tag{1.121}$$

In Eqn. (1.121), for the purpose of simplicity, only the first and the fifth terms corresponding to form drag and buoyancy have been retained. In addition, the parameter f expresses the ratio of the form drag to the Stokes

drag and the gravitational field has been assumed to point in the negative x_3 direction. As characteristic values, $\sqrt{\langle \delta u^2 \rangle}$ for velocity, $\mathrm{T_m}_E$ for time and $\sqrt{\langle \delta u^2 \rangle}\,\mathrm{T_m}_E$ for length have been used.

Particles of different material than the surrounding fluid do not follow equivalent paths with the fluid. This means that the knowledge of the Lagrangian temporal correlation of velocities for the fluid is not adequate but the corresponding fluid-particle correlation (tensor) is required. Here, the possibilities for theoretical treatment are limited on only a few special cases.

If the properties of the particles are close to that of the fluid, it can be assumed that a given particle stays inside the same turbulent eddy for the entire life time of the eddy. This condition can also be stated in the form that the particles essentially stay in the highly correlated part of the flow and, consequently, their dispersion follows that of the fluid. For this case the motion of the particle can be approximated by the linearized form of the equation of motion of the particle, *i.e.*, the Tchen's solution [Tch47], discussed in section 1.6.5. A new theoretical problem, called 'the preferential concentration of particles' [EF94], is raised with these almost neutrally buoyant particles. That indicates a condition where the particles are not randomly distributed in the fluid but become concentrated on certain areas of the turbulent structures.

If, instead, particles have a notable relative speed with respect to the surrounding fluid, the particle will leave the eddy before the eddy decays. Such condition is typically found in gas-particle systems and in the presence of strong external force field. As a consequence of this 'effect of crossing trajectories', the particles rapidly loose their velocity correlation to the fluid. This effect can also lead to strongly unisotropic dispersion. On the other hand, in many engineering problems of particulate flows the dispersion is mainly limited by this effect and, consequently, the difficulties related to more detailed description of turbulence and preferential concentration of particles can be avoided. The effect of crossing trajectories is further discussed in section 1.6.5 based on the work of Csanady [Csa63b, Csa63a].

The theoretical treatment of particle dispersion rests, in general, on the assumption of stationary and homogeneous turbulence field. The fundamental work concerning the statistical diffusion of fluid points was made by Taylor [Tay21] and later generalized by Batchelor [Bat53]. This formalism can be directly applied to the dispersion of particles as well. When Brownian motion is neglected as compared to turbulent contribution, the random continuous motion of a single particle is defined by the mean square displacement tensor over an ensemble of realizations of the system

$$\langle y_{L,i}\, y_{L,j}(t) \rangle = \sqrt{\langle v^2_{L,(i)} \rangle \, \langle v^2_{L,(j)} \rangle} \int_0^t \int_0^{t'} \{ \mathrm{R}_{L\mathrm{p},ij}(\tau) + \quad \mathrm{R}_{L\mathrm{p},ji}(\tau) \} \mathrm{d}\tau \, \mathrm{d}t'$$

$$= \sqrt{\langle v_{L,(i)}^2 \rangle \ \langle v_{L,(j)}^2 \rangle} \int_0^t (t-\tau)\{\mathrm{R}_{Lp,ij}(\tau) + \mathrm{R}_{Lp,ji}(\tau)\}\mathrm{d}\tau, \tag{1.122}$$

where y_L stands for the location of the particle in reference to the coordinate system moving with the mean particle velocity (Lagrangian coordinate system) and v_L the instantaneous Lagrangian velocity of the particle. Here, parentheses around the subscript are used to note that the Einstein summation convention must not be used. The latter equality sign holds for the stationary and homogenous field under study. Further, the Lagrangian temporal correlation tensor for particle velocities is defined as

$$\mathrm{R}_{Lp,ij}(\tau) = \frac{\langle v_{L,i}(0)\, v_{L,j}(\tau)\rangle}{\sqrt{\langle v_{L,(i)}^2 \rangle \ \langle v_{L,(j)}^2 \rangle}}\,. \tag{1.123}$$

By denoting the symmetric part of $\mathrm{R}_{Lp,ij}(\tau)$ as

$$\mathrm{R}^{\mathrm{S}}_{Lp,ij}(\tau) = \frac{1}{2}\{\mathrm{R}_{Lp,ij}(\tau) + \mathrm{R}_{Lp,ji}(\tau)\}\,, \tag{1.124}$$

the mean square displacement tensor can be expressed by

$$\langle y_{L,i}\, y_{L,j}(t)\rangle = 2\sqrt{\langle v_{L,(i)}^2 \rangle \ \langle v_{L,(j)}^2 \rangle} \int_0^t (t-\tau)\mathrm{R}^{\mathrm{S}}_{Lp,ij}(\tau)\ \mathrm{d}\tau\,. \tag{1.125}$$

Since the Lagrangian temporal correlation tensor $\mathrm{R}_{Lp,ij}(\tau)$ and the power spectral density $\mathrm{E}_{Lp,ij}(\omega)$ are Fourier transform pairs of each other [TL72]

$$\mathrm{R}_{Lp,ij}(\tau) = \int_{-\infty}^{\infty} \mathrm{E}_{Lp,ij}(\omega)\exp(-i\omega\tau)\mathrm{d}\omega\,, \tag{1.126}$$

where ω corresponds to the frequency of a temporal harmonic oscillation into which the motion of the particle is decomposed, it is possible to transform Eqn. (1.125) into the form

$$\begin{aligned}\langle y_{L,i}\, y_{L,j}(t)\rangle &= 2\sqrt{\langle v_{L,(i)}^2 \rangle \ \langle v_{L,(j)}^2 \rangle} \int_0^t (t-\tau) \int_0^{\infty} \mathrm{E}^{\mathrm{S}}_{Lp,ij}(\omega)\cos(\omega\tau)\ \mathrm{d}\omega\,\mathrm{d}\tau \\ &= \sqrt{\langle v_{L,(i)}^2 \rangle \ \langle v_{L,(j)}^2 \rangle} \int_0^{\infty} \mathrm{E}^{\mathrm{S}}_{Lp,ij}(\omega)\frac{2(1-\cos\omega t)}{\omega^2}\ \mathrm{d}\omega\,. \end{aligned} \tag{1.127}$$

To calculate $\langle y_{L,i}\, y_{L,j}(t)\rangle$ by Eqn. (1.125) or by Eqn. (1.127) the relationship either between $\mathrm{R}_{Lf,ij}(\tau)$ and $\mathrm{R}_{Lp,ij}(\tau)$ or between $\mathrm{E}_{Lf,ij}(\omega)$ and $\mathrm{E}_{Lp,ij}(\omega)$ is needed. The direct relation between the Lagrangian temporal correlation tensors of the fluid and of the particle is very complicated, in general. Some approximate solutions are, however, available for the relation between the two power spectral densities [TL72].

The classical dispersion tensor for a cloud of particles can now be defined as

$$\begin{aligned} \mathrm{D}_{\mathrm{p},ij} &= \frac{1}{2}\frac{\mathrm{d}}{\mathrm{d}t}\left\{\langle y_{L,i}\, y_{L,j}(t)\rangle\right\} \\ &= \sqrt{\langle v^2_{L,(i)}\rangle\ \langle v^2_{L,(j)}\rangle}\int_0^\infty \mathrm{E}^{\mathrm{S}}_{L\mathrm{p},ij}(\omega)\frac{\sin\omega t}{\omega}\ \mathrm{d}\omega\,. \end{aligned} \tag{1.128}$$

The above analysis has been carried out with ensemble averages as is appropriate in the general theory of random processes. However, as the analysis concerns only stationary and homogeneous fields the random fluctuations are ergodic [TL72] and, consequently, time averages become identical to ensemble averages for long integration times.

Since it is always possible to use a Cartesian frame of reference where $\mathrm{E}^{\mathrm{S}}_{L\mathrm{f},ij}(\omega)$ and $\mathrm{E}^{\mathrm{S}}_{L\mathrm{p},ij}(\omega)$ (and therefore $\mathrm{R}^{\mathrm{S}}_{L\mathrm{f},ij}(\omega)$ and $\mathrm{R}^{\mathrm{S}}_{L\mathrm{p},ij}(\omega)$) are simultaneously diagonal, the real 3-D problem can be reduced to a combination of three one-dimensional problems without any further loss of generality. Therefore, the following treatment utilizes this finding by concentrating only on a single index for which, *e.g.*, the above correlation tensors and power spectral densities are denoted as $\mathrm{R}_{L\mathrm{f}}(\omega)$, $\mathrm{R}_{L\mathrm{p}}(\omega)$, $\mathrm{E}_{L\mathrm{f}}(\omega)$ and $\mathrm{E}_{L\mathrm{p}}(\omega)$.

Thus, in order to calculate the mean square displacement, the rms fluctuating velocities of particles and the Lagrangian temporal correlation tensor must be known. Of these two quantities, the latter poses the main difficulty. Even for fluid particles this correlation tensor is not generally known as there is no device available that would be capable of following the tracked particle and directly measuring it's velocity. Measurement systems commonly utilize fixed Eulerian coordinate system, and consequently, produce data from which Eulerian correlations of velocities can be determined. Unfortunately, no simple relation between these two types of correlation tensor exist, except in the case of stationary homogeneous fields.

Eddy interaction model

The 'eddy interaction model' is a customary approach to calculate (or more accurately, numerically simulate) turbulent dispersion in the Lagrangian approach. It's original version is based on the discrete eddy velocity specification and constant characteristic scales of eddies throughout the flow field [HHD71, BH79]. Later on this approach was extended to complex flows by defining the eddy scales from the turbulent statistics available from the turbulence model used within the carrier fluid. A large number of articles on this approach exist, *e.g.*, [GI81a, Fae83, WBAS84, GHN89, SAW92]. It is also utilized in several commercial flow simulation codes. In the eddy interaction model, the particle motion is determined by the interaction of a particle with a succession of turbulent eddies in which the velocity is kept constant within a finite volume, characterized by the length and time scales

of the eddy. The attraction of this model lies in its conceptual simplicity and in that the only statistics required is given by the characteristic scales of velocity, time and length. In the alternative models the forms of either the temporal Lagrangian or the spatial Eulerian velocity autocorrelation functions are required [BDG90, BB93, LFA93].

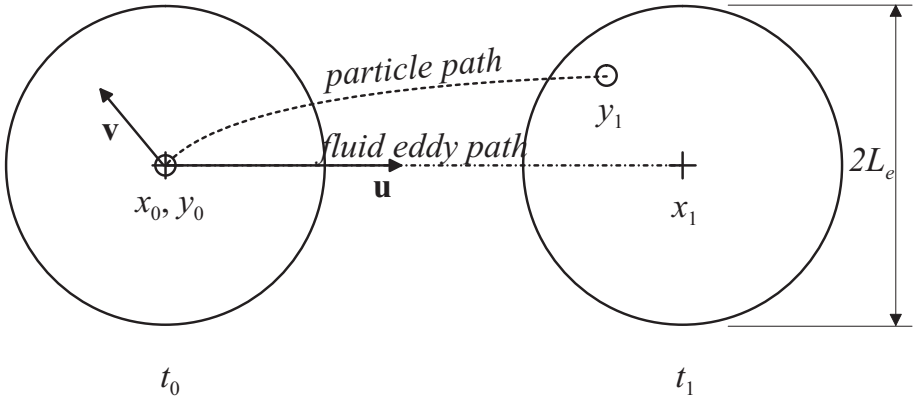

Figure 1.3: Illustration of the eddy interaction model and related parameters.

An illustration of the eddy interaction model and related properties is shown in Fig. 1.3. At initial time t_0, the particle resides at the center of the fluid eddy located at $\mathbf{x}_0$, *i.e.*, $\mathbf{y}_0 = \mathbf{x}_0$. At some later time t_1, the fluid eddy has traveled to a new location $\mathbf{x}_1 = \mathbf{x}_0 + t_1\mathbf{u} = \mathbf{x}_0 + t_1(\overline{\mathbf{u}} + \delta\mathbf{u})$. Because of the velocity difference between the fluid eddy and the particle, their paths are not identical but the particle will be found at $\mathbf{y}_1 = \mathbf{x}_0 + t_1(\mathbf{u} + \mathbf{v})$. The distance between the center of the eddy and the particle is therefore $(\mathbf{y}_1 - \mathbf{x}_1) = t_1\mathbf{v}$. The particle remains under the influence of the current eddy of size L_e until either the life time of the turbulent eddy T_e is exceeded, or it travels out of the eddy due to the velocity difference within an interaction time T_i (the effect of crossing trajectories). When either of these conditions is satisfied, a new eddy is generated and the process is repeated.

For Stokesian drag and negligible contributions from fluid pressure gradient, added mass and Basset history terms, it is possible to derive analytical expressions for the particle velocity and position at the end of interaction with an eddy. For that purpose it is assumed that the particle enters the eddy at x_0 with velocity of v_0. The fluid velocity U_e within the eddy is constant over the interaction time T_i. The equation of motion of the particle is now given by

$$\frac{d}{dt}(v(t)) = \frac{\mathrm{U}_e - v(t)}{t_p}\,, \tag{1.129}$$

where, as before, t_p is the particle hydrodynamic response (relaxation) time, Eqn. (1.116). Solving this equation gives the updated particle velocity after the interaction with the eddy as

$$v_1 = \mathrm{U}_e - (\mathrm{U}_e - v_0)\exp(-\mathrm{T}_i/t_p). \tag{1.130}$$

The updated position of the particle is then given by

$$\begin{aligned} x(t) &= x_0 + \int_0^t v(t')\mathrm{d}t' && (1.131)\\ &= (x_0 + \mathrm{T}_i\mathrm{U}_e) - (\mathrm{U}_e - v_0)t_p(1 - \exp(-\mathrm{T}_i/t_p))\,. && (1.132) \end{aligned}$$

The particle crossing time T_c is defined by the equation $\mid x(\mathrm{T}_c) - x_0 - \mathrm{T}_c\mathrm{U}_e \mid = \mathrm{L}_e$. The solution is given by

$$\mathrm{T}_c = -t_p \log(1 - \frac{\mathrm{L}_e}{\mid V_{\mathrm{fp}} \mid t_p})\,, \tag{1.133}$$

where $V_{\mathrm{fp}} = \mathrm{U}_e - v_0$ is the fluid-particle relative velocity. This expression is valid only if $\mathrm{L}_e/(V_{\mathrm{fp}}t_p) < 1$, and then T_i is set equal to T_c. If this inequality does not hold, *i.e.*, the particle stays inside the eddy, the interaction time T_i is set equal to the eddy life time T_e. Because the interaction time can be determined prior to the interaction, only one integration per eddy is required.

In the case of small relaxation time t_p, the particles are almost always captured by the eddies. The interaction time will thus be equal to the eddy life time and the particle velocity will quickly approach the fluid velocity. Then, in the context of eddy interaction model, the dispersion of particles will be similar to the dispersion of fluid points. For large relaxation times the interaction time is more often set by the particle crossing time and, consequently, fluid-particle interaction will be almost independent of the eddy life time.

As emphasized above the key problem of the eddy interaction model is to find the appropriate scales for the velocity, time and length of the eddies. In general, these scales are random variables and should be given by the statistical properties of fluid turbulence available from the applied turbulence model or from experimental data. Thus, the components of, *e.g*, eddy velocity can be randomly sampled from a Gaussian velocity distribution with a zero mean and standard deviation $\sqrt{\langle \delta u^2 \rangle} = \sqrt{\frac{2}{3}k}$, where k is the kinetic energy of fluid turbulence.

The eddy life time (life time distribution) can be related to the Lagrangian integral time scale of fluid turbulence, given by

$$\mathrm{T}_{L\mathrm{f}} = \int_0^\infty \mathrm{R}_{L\mathrm{f}}(\tau)\,\mathrm{d}\tau, \tag{1.134}$$

where

$$\mathrm{R}_{Lf}(t,\tau) = \frac{\langle u_L(t)\, u_L(t+\tau)\rangle}{\langle u_L^2(t)\rangle} \tag{1.135}$$

is the Lagrangian temporal correlation tensor of fluid.

In a stationary turbulence R_{Lf} is independent of time, *i.e.*, $\mathrm{R}_{Lf}(t,\tau) = \mathrm{R}_{Lf}(\tau)$. Assuming that eddy life times t_e are distributed according to a probability distribution function $f(\mathrm{t}_e)$, we can write the Lagrangian temporal correlation in the form [WS92]

$$\mathrm{R}_{Lf}(\tau) = \frac{\int_\tau^\infty (\mathrm{t}_e - \tau) f(\mathrm{t}_e)\, \mathrm{dt}_e}{\int_0^\infty \mathrm{t}_e f(\mathrm{t}_e)\, \mathrm{dt}_e}\,. \tag{1.136}$$

The most simple choice for the eddy life time distribution is the delta function $f(\mathrm{t}_e) = \delta(\mathrm{t}_e - \mathrm{T}_e)$, which corresponds to a constant eddy life time T_e [HHD71, BH79, JHW80, WAW82, GI81a, GHN89]. The Lagrangian temporal correlation then assumes the form

$$\mathrm{R}_{Lf}(\tau) = \begin{cases} 1 - \tau/\mathrm{T}_e & ,\tau \le \mathrm{T}_e \\ 0 & ,\tau > \mathrm{T}_e \end{cases}\,. \tag{1.137}$$

Using Eqn. 1.134, we then obtain the required correlation within the constant life time scheme as.

$$\mathrm{T}_e = 2\mathrm{T}_{Lf}. \tag{1.138}$$

Another assumption that has been used in the context of eddy interaction simulations [KR89] is the exponential distribution of life times, *i.e.*, $f(\mathrm{t}_e) = \exp(-\mathrm{t}_e/\mathrm{T}_m)/\mathrm{T}_m$, where T_m is the mean life time. In this case, the Lagrangian temporal correlation is given by

$$\mathrm{R}_{Lf}(\tau) = \exp\left(-\tau/\mathrm{T}_m\right). \tag{1.139}$$

Using Eqn. 1.134 we now obtain

$$\mathrm{T}_m = \mathrm{T}_{Lf}, \tag{1.140}$$

which again correlates the eddy life time distribution with the appropriate turbulent time scale within the exponential distribution scheme.

Notice, that for the eddy interaction model it has been shown [GJ96], that the mean eddy life time T_m is subject to the general constraint that $\mathrm{T}_{Lf} \le \mathrm{T}_m \le 2\mathrm{T}_{Lf}$. The two simple schemes discussed above thus correspond to the limiting cases allowed by this inequality. As the number of samples that are required for adequate prediction of particle dispersion in eddy interaction models depends on the mean eddy life time and, therefore, on the selected life time distribution, the constant eddy life time scheme requires the lowest, and the exponential scheme the highest number of samples of all the admissible distributions. Furthermore, to enable a realistic

statistical configuration of particles at the initial time $t = t_0$, *i.e.*, at the moment of particle release, the life time of the first eddy in constant life time scheme has to be randomly distributed according to a uniform distribution $f_0(\mathrm{t}_e) = 1/\mathrm{T}_e$, $0 < \tau < \mathrm{T}_e$ [GJ96]. Within the exponential scheme instead, a realistic configuration of particles at the initial time is automatically generated.

For large slip velocity V_{fp}, the eddy size distribution can be related to the Eulerian integral size scale of fluid turbulence (similarly with the eddy life time discussed above). This size scale is defined by

$$\mathrm{L}_{E\mathrm{f}} = \int_0^\infty \mathrm{R}_{E\mathrm{f}}(\lambda, 0)\, d\lambda, \tag{1.141}$$

where

$$\mathrm{R}_{E\mathrm{f}}(\lambda, \tau) = \frac{\langle u(x,t)u(x+\lambda, t+\tau)\rangle}{\langle u^2(x,t)\rangle} \tag{1.142}$$

is the Eulerian fluid velocity autocorrelation function. (In a general case, a much more complex Lagrangian correlation of fluid along the particle path and a corresponding Lagrangian scale should be used [Csa63b, Csa63a].) Analogously with the eddy life time distribution, this autocorrelation function can be expressed in terms of eddy size distribution $g(\mathrm{l}_e)$. Assuming constant eddy length L_e [HHD71] corresponds to $g(\mathrm{l}_e) = \delta(\mathrm{l}_e - L_e)$ and, in the case of stationary turbulence, gives the autocorrelation function of the form

$$\mathrm{R}_{E\mathrm{f}}(\lambda) = \begin{cases} 1 - \lambda/\mathrm{L}_e & , \lambda \le \mathrm{L}_e \\ 0 & , \lambda > \mathrm{L}_e \end{cases} . \tag{1.143}$$

Using Eqn. (1.141) then gives the result $\mathrm{L}_e = 2\mathrm{L}_{E\mathrm{f}}$. In general, the length scale can be taken to be a random variable with a given distribution function. An exponential probability distribution, *e.g.*, gives results completely analogous to Eqns. (1.139) and (1.140) [BM90].

Another possibility for finding the relevant time and length scales is given by the widely used model of Gosman and Ioannides [GI81a]. Within that model it is assumed that the eddy time and length scales are related to the 'dissipation scales' L_ϵ and T_ϵ, given by

$$\mathrm{L}_\epsilon = C_\mu^{3/4} \frac{k^{3/2}}{\epsilon} \quad \text{and} \quad \mathrm{T}_\epsilon = \sqrt{3/2}\, C_\mu^{3/4} \frac{k}{\epsilon}\,, \tag{1.144}$$

where k is the kinetic energy of turbulence, ϵ its rate of dissipation and C_μ is the constant that appears in definition of eddy viscosity $\mu_{\mathrm{T}} = \rho C_\mu k^2/\epsilon$ in the standard $k - \epsilon$ turbulence model.

Notice, however, that even though we may assume the eddy life time T_e and size L_e to be proportional to the corresponding statistical scales given above, the actual relation depends on the details of the underlying statistical model.

1.6 Practical closure approaches

In this section we shall give more detailed examples of constitutive relations for selected systems. The constitutive relations given here finally render the general flow equations for a given multiphase system derived in section 1.2.2 in a closed form amenable for numerical solution (see Chapter 2 below). The final equations derived here may not however be generally valid for all such systems and should merely be taken as examples of plausible constitutive models that may be used for that particular type of systems. One should also bear in mind that the existing models in particular for turbulence in multiphase flows still lack generality and can be considered inadequate to some extent. For the sake of reliability of the model it is thus essential that the values of various material parameters, that are left unspecified in the constitutive relations, are determined by independent measurements in conditions that closely resemble those of the actual application. It is also essential that the numerical solution is verified experimentally.

1.6.1 Dilute liquid-particle suspension

As a starting point, we use the Eqns. (1.37) through (1.41) derived in section 1.2.2. We thus have eight equations for the eight unknowns which can be taken to be the volume fraction of the fluid ϕ, fluid pressure $\tilde{p}_\mathrm{f}$ and the three components of both the velocities $\bar{\mathbf{u}}_\mathrm{f}$ and $\bar{\mathbf{u}}_\mathrm{d}$. It remains to specify the constitutive relations for the viscous stress tensor of the fluid $\langle\tau_\mathrm{f}\rangle$, the total stress tensor of the particulate phase $\langle\sigma_\mathrm{d}\rangle$, the momentum transfer integral $\mathbf{D}$, and the turbulent stresses $\tau_{\delta\mathrm{d}}$ and $\tau_{\delta\mathrm{f}}$.

The constitutive relation for the viscous stress tensor of the fluid $\langle\tau_\mathrm{f}\rangle$ can be derived simply by performing the volume averaging of the mesoscopic tensor $\tau_\mathrm{f} = \mu_\mathrm{f}((\nabla\mathbf{u}_\mathrm{f}) + (\nabla\mathbf{u}_\mathrm{f})^t)$ and using Eqn. (1.14). We define the averaged surface velocity of the fluid $\bar{\mathbf{U}}_\mathrm{S}$ by

$$\frac{1}{V}\int_{A_\mathrm{f}} \mathbf{u}_\mathrm{f}\hat{\mathbf{n}}_\mathrm{f}\, dA = \bar{\mathbf{U}}_\mathrm{S}\frac{1}{V}\int_{A_\mathrm{f}} \hat{\mathbf{n}}_\mathrm{f}\, dA = -\bar{\mathbf{U}}_\mathrm{S}\nabla\phi, \tag{1.145}$$

and postulate that $\bar{\mathbf{U}}_\mathrm{S} = b\bar{\mathbf{u}}_\mathrm{d} - (1-b)\bar{\mathbf{u}}_\mathrm{f}$, where $b = b(\phi)$ is a free parameter (the 'mobility' of the dispersed phase) which aquires values between 0 and 1. It is then easy to see that the viscous stress tensor of the fluid can be given by

$$\begin{aligned}\langle\tau_\mathrm{f}\rangle &= \phi\tilde{\tau}_\mathrm{f} \\ &= \phi\mu_\mathrm{f}[(\nabla\bar{\mathbf{u}}_\mathrm{f}) + (\nabla\bar{\mathbf{u}}_\mathrm{f})^t] \\ &\quad -b\mu_\mathrm{f}[(\nabla\phi)(\bar{\mathbf{u}}_\mathrm{d} - \bar{\mathbf{u}}_\mathrm{f}) + (\bar{\mathbf{u}}_\mathrm{d} - \bar{\mathbf{u}}_\mathrm{f})(\nabla\phi)].\end{aligned} \tag{1.146}$$

For a very dilute liquid-particle suspension where the collisions between particles can be ignored, the stress state of the particles is determined by the

hydrodynamic forces exerted on the surface of the particles by the surrounding fluid. If the velocity difference between the particles and the fluid is not very high, we may approximate

$$\langle \sigma_{\mathrm{d}} \rangle = -(1-\phi)\tilde{\sigma}_{\mathrm{d}} \approx -(1-\phi)\tilde{p}_{\mathrm{f}} \mathbb{1}. \tag{1.147}$$

The term $\nabla \cdot \langle \sigma_{\mathrm{d}} \rangle - \tilde{p}_{\mathrm{f}} \nabla \phi$ on the right side of Eqn. (1.41) is now reduced to $-(1-\phi)\nabla \tilde{p}_{\mathrm{f}}$. For a dense suspension instead, the tensor $\langle \sigma_{\mathrm{d}} \rangle$ is contributed by particle particle collisions and may have a very complicated form which we do not consider here (see [Hwa89] and references therein).

According to Eqn. (1.36), the transfer integral $\mathbf{D}$ is the force per unit volume acting on particles due to fluctuations of fluid pressure and due to viscous stresses. From the standard fluid mechanics we know that specific hydrodynamic forces act on particles that move through the fluid with constant velocity, with acceleration or with superimposed linear motion and rotation. In principle, the forces acting on such a particle (with low particle Reynolds number) are specified by the BBO equation, Eqn. (1.109) or Eqn. (1.111). Thus, the transfer integral should contain a contribution from all the force terms that appear on the right side of that equation - *except* of the terms that arise from gravitational force and from the fluid pressure gradient, since these effects are already included in Eqns. (1.39) and (1.41)! For a dilute suspension where particles can be considered independent of each other, the terms in $\mathbf{D}$ corresponding to various terms in the selected version of the BBO equation can be derived in a rather straightforward manner. For example, neglegting the effects of fluid velocity gradient, and taking into account only the Stokes drag force and the added mass term (which arises since accelerating a particle immersed in a fluid accelerates an amount of fluid around the particle as well), we may write

$$\mathbf{D} = B(\bar{\mathbf{u}}_{\mathrm{d}} - \bar{\mathbf{u}}_{\mathrm{f}}) + C\Big[(\frac{\partial}{\partial t}(\bar{\mathbf{u}}_{\mathrm{d}} - \bar{\mathbf{u}}_{\mathrm{f}}) + (\bar{\mathbf{u}}_{\mathrm{d}} - \bar{\mathbf{u}}_{\mathrm{f}}) \cdot \nabla(\bar{\mathbf{u}}_{\mathrm{d}} - \bar{\mathbf{u}}_{\mathrm{f}})\Big], \tag{1.148}$$

where B and C are unknown but perhaps measurable parameters. For a very dilute suspension of spherical particles of radius r_{p} and for low particle Reynolds numbers, Eqn. (1.109) suggest that

$$B = \frac{9\mu_{\mathrm{f}}}{2r_{\mathrm{p}}^2}(1-\phi) \tag{1.149}$$

$$C = \frac{1}{2}\tilde{\rho}_{\mathrm{f}}(1-\phi). \tag{1.150}$$

Many other interaction mechanisms than those included in Eqn. (1.148) may be crucial in practical flows of fluid-particle suspensions [Dre83]. For instance if a particle is rotating, moving in the presence of a strong velocity gradient of the fluid or, especially, if the particle is moving near a solid wall, it may experience a 'lift' or 'side' force which is perpendicular to its direction

of relative motion with respect to the fluid. A particle moving in a fluid may also experience hydrodynamic forces which depend on the previous history of its motion. This effect is taken into account in the BBO equation through the Basset history term which may become important for instance in the case of fast oscillatory motions (see [Soo90] and references therein).

The tensors $\langle \tau_{\delta \mathrm{f}} \rangle$ and $\langle \tau_{\delta \mathrm{d}} \rangle$ contain the momentum transfer due to turbulent and "pseudo-turbulent" fluctuations of the two phases. Various models have been proposed for these quantities which are analogous to the ordinary Reynold's stresses in single phase flows. The constitutive relations suggested by Drew and Lahey are [DLJ92]

$$\begin{aligned} \langle \tau_{\delta \mathrm{f}} \rangle &= -\phi p_{\mathrm{f}}^T \mathbb{1} + 2\mu_{\mathrm{ff}}^T \mathbf{\Pi}_{\mathrm{f}} + 2\mu_{\mathrm{fd}}^T \mathbf{\Pi}_{\mathrm{d}} \\ &\quad + (1-\phi)\rho_{\mathrm{f}} [a_{\mathrm{f}} |\bar{\mathbf{u}}_{\mathrm{f}} - \bar{\mathbf{u}}_{\mathrm{d}}|^2 \mathbb{1} + b_{\mathrm{f}} (\bar{\mathbf{u}}_{\mathrm{f}} - \bar{\mathbf{u}}_{\mathrm{d}})(\bar{\mathbf{u}}_{\mathrm{f}} - \bar{\mathbf{u}}_{\mathrm{d}})] \quad (1.151) \end{aligned}$$

$$\begin{aligned} \langle \tau_{\delta \mathrm{d}} \rangle &= -(1-\phi) p_{\mathrm{d}}^T \mathbb{1} + 2\mu_{\mathrm{dd}}^T \mathbf{\Pi}_{\mathrm{d}} + 2\mu_{\mathrm{df}}^T \mathbf{\Pi}_{\mathrm{f}} \\ &\quad + (1-\phi)\rho_{\mathrm{d}} [a_{\mathrm{d}} |\bar{\mathbf{u}}_{\mathrm{f}} - \bar{\mathbf{u}}_{\mathrm{d}}|^2 \mathbb{1} + b_{\mathrm{d}} (\bar{\mathbf{u}}_{\mathrm{f}} - \bar{\mathbf{u}}_{\mathrm{d}})(\bar{\mathbf{u}}_{\mathrm{f}} - \bar{\mathbf{u}}_{\mathrm{d}})], \quad (1.152) \end{aligned}$$

where $\mathbf{\Pi}_\alpha = \frac{1}{2}[(\nabla \bar{\mathbf{u}}_\alpha) + (\nabla \bar{\mathbf{u}}_\alpha)^t]$ for $\alpha = \mathrm{f}, \mathrm{d}$. The turbulent pressures p_α^T, the eddy viscosities $\mu_{\alpha\beta}^T$ and the coefficients a_α and b_α are still to be correlated with appropriate variables that characterise the turbulent and pseudoturbulent motion of the phases. This might be accomplished through experiments or through additional turbulence modelling [CTC96]. Here, we shall consider a simple generalization of the ordinary $k-\epsilon$ model for onephase flows.

In this illustrative multiphase version or the $k-\varepsilon$ model we ignore all the other terms on the right side of Eqns. (1.151) and (1.152) than those proportional to the eddy viscosities μ_{ff}^T and μ_{dd}^T. We also assume that the eddy viscosity hypothesis holds for each individual phase. Thus we can define the eddy viscosity for phase α in analogy with single phase flows as

$$\mu_{\alpha\alpha}^T = C_\mu \tilde{\rho}_\alpha \frac{k_\alpha^2}{\varepsilon_\alpha}, \quad (1.153)$$

where k_α and ε_α are the turbulent kinetic energy and the dissipation for phase α, respectively, and C_μ is an empirical constant. The transport equations for k_α and ε_α are postulated to have the form

$$\begin{aligned} &\frac{\partial}{\partial t}(\phi_\alpha \tilde{\rho}_\alpha k_\alpha) + \nabla \cdot (\phi_\alpha \tilde{\rho}_\alpha \bar{\mathbf{u}}_\alpha k_\alpha) - \nabla \cdot [\phi_\alpha (\mu_\alpha + \frac{\mu_{\alpha\alpha}^T}{\sigma_k}) \nabla k_\alpha] \\ &\quad = \phi_\alpha S_{k\alpha} + \Gamma_{k\alpha} \quad (1.154) \\ &\frac{\partial}{\partial t}(\phi_\alpha \tilde{\rho}_\alpha \varepsilon_\alpha) + \nabla \cdot (\phi_\alpha \tilde{\rho}_\alpha \bar{\mathbf{u}}_\alpha \varepsilon_\alpha) - \nabla \cdot [\phi_\alpha (\mu_\alpha + \frac{\mu_{\alpha\alpha}^T}{\sigma_\varepsilon}) \nabla \varepsilon_\alpha] \\ &\quad = \phi_\alpha S_{\varepsilon\alpha} + \Gamma_{\varepsilon\alpha}. \quad (1.155) \end{aligned}$$

Analogously with single phase flows the source terms are divided into production and dissipation terms as follows

$$S_{k\alpha} = P_\alpha - \tilde{\rho}_\alpha \varepsilon_\alpha \tag{1.156}$$

$$S_{\varepsilon\alpha} = \frac{\varepsilon_\alpha}{k_\alpha}(C_{1\varepsilon} P_\alpha - C_{2\varepsilon}\tilde{\rho}_\alpha \varepsilon_\alpha) \tag{1.157}$$

$$P_\alpha = \mu^T_{\alpha\alpha} \nabla \bar{\mathbf{u}}_\alpha \cdot [\nabla \bar{\mathbf{u}}_\alpha + (\nabla \bar{\mathbf{u}}_\alpha)^t]. \tag{1.158}$$

Interphasial turbulence exchange terms $\Gamma_{k\alpha}, \Gamma_{\varepsilon\alpha}$ must be defined separately for each case. Assuming that the turbulence quantities are equal for both phases, *i.e.*, that $k_\alpha \equiv k$ and $\varepsilon_\alpha = \varepsilon$ for all $\alpha = \mathrm{f}, \mathrm{d}$, and summing the above transport equations, we get

$$\frac{\partial}{\partial t}(\rho k) + \nabla \cdot [\rho \bar{\mathbf{u}} k - (\mu + \frac{\mu^T}{\sigma_k}\nabla k)] = S_k \tag{1.159}$$

$$\frac{\partial}{\partial t}(\rho \varepsilon) + \nabla \cdot [\rho \bar{\mathbf{u}} \varepsilon - (\mu + \frac{\mu^T}{\sigma_\varepsilon}\nabla \varepsilon)] = S_\varepsilon, \tag{1.160}$$

where

$$\rho = \sum_\alpha \phi_\alpha \tilde{\rho}_\alpha \tag{1.161}$$

$$\bar{\mathbf{u}} = \frac{1}{\rho}(\sum_\alpha \phi_\alpha \tilde{\rho}_\alpha \bar{\mathbf{u}}_\alpha) \tag{1.162}$$

$$\mu = \sum_\alpha \phi_\alpha \mu_\alpha \tag{1.163}$$

$$\mu^T = \sum_\alpha \phi_\alpha \mu^T_{\alpha\alpha} \tag{1.164}$$

$$S_k = \sum_\alpha \phi_\alpha S_{k\alpha} \tag{1.165}$$

$$S_\varepsilon = \sum_\alpha \phi_\alpha S_{\varepsilon\alpha}. \tag{1.166}$$

1.6.2 Flow in a porous medium

Most porous materials of practical interest consist either of particles packed in a more or less distordered manner or of a consolidated irregular porous structure of some kind. Examples of such materials are numerous: sand, soil, fractured rock, ceramics, sponge, paper *etc.* Many important processes found in geophysics or in various industrial applications involve flow of fluid through a porous medium. In some cases, such as in slow transport of ground water through an aquifer, the porous material can be considered rigid so that the structure of the solid matrix is not significantly deformed during the process. The basic equation for such a flow is given by the famous Darcy's law, which was originally inferred from purely empirical results for a

stationary creeping flow of Newtonian liquid through a homogeneous column of sand [Bea72]. With processes such as removal of water from a sponge by squeezing it, the porous structure appears soft and may thus be extensively deformed by external forces and by hydrodynamical forces exerted on the solid matrix by the fluid flow.

In this section, we shall utilize Darcy's experimental formula in the context of the multiphase flow theory and derive the governing equations for time dependent creeping flow of Newtonian liquid through a soft porous medium. Formally, we treate the system of the highly deformable solid matrix and the liquid flowing through the interstities of the matrix as a binary mixture of two fluids. We assume again that both phases are incompressible, that there is no mass transfer between the two phases and that surface tension between the solid material and the liquid is negligible. The situation is thus analogous with the liquid-particle suspension discussed in section (1.2.2). However, instead of a contiunous liquid phase and a dispersed particle phase we now have two continuous phases. Replacing the subscript 'd' for 'dispersed' phase by 's' for 'solid' phase, the Eqns. (1.37) through (1.41) are thus formally valid also for the present system. Several simplifications as compared to the liquid-particle suspension can however be made in this case. Assuming creeping flow indicates that the inertial terms that appear on the left side of Eqns. (1.39) and (1.41) can be neglected. Furthermore, the pseudoturbulent stress term $\nabla \cdot \langle \tau_{\delta \mathrm{d}} \rangle$ vanishes for the solid phase and is expected to be very small also for the fluid phase in this flow regime. According to Darcy's early experiments and to innumerable later experiments, the dominant interaction mechanism in a flow through porous medium is viscous drag. The results of these experiments, as summarized by the Darcy's law, indicate that the momentum transfer integral $\mathbf{D}$ should be written in a form

$$\mathbf{D} = -\frac{\mu}{k}(\bar{\mathbf{u}}_{\mathrm{f}} - \bar{\mathbf{u}}_{\mathrm{s}}). \tag{1.167}$$

Here, $k = k(\phi)$ is the permeability of the porous material which remains to be measured. Several experimental correlations for k has been reported in literature for different types of porous media [Bea72]. Perhaps the most common formula which can be derived analytically for simplified capillary models of porous materials and which at least qualitatively grasps the correct behaviour for many materials, is the Kozeny-Carman relation

$$k = \frac{1}{cS_0^2} \frac{\phi}{(1-\phi)^2}. \tag{1.168}$$

Here, S_0 is the specific pore surface area and c is the dimensionless Kozeny constant which aquires values between 2 and 10, in practice. (Notice that due to the conventions used here, Eqn. (1.168) differs from its more usual form where ϕ^3 instead of ϕ appears in the nominator, see Eqn. (1.177) below.) Furthermore, if the porosity ϕ is not too close to unity, the viscous

shear stress term $\nabla \cdot \langle \tau_{\rm f} \rangle$ is small as compared to the viscous drag term and can be neglected. Taking gravitation to be the only body force, the equations for a flow of liquid in a deformable porous medium can thus be written in a form

$$\frac{\partial}{\partial t}\phi + \nabla \cdot (\phi \bar{\mathbf{u}}_{\rm f}) = 0 \tag{1.169}$$

$$\frac{\partial}{\partial t}(1-\phi) + \nabla \cdot [(1-\phi)\bar{\mathbf{u}}_{\rm s}] = 0 \tag{1.170}$$

$$\phi \nabla \tilde{p}_{\rm f} = -\frac{\mu}{k}(\bar{\mathbf{u}}_{\rm f} - \bar{\mathbf{u}}_{\rm s}) + \phi \tilde{\rho}_{\rm f}\mathbf{g} \tag{1.171}$$

$$-\nabla \cdot \langle \sigma_{\rm s} \rangle = +\frac{\mu}{k}(\bar{\mathbf{u}}_{\rm f} - \bar{\mathbf{u}}_{\rm s}) - \tilde{p}_{\rm f}\,\nabla\phi + (1-\phi)\tilde{\rho}_{\rm s}\mathbf{g}. \tag{1.172}$$

Adding Eqns. (1.169) and (1.170) and Eqns. (1.171) and (1.172) we arrive at the mixture equations

$$\nabla \cdot \langle \mathbf{q} \rangle = 0 \tag{1.173}$$

$$\nabla \cdot \langle \mathbf{T} \rangle = -\langle \rho \rangle \mathbf{g}, \tag{1.174}$$

where $\langle \mathbf{q} \rangle = \phi \bar{\mathbf{u}}_{\rm f} + (1-\phi)\bar{\mathbf{u}}_{\rm s}$ is the volume flux, $\langle \mathbf{T} \rangle = -\phi \tilde{p}_{\rm f} \mathbb{1} + \langle \sigma_{\rm s} \rangle$ is the total stress, and $\langle \rho \rangle = \phi \tilde{\rho}_{\rm f} + (1-\phi)\tilde{\rho}_{\rm s}$ is the density of the mixture.

For linearly elastic materials, the stress tensor $\langle \sigma_{\rm s} \rangle$ is readily given as a function of local strain by Hooke's law. For viscoelastic materials instead, $\langle \sigma_{\rm s} \rangle$ may depend both on the strain and on the rate of strain (*i.e.* on $\bar{\mathbf{u}}_{\rm s}$). Since the solid phase is actually not a fluid in an ordinary sense, a finite stress implies finite strain on the solid matrix. It follows that the velocity of the solid phase can be non-zero only in a transient state. In a stationary state (and in the case of rigid porous material) we have $\bar{\mathbf{u}}_{\rm s} = 0$. The porosity ϕ is then independent of time, and the flow equations are reduced to

$$\nabla \cdot \mathbf{q}_{\rm f} = 0 \tag{1.175}$$

$$\mathbf{q}_{\rm f} = -\frac{\bar{k}}{\mu}(\nabla \tilde{p}_{\rm f} + \tilde{\rho}_{\rm f}\mathbf{g}), \tag{1.176}$$

and one of Eqns. (1.172) or (1.174). Here $\mathbf{q}_{\rm f} = \phi \bar{\mathbf{u}}_{\rm f}$ is the volume flux of the fluid (the 'seepage' velocity), and

$$\bar{k} = \frac{1}{cS_0^2}\frac{\phi^3}{(1-\phi)^2}. \tag{1.177}$$

Eqn. (1.176) is the Darcy's formula in its conventional form.

1.6.3 Dense gas-solid suspensions

The behaviour of solid particles in a dense gas-solid suspension is strongly affected by the binary interparticle collisions. The kinetic theory of granular flow is derived for this special case of twophase flow in analogy with the kinetic theory of dense gases.

A conservation equation (the Bolzmann equation) for the particulate phase is formulated in terms of the single particle velocity distribution function $f^1(\mathbf{x}, \mathbf{u}, t)$

$$\frac{\partial}{\partial t} f^1 + \frac{\partial}{\partial x_i}(u_i f^1) + \frac{\partial}{\partial u_i}(F_i f^1) = \left(\frac{\partial}{\partial t} f^1\right)_{coll} \tag{1.178}$$

where F is the external force per unit of mass acting on a sphere and the right side describes the rate of change of the distribution function due to particle collisions. In the kinetic theory of granular flow the ensemble-average (1.59) of a function $\psi(\mathbf{u})$ is defined by

$$\langle \psi(\mathbf{u}) \rangle = \frac{1}{n_p} \int \psi(\mathbf{u}) f^1(\mathbf{x}, \mathbf{u}, t) du \tag{1.179}$$

where n_p is the number of particles per unit volume. A transport equation for $\langle \psi(\mathbf{u}) \rangle$ can be derived from Eqn. (1.178) by multiplying it by $\psi(\mathbf{u})$ and integrating it over the velocity domain [CC70]:

$$\begin{aligned} \frac{\partial}{\partial t}(n_p \langle \psi \rangle) \quad &+ \quad \frac{\partial}{\partial x_i}(n_p \langle \psi u_i \rangle) \\ &- \quad n_p \left(\left\langle \frac{\partial \psi}{\partial t} \right\rangle + \left\langle u_i \frac{\partial \psi}{\partial x_i} \right\rangle + \left\langle F_i \frac{\partial \psi}{\partial u_i} \right\rangle \right) = C(\psi), \end{aligned} \tag{1.180}$$

where the collisional rate of change for ψ is defined by ([JR85], cited in [Pei98])

$$C(\psi) = \chi(\psi) - \frac{\partial}{\partial x_i}\theta_i(\psi) - \frac{\partial \overline{u}_{s,j}}{\partial x_i}\theta_i \left\langle \frac{\partial \psi}{\partial \delta u_j} \right\rangle \tag{1.181}$$

where $\overline{u}_{s,j}$ is the mean velocity of the discrete phase. Alternative formulations of $C(\psi)$, where the last term is missing, can be found in literature (e.g. [JS83, DG90]). The source term $\chi(\psi)$ describes loss of ψ due to inelastic collisions and $\theta_i(\psi)$ transport of property ψ during collisions. These terms are defined by integrals involving the pair distribution function $f^2(x_1, x_2, u_1, u_2, t)$ and can be calculated analytically. In the derivation, the pair distribution function is given as a product of the single velocity distribution functions and a correction function g_0.

Kinetic theory yields the continuity equation and the momentum equation of a phase in a form similar with the traditional multifluid equations.

The continuity equation is obtained using $\psi = 1$ and the momentum equation by using $\psi = u$. In the resulting equations, the kinetic and collisional contributions of the particulate phase stress are treated together. The isotropic parts are described as a solid pressure and the rest as a shear stress term. In addition to the continuity and the momentum equations, a field equation for the particle fluctuating kinetic energy must be solved. The following formulation can be found, *e.g.*, in [Boe97].

The continuity equation without mass transfer can be written in the form

$$\frac{\partial}{\partial t}(\phi_\alpha \tilde{\rho}_\alpha) + \nabla \cdot (\phi_\alpha \tilde{\rho}_\alpha \bar{\mathbf{u}}_\alpha) = 0. \tag{1.182}$$

Using the notation of total averaged stresses the momentum equations can be written in the form

$$\frac{\partial}{\partial t}(\phi_\alpha \tilde{\rho}_\alpha \bar{\mathbf{u}}_\alpha) + \nabla \cdot (\phi_\alpha \tilde{\rho}_\alpha \bar{\mathbf{u}}_\alpha \bar{\mathbf{u}}_\alpha) = \nabla \cdot \langle \sigma_\alpha \rangle + \mathbf{M}_\alpha + \phi_\alpha \tilde{\mathbf{F}}_\alpha. \tag{1.183}$$

Averaged total stresses are given by

$$\langle \sigma_\mathrm{p} \rangle = \phi_\mathrm{p} \tilde{\tau}_\mathrm{p} - \phi_\mathrm{p} \tilde{p}_\mathrm{p} \mathbb{1} - \phi_\mathrm{p} \tilde{p}_\mathrm{g} \mathbb{1} \tag{1.184}$$

$$\langle \sigma_\mathrm{g} \rangle = \phi_\mathrm{g} \tilde{\tau}_\mathrm{g} - \phi_\mathrm{g} \tilde{p}_\mathrm{g} \mathbb{1}, \tag{1.185}$$

where $\tilde{p}_\mathrm{p}$ is an 'extra stress' due to collision of particles and

$$\tilde{\tau}_\alpha = 2\mu_\alpha \mathbf{\Pi}_\alpha + (\mu_{\alpha,b} - \frac{2}{3}\mu_\alpha) \cdot \mathrm{tr}(\mathbf{\Pi}_\alpha)\mathbb{1}, \tag{1.186}$$

where μ_α is the shear viscosity and $\mu_{\alpha,b}$ is the bulk viscosity of phase α and

$$\mathbf{\Pi}_\alpha = \frac{1}{2}\Big[\nabla \bar{\mathbf{u}}_\alpha + (\nabla \bar{\mathbf{u}}_\alpha)^t\Big]. \tag{1.187}$$

Furthermore assuming that the interfacial momentum exchange term consist of bouyancy and viscous drag term, *i.e.*,

$$\mathbf{M}_\mathrm{g} = \tilde{p}_\mathrm{g} \nabla \phi_\mathrm{g} + B(\bar{\mathbf{u}}_\mathrm{p} - \bar{\mathbf{u}}_\mathrm{g})$$
$$\mathbf{M}_\mathrm{p} = -\mathbf{M}_\mathrm{g}$$

we get

$$\begin{aligned} \frac{\partial}{\partial t}(\phi_\mathrm{g} \tilde{\rho}_\mathrm{g} \bar{\mathbf{u}}_\mathrm{g}) + \nabla \cdot (\phi_\mathrm{g} \tilde{\rho}_\mathrm{g} \bar{\mathbf{u}}_\mathrm{g} \bar{\mathbf{u}}_\mathrm{g}) &= -\phi_\mathrm{g} \nabla \tilde{p}_\mathrm{g} + \nabla \cdot (\phi_\mathrm{g} \tilde{\tau}_\mathrm{g}) \\ &\quad + \mathbf{D}_\mathrm{g} + \phi_\mathrm{g} \tilde{\mathbf{F}}_\mathrm{g} \end{aligned} \tag{1.188}$$

$$\begin{aligned} \frac{\partial}{\partial t}(\phi_\mathrm{p} \tilde{\rho}_\mathrm{p} \bar{\mathbf{u}}_\mathrm{p}) + \nabla \cdot (\phi_\mathrm{p} \tilde{\rho}_\mathrm{p} \bar{\mathbf{u}}_\mathrm{p} \bar{\mathbf{u}}_\mathrm{p}) &= -\phi_\mathrm{p} \nabla \tilde{p}_\mathrm{g} + \nabla \cdot [\phi_\mathrm{p} (\tilde{\tau}_\mathrm{p} - \tilde{p}_\mathrm{p} \mathbb{1})] \\ &\quad - \mathbf{D}_\mathrm{g} + \phi_\mathrm{p} \tilde{\mathbf{F}}_\mathrm{p}, \end{aligned} \tag{1.189}$$

where

$$\mathbf{D}_\mathrm{g} = B(\bar{\mathbf{u}}_\mathrm{p} - \bar{\mathbf{u}}_\mathrm{g}). \tag{1.190}$$

Both the shear viscosity and the solids 'extra stress' consist of a kinetic part and a collisional part. The extra stress can be written as follows

$$\tilde{p}_{\mathrm{p}} = \tilde{\rho}_{\mathrm{p}}\Theta_{\mathrm{p}}[1 + 2(1+e)\phi_{\mathrm{p}}g_o], \tag{1.191}$$

where Θ_{p} is the granular temperature describing the fluctuating kinetic energy of the solid material

$$\Theta_{\mathrm{p}} = \frac{1}{3}\mathrm{tr}\langle\delta\mathbf{u}_{\mathrm{p}}\delta\mathbf{u}_{\mathrm{p}}\rangle \tag{1.192}$$

and e is the coefficient of restitution for particle collisions and g_o is the radial distribution function given by [DG90]

$$g_o = \frac{3}{5}\left[1 - \left(\frac{\phi_{\mathrm{p}}}{\phi_{\mathrm{p,max}}}\right)^{1/3}\right]^{-1}, \tag{1.193}$$

where $\phi_{\mathrm{p,max}}$ is the maximum packing of the solids. Several alternative forms of the radial distribution function have been proposed in the literature.

The shear viscosity can be written as a sum of the kinetic part and the collisional part as follows

$$\mu_{\mathrm{p}} = \mu_{\mathrm{p,kin}} + \mu_{\mathrm{p,col}}, \tag{1.194}$$

where [LSJC84]

$$\mu_{\mathrm{p,col}} = \frac{4}{5}\phi_{\mathrm{p}}\tilde{\rho}_{\mathrm{p}}d_{\mathrm{p}}g_o(1+e)\sqrt{\frac{\Theta_{\mathrm{p}}}{\pi}} \tag{1.195}$$

and [GBD92]

$$\mu_{\mathrm{p,kin}} = \frac{10\sqrt{\pi}\tilde{\rho}_{\mathrm{p}}d_{\mathrm{p}}\sqrt{\Theta_{\mathrm{p}}}}{96\phi_{\mathrm{p}}(1+e)g_o}\left[1 + \frac{4}{5}g_o\phi_{\mathrm{p}}(1+e)\right]^2 \tag{1.196}$$

Also for the shear viscosity several alternatives exist, with biggest differences in the dilute regions.

The bulk viscosity expresses the resistance against compression and is given by

$$\mu_{\mathrm{p,b}} = \frac{4}{3}\phi_{\mathrm{p}}\tilde{\rho}_{\mathrm{p}}d_{\mathrm{p}}g_o(1+e)\sqrt{\frac{\Theta_{\mathrm{p}}}{\pi}}. \tag{1.197}$$

The solids pressure, the shear viscosity and the bulk viscosity above are all given as functions of the granular temperature Θ. The following transport equation has been derived for the fluctuating kinetic energy thus yielding the granular temperature [DG90]

$$\begin{aligned}\frac{3}{2}\left[\frac{\partial}{\partial t}(\phi_{\mathrm{p}}\tilde{\rho}_{\mathrm{p}}\Theta_{\mathrm{p}}) \;+\; \nabla\cdot(\phi_{\mathrm{p}}\tilde{\rho}_{\mathrm{p}}\Theta_{\mathrm{p}}\mathbf{u}_{\mathrm{p}})\right] \\ = \;(-p_{\mathrm{p}}\mathbb{1} + \tau_{\mathrm{p}}) : \nabla\mathbf{u}_{\mathrm{p}} + \nabla\cdot(k_\Theta\nabla\Theta_{\mathrm{p}}) - \gamma_\Theta + \phi_\Theta,\end{aligned} \tag{1.198}$$

where the first term on the right hand side presents the generation by local acceleration of particles, the second term the diffusion of Θ, the third term the dissipation of Θ and the fourth term the exchange between gas and solid phases. Several different closure relations for these different terms have been suggested (see the review in [Boe97]).

The diffusion coefficient can be divided as follows [GBD92]

$$k_\Theta = k_{\Theta,dilute} + k_{\Theta,dense}, \tag{1.199}$$

where

$$k_{\Theta,dense} = 2\phi_\mathrm{p}^2\tilde{\rho}_\mathrm{p}d_\mathrm{p}g_0(1+e)\sqrt{\frac{\Theta_\mathrm{p}}{\pi}} \tag{1.200}$$

and

$$k_{\Theta,dilute} = \frac{75}{192}\frac{\tilde{\rho}_\mathrm{p}d_\mathrm{p}\sqrt{\pi\Theta_\mathrm{p}}}{(1+e)g_0}\left[1+\frac{6}{5}(1+e)g_0\phi_\mathrm{p}\right]^2. \tag{1.201}$$

The dissipation of fluctuating energy can be described as [JS83]

$$\gamma_\Theta = 3(1-e^2)\phi_\mathrm{p}^2\tilde{\rho}_\mathrm{p}g_0\Theta_\mathrm{p}\left(\frac{4}{d_\mathrm{p}}\sqrt{\frac{\Theta_\mathrm{p}}{\pi}} - \nabla\cdot\bar{\mathbf{u}}_\mathrm{p}\right) \tag{1.202}$$

and the interphase exchange term as [DG90]

$$\phi_\Theta = -3B\Theta_\mathrm{p}. \tag{1.203}$$

Due to the time consumption of the solution of an extra field equation, an algebraic equation is often used for calculation of the granular temperature. It is based on the assumption that there is a local equilibrium and all terms but the generation and dissipation of granular temperature can be neglected. The resulting algebraic equation is ([SRO93], cited in [Boe97])

$$\begin{aligned}\sqrt{\Theta_\mathrm{p}} &= \frac{-K_1\phi_\mathrm{p}\mathrm{tr}(\mathbf{\Pi}_\mathrm{p})}{2K_4\phi_\mathrm{p}} \\ &+ \frac{\sqrt{(K_1\phi_\mathrm{p})^2\mathrm{tr}^2(\mathbf{\Pi}_\mathrm{p}) + 4K_4\phi_\mathrm{p}\left[K_2\mathrm{tr}^2(\mathbf{\Pi}_\mathrm{p}) + 2K_3\mathrm{tr}(\mathbf{\Pi}_\mathrm{p}^2)\right]}}{2K_4\phi_\mathrm{p}},\end{aligned} \tag{1.204}$$

where

$$K_1 = 2(1+e)\tilde{\rho}_\mathrm{p}g_o + \frac{\tilde{\rho}_\mathrm{p}}{\phi_\mathrm{p}} \tag{1.205}$$

$$K_2 = \frac{4d_\mathrm{p}\tilde{\rho}_\mathrm{p}(1+e)\phi_\mathrm{p}g_o}{3\sqrt{\pi}} - \frac{2}{3}K_3 \tag{1.206}$$

$$K_3 = \frac{d_\mathrm{p}\tilde{\rho}_\mathrm{p}}{2}\left\{\frac{\sqrt{\pi}}{3(3-e)}[1+0.4(1+e)(3e-1)\phi_\mathrm{p}g_o] + \frac{8\phi_\mathrm{p}g_o(1+e)}{5\sqrt{\pi}}\right\} \tag{1.207}$$

$$K_4 = \frac{12(1-e^2)\tilde{\rho}_\mathrm{p} g_o}{d_\mathrm{p}\sqrt{\pi}} \tag{1.208}$$

The typical applications of the kinetic theory of granular flow are in bubbling and circulating fluidized beds. In dense flows of this type the inter-phase drag forces require special closure relations that are based on measurements in dense suspensions. For bubbling beds the models are based on the models for packed beds (Ergun equation [Erg52]) and on the measurements of Richardson and Zaki who studied liquid-solid fluidization [RZ54]. For circulating fluidized beds it is often necessary to apply clustering corrections to the drag forces [Boe97]. In bubbling beds the inter-particle distances are short and particle-particle collisions dominate the flow. In very dense regions the inter-particle friction can dominate over the fluctuating motion and special description of the shear stress term is required [Boe97]. In circulating fluidized beds the gas phase turbulence and particle-gas interactions are important and corrections to the drag force and several others of the closure relations above may be necessary [BBS95].

1.6.4 Constitutive equations for the mixture model

The equations of the mixture model were derived from the general multiphase equations in Section 1.4. For practical applications, constitutive relations are needed for the diffusion velocity and the viscous and turbulent stresses. Some formulations of the constitutive relations are given below.

Diffusion velocity

In a liquid-particle suspension, the momentum source term $\mathbf{D_p}$ can be written in the form

$$\mathbf{D}_\mathrm{p} = \frac{\phi_\mathrm{p}\mathbf{F}_\mathrm{p}}{V_\mathrm{p}}, \tag{1.209}$$

where V_p is the particle volume. Neglecting all other effects except the viscous drag and assuming spherical particles, we can write in the Stokes regime

$$\mathbf{F}_\mathrm{p} = 3\pi d_\mathrm{p}\mu_c\mathbf{u}_\mathrm{cp}. \tag{1.210}$$

Using Eqns. (1.209) and (1.210) together with (1.102), the expression for the slip velocity is

$$\mathbf{u}_\mathrm{cp} = \frac{d_\mathrm{p}^2(\rho_\mathrm{p}-\rho_\mathrm{m})}{18\mu_c}\left[\mathbf{g} - (\bar{\mathbf{u}}_\mathrm{m}\cdot\nabla)\bar{\mathbf{u}}_\mathrm{m} - \frac{\partial}{\partial t}\bar{\mathbf{u}}_\mathrm{m}\right] \tag{1.211}$$

and the diffusion velocity follows from Eqn. (1.103). For larger particle Reynolds numbers, Eqn. (1.210) must be replaced by a corresponding model for the drag force.

Viscous stress

The viscous stress tensor is approximated in the mixture model by an expression analogous to incompressible single phase flow

$$\tau_{\mathrm{m}} = \mu_{\mathrm{m}}[\nabla \bar{\mathbf{u}}_{\mathrm{m}} + (\nabla \bar{\mathbf{u}}_{\mathrm{m}})^t] \tag{1.212}$$

It should be noted that the apparent viscosity of a suspension μ_{m} is not a well defined property of the mixture, but depends on many factors, including the method of measurement. However, it turns out that, at reasonably low concentrations, it can be correlated in a simple way to the concentration.

In mixture model applications, the most often used correlation for the mixture viscosity is that according to Ishii and Zuber [IZ79]; see also [IM84] for a summary of the results. The general expression for the mixture viscosity, valid for solid particles as well as bubbles or drops, is given by

$$\mu_{\mathrm{m}} = \mu_{\mathrm{c}} \left(1 - \frac{\phi_{\mathrm{p}}}{\phi_{\mathrm{pm}}} \right)^{2.5\phi_{\mathrm{pm}}\mu^*} \tag{1.213}$$

where ϕ_{pm} is a concentration for maximum packing. For solid particles $\phi_{pm} \approx 0.62$. In Eqn. (1.213), $\mu^* = 1$ for solid particles and

$$\mu^* = \frac{\mu_{\mathrm{p}} + 0.4\mu_{\mathrm{c}}}{\mu_{\mathrm{p}} + \mu_{\mathrm{c}}} \tag{1.214}$$

for bubbles or drops. Numerous other correlations for the viscosity of solid suspensions are presented in the literature. Rutgers [Rut62] presented a review of various empirical formulas for the relative viscosity. One of the correlations with a theoretical foundation is due to Mooney (cited in [Rut62])

$$\ln\left(\frac{\mu_{\mathrm{m}}}{\mu_{\mathrm{c}}} \right) = \frac{2.5\phi_{\mathrm{p}}}{1 - 1.4\phi_{\mathrm{p}}} \tag{1.215}$$

Turbulence

In the mixture model the effects of turbulence appear in the mixture momentum equation as part of the general stress term. Additionally, turbulent effects appear in the fluid-particle interaction term and in the fluctuating components of particle velocity, *i.e.*, as a turbulent stress in the particle momentum equation.

In turbulent multiphase flow at low loadings, it can be assumed that both the viscous stresses of the carrier phase and the turbulent stresses of the particulate phase are negligible. The effective viscosity of the continuous phase can then be calculated directly from a turbulence model for the continuous phase, *e.g.*, from the $k-\epsilon$ model. There a correction can be applied

to reduce the turbulence intensity. The models for correcting turbulent viscosity are unfortunately very uncertain. In some cases the results with the corrections can be less accurate than those obtained using the standard $k-\epsilon$ model. Therefore, simulations should be performed without the corrections and with various correction methods.

In turbulent flows the fluid particle interaction force should be written in the form

$$\mathbf{D}_\mathrm{p} = -B\bar{\mathbf{u}}_\mathrm{cp} + \mathbf{D}'_\mathrm{p} \tag{1.216}$$

where $\mathbf{D}'_\mathrm{p}$ is the fluctuating part of the force that causes particle dispersion. In turbulent flow the term $\mathbf{D}'_\mathrm{p}$ should be added to the right hand side of Eqn. (1.100).

In the original multiphase equations, the turbulent dispersion terms are included in the momentum equations of dispersed phases, Eqn. (1.28). In the mixture model, the influence of turbulence must be contained in the equation for the diffusion velocity. This implies additional terms in (1.211) due to the turbulent stresses and the fluctuation part of $\mathbf{D}_\mathrm{p}$. Instead of developing a model for those terms directly, we adopt a simpler and more intuitive method. The main effect of the slip velocity is the diffusion term introduced in the continuity equation of the dispersed phase. If the turbulent terms are taken into account, other terms will appear in the continuity equation representing the turbulent diffusion. The simplest way is to model these terms as Fickian diffusion. The continuity equation of the particulate phase is then

$$\frac{\partial}{\partial t}(\phi_\mathrm{p}\tilde{\rho}_\mathrm{p}) + \nabla\cdot(\phi_\mathrm{p}\tilde{\rho}_\mathrm{p}\bar{\mathbf{u}}_\mathrm{p}) = \nabla\cdot(D_\mathrm{mp}\nabla\phi_\mathrm{p}) - \nabla\cdot(\phi_\mathrm{p}\bar{\rho}_\mathrm{p}\bar{\mathbf{u}}_\mathrm{mp}), \tag{1.217}$$

where D_mp is a dispersion (or diffusion) coefficient.

One simple way to estimate the dispersion coefficient is to estimate it from the turbulent particle viscosity as follows ([SCQM96])

$$D_\mathrm{mp} = \frac{\mu_\mathrm{p}^T}{\sigma_\mathrm{p}^T\tilde{\rho}_\mathrm{p}}, \tag{1.218}$$

where σ_p^T is the turbulent particle Schmidt number for which values of, *e.g.*, 0.34 and 0.7 have been suggested.

Csanady's model [Csa63b] for the turbulent diffusion takes into account the crossing trajectory effect. It was developed for a special boundary layer application under special assumptions. Csanady's model is still today the best model available for predicting particle dispersion and has shown to be fairly accurate even for other applications. The following equation is based on Csanady's work and the $k-\epsilon$ model [PBG86]

$$D_\mathrm{mp} = \nu_\mathrm{c}^T\left(1 + 0.85\frac{\bar{u}_\mathrm{cp}^2}{2k/3}\right)^{-1/2}, \tag{1.219}$$

where 0.85 is an empirical value determined from particle dispersion data. The equation above is based on the assumption that the carrier phase turbulent Schmidt number is equal to one. In addition, the turbulent Schmidt number of the dispersed phase was defined using the carrier phase diffusivity as a reference.

1.6.5 Dispersion models

The theoretical treatment of particle dispersion was discussed earlier in Section 1.5.2. There, this treatment was further supplemented with the most common approach utilized in numerical simulations involving turbulent particle dispersion, i.e., the eddy interaction model. In that context the two extreme conditions of particles almost following the turbulent fluid motions, and heavy particles crossing the eddies were mentioned. In the following, an analytic approach of particle dispersion is given for these two limiting cases. They constitute the only theoretical conditions for which practical numerical models can be compared.

Linearized equation of motion

To examine the relation between fluid and particle correlations or spectral densities we need to solve the equation of motion of a particle. To this end we study the BBO-equation (1.109), which is a nonlinear integro-differential equation. For the Stokes regime $\mathrm{Re_p} < 1$ the nonlinearity is caused mainly by the pressure gradient term (II). By using the Lumley's approximation for this term [Lum57] the BBO-equation for the velocity component i can be written as

$$\begin{aligned}
&\frac{\mathrm{d}v_{L,i}}{\mathrm{d}t} - b\left(\frac{\mathrm{d}u_{L,i}}{\mathrm{d}t} - \frac{2}{3}\nu_\mathrm{f}\frac{\partial^2 u_{L,i}}{\partial x_j \partial x_j}\right) \\
&+ab\left\{(v_{L,i} - u_{L,i}) + \frac{2}{3a}(v_{L,j} - u_{L,j})\frac{\partial u_{L,i}}{\partial x_j}\right\} \\
&+b\sqrt{\frac{3a}{\pi}}\int_{t_0}^{t}\frac{\frac{\mathrm{d}}{\mathrm{d}\tau}\{v_{L,i}(\tau) - u_{L,i}(\tau)\}}{\sqrt{t-\tau}}\,\mathrm{d}\tau + f_i = 0\,. \qquad (1.220)
\end{aligned}$$

In this equation f_i denotes an external field force per unit effective mass (real mass + virtual mass) of the particle. The parameters a and b are given by

$$a = \frac{3\nu_\mathrm{f}}{r_\mathrm{p}^2} \quad \text{and} \quad b = \frac{3\rho_\mathrm{f}}{2\rho_\mathrm{p} + \rho_\mathrm{f}}\,. \qquad (1.221)$$

Hinze [Hin75] pointed out that the nonlinearity becomes negligible if the term including derivative in the third term of Eqn. (1.220) is very small, *i.e.*,

$$\frac{2}{3a}\frac{\partial u_{L,i}}{\partial x_j} \ll 1\,. \qquad (1.222)$$

This requirement is fulfilled if the particle size is small as compared to the Taylor microscale. However, the restrictions of validity of the particle equation of motion in turbulent field, set by Eqns. (1.115), already includes this requirement. It was further realized by Hinze that additional simplification is possible if the latter part of also the second term of Eqn. (1.220) is negligible. It is reasonable to assume that this requirement is also met if the particle size is sufficiently small as compared to the turbulent structures. Implicit in both these simplifying conditions is the assumption that the particle resides in a locally uniform fluid field. In other words, it is restricted to move in the strongly correlated region of the turbulent field (inside an eddy) for a time comparable to the eddy decay time.

In what follows we consider an arbitrary coordinate direction i in a coordinate system where the correlation tensors and spectral densities are diagonal (see discussion at the end of Sect. 1.5.2), and omit subscript i. Under the assumptions made above, the linearized BBO-equation for a velocity component can be written as

$$\begin{aligned}&\frac{\mathrm{d}v_L}{\mathrm{d}t} - b\frac{\mathrm{d}u_L}{\mathrm{d}t} + ab(v_L - u_L)\\ &+b\sqrt{\frac{3a}{\pi}}\int_{t_0}^{t}\frac{\frac{\mathrm{d}}{\mathrm{d}\tau}\{v_L(\tau)-u_L(\tau)\}}{\sqrt{t-\tau}}\,\mathrm{d}\tau + f = 0\,.\end{aligned} \tag{1.223}$$

By defining the Fourier transforms of the fluid and particle velocity components as

$$\begin{aligned}\hat{u}_L(\omega) &= \int_{-\infty}^{\infty} u_L(t)\exp(-i\omega t)\,\mathrm{d}t\\ \hat{v}_L(\omega) &= \int_{-\infty}^{\infty} v_L(t)\exp(-i\omega t)\,\mathrm{d}t\,,\end{aligned} \tag{1.224}$$

and by applying them in Eqn. (1.223), leads to simple relationship between the velocities [Cha64]

$$\hat{v}_L = \frac{\left\{a+\sqrt{\frac{3a\omega}{2}}\right\} + i\left\{\omega+\sqrt{\frac{3a\omega}{2}}\right\}}{\left\{a+\sqrt{\frac{3a\omega}{2}}\right\} + i\left\{\frac{\omega}{b}+\sqrt{\frac{3a\omega}{2}}\right\}}\hat{u}_L\,. \tag{1.225}$$

Multiplying each side of this equation by its complex conjugate and applying ensemble averaging on the resulting equation gives

$$\frac{\langle\hat{v}_L(\omega)\,\hat{v}_L^{\star}(\omega)\rangle}{\langle\hat{u}_L(\omega)\,\hat{u}_L^{\star}(\omega)\rangle} = \frac{\Omega_{(1)}}{\Omega_{(2)}}\,, \tag{1.226}$$

where

$$\begin{aligned}\Omega_{(1)}\left(\frac{\omega}{a}\right) &= \left(\tfrac{\omega}{a}\right)^2 + \sqrt{6}\left(\tfrac{\omega}{a}\right)^{3/2} + 3\left(\tfrac{\omega}{a}\right) + \sqrt{6}\left(\tfrac{\omega}{a}\right)^{1/2} + 1 \qquad (1.227)\\ \Omega_{(2)}\left(\frac{\omega}{a},b\right) &= \tfrac{1}{b^2}\left(\tfrac{\omega}{a}\right)^2 + \tfrac{\sqrt{6}}{b}\left(\tfrac{\omega}{a}\right)^{3/2} + 3\left(\tfrac{\omega}{a}\right) + \sqrt{6}\left(\tfrac{\omega}{a}\right)^{1/2} + 1\,.\end{aligned}$$

The Lagrangian spectral densities (see Eqn. (1.126)) can be given in terms of the Fourier transformed velocities as

$$\mathrm{E}_{L\mathrm{f}}(\omega) = \frac{\langle \hat{u}_L(\omega)\, \hat{u}_L^\star(\omega)\rangle}{\langle u_L^2\rangle} \qquad (1.228)$$
$$\mathrm{E}_{L\mathrm{p}}(\omega) = \frac{\langle \hat{v}_L(\omega)\, \hat{v}_L^\star(\omega)\rangle}{\langle v_L^2\rangle}\,.$$

It thus follows that

$$\frac{\mathrm{E}_{L\mathrm{p}}}{\mathrm{E}_{L\mathrm{f}}} = \frac{\langle u_L^2\rangle}{\langle v_L^2\rangle}\frac{\Omega_{(1)}}{\Omega_{(2)}}\,. \qquad (1.229)$$

Consequently, the (diagonal elements of) the mean square displacement and dispersion tensors of the particle, Eqns. (1.127) and (1.128), can be given in terms of variables defined by the turbulent field of the fluid as

$$\langle y_L^2(t)\rangle = \langle u_L^2\rangle \int_0^\infty \frac{\Omega_{(1)}}{\Omega_{(2)}}\mathrm{E}_{L\mathrm{f}}(\omega)\frac{2(1-\cos\omega t)}{\omega^2}\,\mathrm{d}\omega \quad \text{and} \qquad (1.230)$$

$$\mathrm{D}_\mathrm{p} = \langle u_L^2\rangle \int_0^\infty \frac{\Omega_{(1)}}{\Omega_{(2)}}\mathrm{E}_{L\mathrm{f}}(\omega)\frac{\sin\omega t}{\omega}\,\mathrm{d}\omega\,. \qquad (1.231)$$

A number of conclusions concerning Eqns. (1.230) and (1.231) can be made without actually solving the spectral densities or calculating the integrals. For the low and high frequency limits, the amplitude ratio of the phases is seen to behave as

$$\tfrac{\omega}{a} \to 0\,, \quad \frac{\Omega_{(1)}}{\Omega_{(2)}} \to 1 \quad \text{and} \qquad (1.232)$$

$$\tfrac{\omega}{a} \to \infty\,, \quad \frac{\Omega_{(1)}}{\Omega_{(2)}} \to b^2\,. \qquad (1.233)$$

For the ratio of the effective masses of the phases b, it is observed that in the case of very heavy particles, where $\rho_\mathrm{f}/\rho_\mathrm{p} \to 0$, and in the case of equal densities, where $\rho_\mathrm{f} = \rho_\mathrm{p}$, the amplitude ratio is given by

$$b \to 0\,, \quad \frac{\Omega_{(1)}}{\Omega_{(2)}} \to 0 \quad \text{and} \qquad (1.234)$$

$$b = 1\,, \quad \frac{\Omega_{(1)}}{\Omega_{(2)}} = 1\,, \qquad (1.235)$$

respectively. These results are all physically very plausible. Furthermore, the asymptotic values of the dispersion coefficient for short and long dispersion times are given by

$$\lim_{t\to 0}\mathrm{D}_\mathrm{p} = \langle u_L^2\rangle\, t \quad \text{and} \quad \lim_{t\to\infty}\mathrm{D}_\mathrm{p} = \frac{\pi}{2}\,\langle v_L^2\rangle\,\mathrm{E}_{L\mathrm{p}}(0)\,. \qquad (1.236)$$

The relative degree of the dispersion of particles and fluid is given by

$$\frac{\mathrm{D_p}}{\mathrm{D_f}} = \frac{\langle v_L^2 \rangle}{\langle u_L^2 \rangle} \frac{\int_0^t \mathrm{R}_{L\mathrm{p}}(\tau)\,\mathrm{d}\tau}{\int_0^t \mathrm{R}_{L\mathrm{f}}(\tau)\,\mathrm{d}\tau} = \frac{\langle v_L^2 \rangle}{\langle u_L^2 \rangle} \frac{\int_0^\infty \frac{\sin\omega t}{\omega} \mathrm{E}_{L\mathrm{p}}(\omega)\,\mathrm{d}\omega}{\int_0^\infty \frac{\sin\omega t}{\omega} \mathrm{E}_{L\mathrm{f}}(\omega)\,\mathrm{d}\omega}\,, \tag{1.237}$$

For short and long dispersion times, the limiting behavior of that ratio is given by

$$\lim_{t\to 0} \frac{\mathrm{D_p}}{\mathrm{D_f}} = \frac{\langle v_L^2 \rangle}{\langle u_L^2 \rangle} \quad \text{and} \quad \lim_{t\to\infty} \frac{\mathrm{D_p}}{\mathrm{D_f}} = 1\,. \tag{1.238}$$

The latter limit results since for $\omega = 0$, $\mathrm{E}_{L\mathrm{p}}(0) = \mathrm{E}_{L\mathrm{f}}(0)$ and $\Omega_{(1)} = \Omega_{(2)}$ (see Eqn. (1.232)). These asymptotic expressions for both short and long dispersion times should hold regardless of the detailed form of either the Lagrangian temporal correlation or power spectral density.

The equality of the particle dispersion and the fluid diffusion at long dispersion times is a consequence of the assumptions made while linearizing the particle equation of motion. As stated above, these assumptions indicate that the particle moves in the strongly correlated area of the fluid eddy, since it's motion has been related to the surrounding fluid through the Lagrangian correlation coefficient. This is plausible if the particle is very small as compared to the fluid eddy or if the densities of the phases are close to each other. Considerably heavier or lighter particles can not follow the fluid motion. However, if the particles are very much smaller than the fluid eddies, e.g. dust particles in the athmosphere, the assumptions may still be valid.

Crossing trajectories

In general, a heavy particle can have a significant mean velocity relative to the fluid, while a particle with a density comparable with that of the fluid tends to follow the motion of the fluid more closely. Therefore, a heavy particle continuously changes it's fluid neighborhood and drifts away from the fluid eddy in a time scale that is small as compared with the eddy decay time. The velocity correlation of heavy particles with the surrounding fluid thus decreases rapidly and their dispersion rate is low. This phenomenon is known as the effect of crossing trajectories.

The approach of Csanady [Csa63b, Csa63a] is essentially based on an extended form of Taylor's hypothesis according to which the Eulerian temporal velocity correlation in the streamwise direction approaches the corresponding Eulerian spatial velocity correlation as the ratio of turbulent velocity fluctuations to mean velocity approaches zero. Within Csanady's extension it is assumed that in a frame of reference moving with the mean flow, the Lagrangian spatial velocity correlation can be approximated by the Eulerian temporal velocity correlation. Both theoretical and experimental support to this approximation exist. However, by analogy with Taylor's hypothesis,

mean relative velocity of particles exceeding the standard deviation of velocity fluctuations at least by a factor of four is required for the approximation to be valid.

In hes study of atmospheric dispersion Csanady used a coordinate system where x_1 is the horizontal component (direction of atmospheric wind), x_2 is the span-wise component and x_3 is the vertical component (upwards). Based mainly on experimental observations [Csa63a] he expressed the Lagrangian spatial correlation functions in the three directions as

$$R^{\lambda}_{L\mathrm{p},11} = \exp\left(-\frac{W_3\tau}{L}\right) \tag{1.239}$$

$$R^{\lambda}_{L\mathrm{p},22} = \left(1-\frac{W_3\tau}{2L}\right)\exp\left(-\frac{W_3\tau}{L}\right) \tag{1.240}$$

$$\mathrm{R}^{\lambda}_{L\mathrm{p},33} = \exp\left\{-\frac{\tau}{L}\sqrt{W_3^2+\frac{\langle w_3^2\rangle}{\beta^2}}\right\}. \tag{1.241}$$

Here L is the characteristic size of an eddy (assumed to be approximately the same in all directions), W_3 is the vertical component of mean relative velocity and w_3 it's fluctuating part. The coefficient β is given by

$$\beta = \frac{\sqrt{\langle w_3^2\rangle}T_L}{L}, \tag{1.242}$$

where T_L the Lagrangian time scale. Using the exponential approximation of the correlation function Eqn. (1.241) and Taylor's theorem Eqn. (1.122) the mean square displacement in the vertical direction can be expressed in the non-dimensional form as

$$\eta = 2\xi\left\{1-\frac{1}{\xi}\left(1-\exp(-\xi)\right)\right\}, \tag{1.243}$$

where the dimensionless displacement η and the dimensionless time ξ are defined by

$$\eta = \frac{\langle y_{L,3}^2(t)\rangle}{\langle w_3^2\rangle L^2}\left(W_3^2+\frac{\langle w_3^2\rangle}{\beta^2}\right)$$

$$\xi = \frac{t}{L}\sqrt{W_3^2+\frac{\langle w_3^2\rangle}{\beta^2}}.$$

The asymptotic long time vertical dispersion coefficient now becomes (see Eqn. (1.128))

$$\lim_{t\to\infty}\mathrm{D}_{\mathrm{p},3} = D^{\infty}_{\mathrm{p},3} = \frac{\langle w_3^2\rangle L}{\sqrt{W_3^2+\frac{\langle w_3^2\rangle}{\beta^2}}}. \tag{1.244}$$

Therefore, at large mean relative velocity the mean square displacement and the long time dispersion coefficient are seen to be proportional to $1/W_3$. By dividing Eqn. (1.244) with the long time diffusivity of the fluid we finally obtain

$$\frac{D^{\infty}_{\mathrm{p},3}}{D^{\infty}_{\mathrm{f},3}} = \frac{1}{\sqrt{1+\frac{\beta^2 W_3^2}{\langle w_3^2\rangle}}}\,. \tag{1.245}$$

Similarly, for dispersion in the horizontal and span-wise directions we find

$$D^{\infty}_{\mathrm{p},1} = \frac{\langle w_1^2\rangle L}{W_3} \tag{1.246}$$

$$D^{\infty}_{\mathrm{p},2} = \frac{1}{2}\frac{\langle w_2^2\rangle L}{W_3}\,, \tag{1.247}$$

and

$$\frac{D^{\infty}_{\mathrm{p},1}}{D^{\infty}_{\mathrm{f},1}} = \frac{1}{\sqrt{1+\frac{\beta^2 W_3^2}{\langle w_3^2\rangle}}} \tag{1.248}$$

$$\frac{D^{\infty}_{\mathrm{p},2}}{D^{\infty}_{\mathrm{f},2}} = \frac{1}{\sqrt{1+\frac{4\beta^2 W_3^2}{\langle w_3^2\rangle}}}\,. \tag{1.249}$$

Notice, however, that the equation for horizontal direction is derived here exactly as for vertical direction, Eqn. (1.245), whereas the equation of lateral direction is written purely by analogy so as to give the correct behavior in the limits $W_3 \to 0$ and $W_3 \to \infty$.

2. Numerical methods

2.1 Introduction

Since the various multiphase flow models introduced in the previous chapter are, in general, complex set of heavily coupled nonlinear equations it is impossible, without dramatic simplifications, to get an analytic solution to any of those models. Without an exception numerical methods are needed.

Most of the numerical work done on the multiphase flow equations has been focused to particle tracking algorithms (see section 1.5 for the theory of particle tracking) and solution of multifluid equations (1.57) and (1.58). We thus restrict ourselves to these traditional topics in this monoghraph. We also give a brief introduction to novel numerical methods that are especially suitable for direct simulation of certain types of multiphase flows in a 'mesoscopic' scale. These include the lattice-gas, the lattice-Boltzmann and the dissipative particle dynamics methods.

Until now, the numerical development of multifluid equations is done mainly within the finite difference method (FDM) or within the finite volume method (FVM). Applications using finite element method (FEM) seem to be less extensively studied. Independently of the applied discretization method the nature of the multifluid equations will end up to the same difficulties in the numerical solution procedures. While having the same mathematical form as the one phase Navier-Stokes equations also the same problems are encountered, including the problems of pressure-velocity coupling and dominating convection. Furthermore in multifluid flow equations, the inter-phase coupling terms pose specific demands to the numerical algorithms.

Contrary to the multifluid flow models the particle tracking reveals no specific theoretical difficulties in numerical methods. The particle tracks are computed by numerical integration of the equation for particle motion and then the set of ordinary differential equations is solved along these tracks. It is a relatively easy method with some technical tricks and can be adopted to any existing one phase flow solver.

As compared to conventional methods discussed above, mesoscopic simulation methods provide a completely different approach to multiphase flows as they do not resort to solving the averaged continuum equations. Instead, they are based on describing the fluid in terms of a large number of 'particles'

that move and collide in a discrete lattice.

In sections 2.2 and 2.3 numerical solution algorithms based on the finite volume method (FVM) and finite element method (FEM) of the continuum multifluid flow equations are represented. In section 2.2 FVM algorithms and schemes are given in detail using Body-Fitted Coordinates. Also the methods, like pressure correction algorithm SIMPLE, mimicked from the one phase context are extended to cover multifluid equations. In section 2.3 the stabilized FEM algorithms are introduced. The presentation covers twofluid flow equations but can easily be extended to multifluid flow equations. In section 2.4 an overview of the basic numerical methods needed in particle tracking and finally in section 2.5 a brief introduction to mesoscopic numerical methods is given.

Balance equations

In what follows we will consider the following continuum multifluid flow equations

$$\begin{aligned} \frac{\partial}{\partial t}(\phi_\alpha \tilde{\rho}_\alpha) &+ \nabla \cdot (\phi_\alpha \tilde{\rho}_\alpha \bar{\mathbf{u}}_\alpha) = 0 \qquad (2.1)\\ \frac{\partial}{\partial t}(\phi_\alpha \tilde{\rho}_\alpha \bar{\mathbf{u}}_\alpha) &+ \nabla \cdot (\phi_\alpha \tilde{\rho}_\alpha \bar{\mathbf{u}}_\alpha \bar{\mathbf{u}}_\alpha) - \nabla \cdot \left(\phi_\alpha \mu_\alpha [\nabla \bar{\mathbf{u}}_\alpha + (\nabla \bar{\mathbf{u}}_\alpha)^t]\right) \\ &= -\phi_\alpha \nabla \tilde{p} + \sum_{\beta=1}^{N_p} B_{\alpha\beta}(\bar{\mathbf{u}}_\beta - \bar{\mathbf{u}}_\alpha) + \phi_\alpha \tilde{\mathbf{F}}_\alpha. \end{aligned}$$

These equations are derived from the general multifluid equations (1.57) and (1.58) neglecting the pseudo-turbulent stress and assuming that all the phases behave like Newtonian fluids, *i.e.*,

$$\nabla \cdot \langle \tau_\alpha \rangle = \phi_\alpha \mu_\alpha [\nabla \bar{\mathbf{u}}_\alpha + (\nabla \bar{\mathbf{u}}_\alpha)^t]. \qquad (2.2)$$

Furthermore the momentum exchange term $\mathbf{D}_\alpha$ is assumed to be due to inter-phase drag only, *i.e.*,

$$\mathbf{D}_\alpha = \sum_{\beta=1}^{N_p} B_{\alpha\beta}(\bar{\mathbf{u}}_\beta - \bar{\mathbf{u}}_\alpha). \qquad (2.3)$$

Using a general dependent variable Φ_α the flow equations for phase α can be given in a generic form

$$\begin{aligned} \frac{\partial}{\partial t}(\phi_\alpha \tilde{\rho}_\alpha \Phi_\alpha) &+ \nabla \cdot [\phi_\alpha (\tilde{\rho}_\alpha \bar{\mathbf{u}}_\alpha \Phi_\alpha - \Gamma_\alpha \nabla \Phi_\alpha)] \qquad (2.4)\\ &= \sum_{\beta=1}^{N_p} B^I_{\alpha\beta}(\Phi_\beta - \Phi_\alpha) + S_\alpha. \end{aligned}$$

The continuity equation and the momentum equation for phase α follow from Eqn. (2.4) by setting $\Phi_\alpha = 1$ and $\Phi_\alpha = \bar{\mathbf{u}}_\alpha$, respectively.

2.2 Multifluid Finite Volume Method

The development of numerical methods for multifluid flow equations within FVM methods is based heavily on the extensions of single phase flow algorithms, such as the pressure-correction algorithm SIMPLE and its improvements to the multifluid context [Spa77, Spa80, Spa83, Kar02].

As discussed in the previous chapter, multifluid flow equations typically include for each phase equations that are formally similar to the conventional single fluid equations (unless simplified models such as the mixture model is considered), except of additional terms that arise due to the presence of other phases. These terms provide coupling between the equations and pose one of the major problems for modelling and for numerical solution of the multifluid flow equations. The coupling terms are often expressed in the form of a coupling constant times the difference between the values of the dependent variable of the two phases. When the coupling is strong the coupling constant is large and the value of the dependent variables in different phases are nearly equal. This condition with a large number multiplying a very small number often leads to convergence problems. The Partial Elimination Algorithm (PEA) developed by Spalding [Spa80] for twophase equations and the SINCE algorithm [Lo89, Lo90] for multifluid equations handles this problem by separating the solution of the phases of the dependent variable. This can be done effectively in the cell level. Further details of SINCE algorithm can be found in Ref. [KL99].

Until now the multifluid algorithms in FVM are based on structured grid approach. Complex geometries are handled by changing to Body Fitted Coordinates (BFC) and by using multi-block grids. A better way to approximate the physical geometry would be to use an unstructured grid where local refinements and adaptation are possible. Also, the ease of grid generation in complex geometries using automatic generation algorithms is a tempting feature of unstructured grids. Within FVM, the development of unstructured grid solvers has been distinct from the development of structured solvers where the benefits of the grid structure are exploited. More recently, development of unstructured grid FVM solvers has followed same guidelines as the development of structured grid solvers. In this method [MM97] the values are stored, like in structured solvers, in the cell centers and the use of the so called reconstruction gradient enables the construction of higher order schemes. Earlier, the problem of pressure oscillation was dealt with a staggered grid for velocity components and pressure. Recently this unwanted staggering (especially in complex geometries) is overcome using the Rhie-Chow algorithm [RC83, BW87], where the cell-boundary velocity components are obtained by interpolating the discrete momentum equations instead of the velocity values. In Control Volume Finite Element Method (CVFEM) by Baliga and Patankar [BP80] finite volume equations and element by element assembling, typical to FEM, are combined. In this

method the variables are attached to discretization points similarly to FEM. For this method some development is done also in twophase context [MB94].

In this Section the FVM method in general Body-Fitted Coordinates (BFC) for multifluid equations is represented. Pressure stabilization is dealt with the Rhie-Chow algorithm, where the cell-boundary velocity components are obtained by interpolating the discrete momentum equations instead of the velocity values. Three different treatments of the inter-phase coupling are given including explicit algorithm, PEA algorithm for two phase situation and an extension of the PEA algorithm to multifluid equations. The solution of the volume fraction equations is obtained from the scheme which ensures the volume fraction sum to unity. The pressure-velocity coupling is handled with the SIMPLE method which extension to multifluid equations is given in detail. In the end the overall algorithm called IPSA (Inter Phase Slip Algorithm) for the solution of the system of multifluid flow equations is given.

2.2.1 General coordinates

In order to facilitate the numerical solution of the macroscopic balance equations (2.1), (2.3) and (2.4) in a general 3D geometry using Body-Fitted Coordinates (BFC), these equations are expressed in the covariant tensor form. The coordinate system used in this context is the local non-orthogonal coordinate system (ξ^1, ξ^2, ξ^3), referred to as the computational space, obtained from the Cartesian coordinate system (x^1, x^2, x^3), i.e. the physical space, by the curvilinear coordinate transformation $x^i(\xi^j)$ (Fig. 2.1). Because there is no danger of confusion, the phase and mass-weighted phase average notations above, *e.g.*, $\tilde{\rho}_\alpha$ and $\bar{\mathbf{u}}_\alpha$, have been omitted in the subsequent treatment in order to enhance the readability of the equations. Thus the balance equations in the computational space are

$$\frac{\partial}{\partial t}(|\mathbf{J}|\phi_\alpha\rho_\alpha) + \frac{\partial}{\partial \xi^i}(\hat{I}^i_{m_\alpha}) = 0 \tag{2.5}$$

$$\frac{\partial}{\partial t}(|\mathbf{J}|\phi_\alpha\rho_\alpha u^k_\alpha) + \frac{\partial}{\partial \xi^i}(\hat{I}^i_{u^k_\alpha}) = -\phi_\alpha A^i_k \frac{\partial p}{\partial \xi^i} + \frac{\partial}{\partial \xi^i}(\phi_\alpha \mu_\alpha \frac{A^i_m A^j_k}{|\mathbf{J}|}\frac{\partial u^m_\alpha}{\partial \xi^j}) + \sum_{\beta=1}^{N_p} |\mathbf{J}| B_{\alpha\beta}(u^k_\beta - u^k_\alpha) + |\mathbf{J}|\phi_\alpha F^k_\alpha \tag{2.6}$$

$$\frac{\partial}{\partial t}(|\mathbf{J}|\phi_\alpha\rho_\alpha\Phi_\alpha) + \frac{\partial}{\partial \xi^i}(\hat{I}^i_{\Phi_\alpha}) = \sum_{\beta=1}^{N_p} |\mathbf{J}| B_{\alpha\beta}(u^k_\beta - u^k_\alpha) + |\mathbf{J}| S_\alpha, \tag{2.7}$$

where $|\mathbf{J}|$ is the Jacobian determinant of the mapping $x^i \to \xi^j(x^i)$ and the total normal phasic fluxes $\hat{I}^i_{m_\alpha}$, $\hat{I}^i_{u^k_\alpha}$ and $\hat{I}^i_{\Phi_\alpha}$ are defined as

$$\hat{I}^i_{m_\alpha} = \phi_\alpha\rho_\alpha\hat{u}^i_\alpha, \tag{2.8}$$

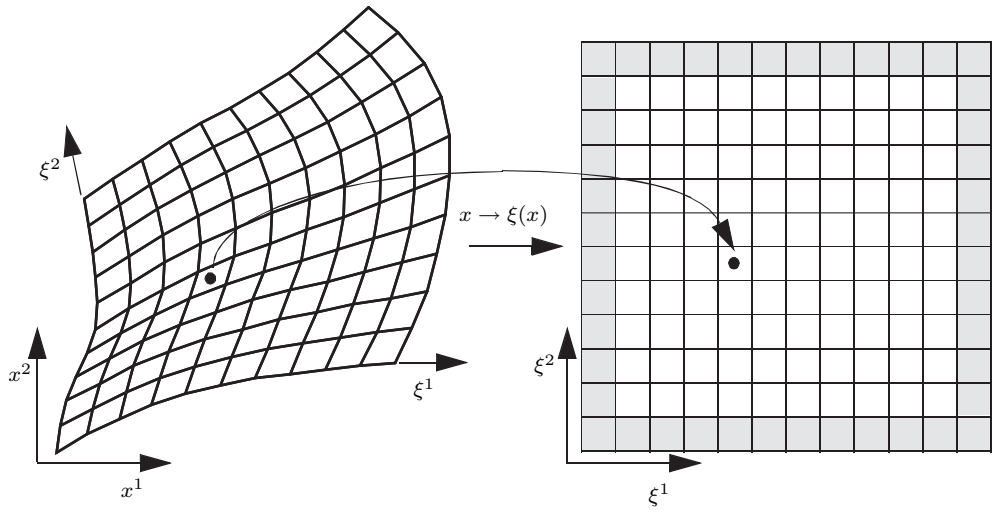

Figure 2.1: A single block of a collocated BFC-grid in the physical space (x^1, x^2, x^3) and in the computational space (ξ^1, ξ^2, ξ^3) with the dummy cells on the boundaries.

$$\hat{I}^i_{u^k_\alpha} = \phi_\alpha(\rho_\alpha \hat{u}^i_\alpha u^k_\alpha - \mu_\alpha \frac{A^i_m A^j_m}{|\mathbf{J}|} \frac{\partial u^k_\alpha}{\partial \xi^j}), \tag{2.9}$$

$$\hat{I}^i_{\Phi_\alpha} = \phi_\alpha(\rho_\alpha \hat{u}^i_\alpha \Phi_\alpha - \mu_\alpha \frac{A^i_m A^j_m}{|\mathbf{J}|} \frac{\partial \Phi_\alpha}{\partial \xi^j}). \tag{2.10}$$

The notations $\hat{u}^i_\alpha = A^i_m u^m_\alpha$ and A^i_m in the above equations stand for the normal flux velocity component and the adjugate Jacobian matrix of the mapping $x^i \to \xi^j(x^i)$. The area vectors of the surfaces of an elementary grid cell $\mathbf{A}^{(i)}$ (Fig. 2.2), i.e., the vectors pointing to the outward normal direction of the cell faces and having the magnitude of the length equal to the magnitude of the area of these faces, are obtained as

$$\mathbf{A}^{(1)} = \mathbf{e}_{(2)} \times \mathbf{e}_{(3)},\ \mathbf{A}^{(2)} = \mathbf{e}_{(3)} \times \mathbf{e}_{(1)} \text{ and } \mathbf{A}^{(3)} = \mathbf{e}_{(1)} \times \mathbf{e}_{(2)}, \tag{2.11}$$

where $\mathbf{e}_{(i)}$ are the contravariant basis vectors associated with the curvilinear frame $\xi^i(x^j)$ (tangential to the coordinate curves). Covariant basis vectors (normal to the coordinate surfaces) are denoted by $\mathbf{e}^{(i)}$. The cartesian components of contravariant vectors are given by

$$\mathbf{e}_{(i)_k} = \mathbf{J}^k_i. \tag{2.12}$$

With the help of these area vectors the volume of elementary grid cell V_P is then related to the Jacobian determinant as

$$\mathbf{A}^{(i)} \cdot \mathbf{e}_{(j)} = \mathbf{e}_{(1)} \cdot \mathbf{e}_{(2)} \times \mathbf{e}_{(3)} \delta^i_j = V_P \delta^i_j = |\mathbf{J}| \delta^i_j. \tag{2.13}$$

Because the two frames of basis vectors are dual to each other $\mathbf{e}^{(i)} \cdot \mathbf{e}_{(j)} = \delta^i_j$ the Eqn. (2.13) can be written in the form

$$\mathbf{A}^{(i)} \cdot \mathbf{e}_{(j)} = |\mathbf{J}| \mathbf{e}^{(i)} \cdot \mathbf{e}_{(j)}. \tag{2.14}$$

It can be shown that the cartesian components of the area vectors $\mathbf{A}^{(i)}_k$ are determined by the adjugate Jacobian matrix as

$$\mathbf{A}^{(i)}_k = A^i_k. \tag{2.15}$$

The necessary information to perform the coordinate transformation includes only the volumes and the cartesian components of the area vectors of the grid cells in the physical space. This information is completed by calculation of the Jacobian determinant $|\mathbf{J}|$ and the adjugate Jacobian matrix A^i_k of the transformation.

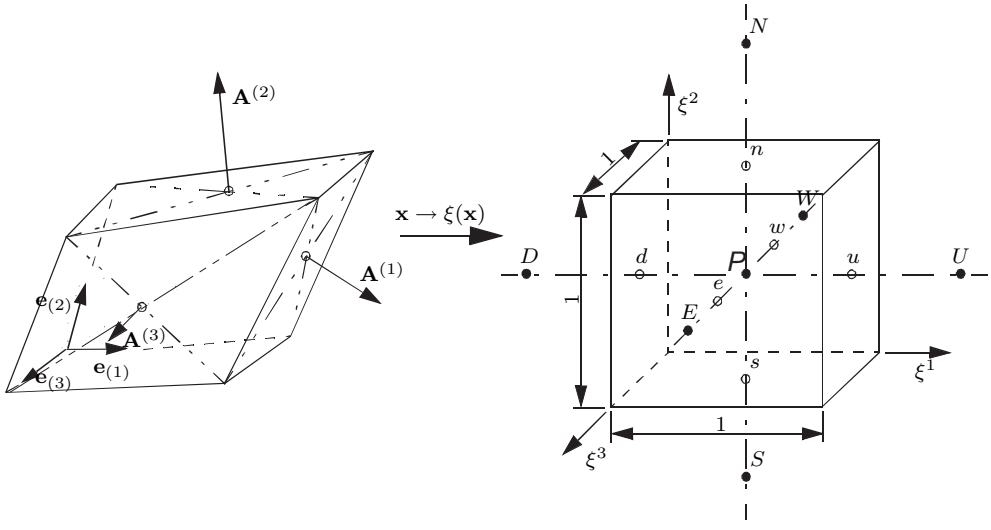

Figure 2.2: Area vectors on the faces of the finite-volume cell in the physical space and the notation of the neighboring cell centers and cell faces in the computational space.

2.2.2 Discretization of the balance equations

Within the coordinate transformation all the derivatives of the macroscopic balance equations in the physical space have been expressed with the corresponding terms in the computational space, in which the transformed macroscopic balance equations are discretized. Now we are free to use any discretization method we prefer. In what follows the conservative finite volume approach with collocated dependent variables is applied.

Integration of the generic balance equation over a single finite volume cell (Fig. 2.2) in the computational space and the use of Gauss' law results in

$$\int_{V_c} \frac{\partial}{\partial t}(|\mathbf{J}|\phi_\alpha\rho_\alpha\Phi_\alpha)\,\mathrm{d}V_c + \int_{A_c} \hat{I}^i_{\Phi_\alpha}\cdot\mathbf{n}\,\mathrm{d}A_c = \int_{V_c}\sum_{\beta=1}^{N_p}|\mathbf{J}|B^I_{\alpha\beta}(\Phi_\beta-\Phi_\alpha)\,\mathrm{d}V_c + \int_{Vc}|\mathbf{J}|S_\alpha\,\mathrm{d}V_c, \tag{2.16}$$

where V_c is the volume of cell and A_c is the surface of that cell in the computational space.

In a same way the macroscopic balance equations (2.5), (2.6) and (2.7) can be formally represented as

$$\left[\frac{\{|\mathbf{J}|\phi_\alpha\rho_\alpha\}}{\Delta t}\right]_t^{t+\Delta t} + \left[\hat{I}^1_{m_\alpha}\right]_d^u + \left[\hat{I}^2_{m_\alpha}\right]_s^n + \left[\hat{I}^3_{m_\alpha}\right]_w^e = 0 \tag{2.17}$$

$$\begin{aligned}\left[\frac{\{|\mathbf{J}|\phi_\alpha\rho_\alpha u^k_\alpha\}}{\Delta t}\right]_t^{t+\Delta t} &+ \left[\hat{I}^1_{u^k_\alpha}\right]_d^u + \left[\hat{I}^2_{u^k_\alpha}\right]_s^n + \left[\hat{I}^3_{u^k_\alpha}\right]_w^e = -\left\{\phi_\alpha|\mathbf{J}|\frac{\partial p}{\partial\xi^i}\right\} \\ &+ \left[\phi_\alpha\mu_\alpha\frac{A^1_mA^j_k}{|\mathbf{J}|}\frac{\partial u^m_\alpha}{\partial\xi^j}\right]_d^u + \left[\phi_\alpha\mu_\alpha\frac{A^2_mA^j_k}{|\mathbf{J}|}\frac{\partial u^m_\alpha}{\partial\xi^j}\right]_s^n \\ &+ \left[\phi_\alpha\mu_\alpha\frac{A^3_mA^j_k}{|\mathbf{J}|}\frac{\partial u^m_\alpha}{\partial\xi^j}\right]_w^e + \{|\mathbf{J}|\phi_\alpha F^k_\alpha\} \\ &+ \sum_{\beta=1}^{N_p}\{|\mathbf{J}|B_{\alpha\beta}(u^k_\beta-u^k_\alpha)\}\end{aligned} \tag{2.18}$$

$$\left[\frac{\{|\mathbf{J}|\phi_\alpha\rho_\alpha\Phi_\alpha\}}{\Delta t}\right]_t^{t+\Delta t} + \left[\hat{I}^1_{\Phi_\alpha}\right]_d^u + \left[\hat{I}^2_{\Phi_\alpha}\right]_s^n + \left[\hat{I}^3_{\Phi_\alpha}\right]_w^e = \sum_{\beta=1}^{N_p}\{|\mathbf{J}|B^I_{\alpha\beta}(\Phi_\beta-\Phi_\alpha)\} + \{|\mathbf{J}|S_\alpha\}. \tag{2.19}$$

In the above equations the notation { } indicates that the operand is integrated over the volume of the finite volume cell in question. Because the computational space cells all are of unit volume, the resulting mean value is directly expressed per unit volume basis. In addition, the notation $[\ ]_d^u$ expresses a difference between the values of the operand at the specified faces or time, *e.g.*,

$$[I^i_{\Phi_\alpha}]_d^u = I^i_{\Phi_\alpha}\big|_u - I^i_{\Phi_\alpha}\big|_d. \tag{2.20}$$

When spatial integration over cell face is considered the right hand side notation $I^i_{\Phi_\alpha}\big|_u$ implies that the operand is integrated over the respective face (face corresponding to point u in this case) of the finite volume cell.

Integration over finite volume cell

It is seen from the Eqns. (2.17), (2.18) and (2.19) that the integration of the operand over the finite- volume cell noted as $\{\Phi\}$ is applied to the terms including time derivatives and to the source terms. To perform the integration the real field of the operand inside the cell is approximated with a constant value found at the center of the cell. So we apply a one point integration rule. Because the discretization is done in the computational space the integration results simply in

$$\{\Phi\} \equiv \Phi|_P \, V_c = \Phi|_P = \Phi_P. \tag{2.21}$$

Integration over cell surface

The rest of the terms expressing the flux of the operand through the faces of the finite volume cell are integrated over the cell face. For the averaging the real profile of the operand over the face is approximated with a constant value located at the center of the face. Thus we apply again one point integration rule which results in

$$\int_{A_c^i} \Phi \, \mathrm{d}A_c \equiv \Phi|_c \, A_c^i = \Phi|_c = \Phi_c. \tag{2.22}$$

Now the integral forms of the phasic fluxes can be represented as

$$\begin{aligned}
&[\hat{I}^i_{m_\alpha}]^h_l = C^i_\alpha\big|_h - C^i_\alpha\big|_l \qquad (2.23)\\
&[\hat{I}^i_{u^k_\alpha}]^h_l = C^i_\alpha\big|_h \, u^k_\alpha\Big|_h - C^i_\alpha\big|_l \, u^k_\alpha\Big|_l - D^{ij}_\alpha\big|_h \, \frac{\partial u^k_\alpha}{\partial \xi^j}\Big|_h + D^{ij}_\alpha\big|_l \, \frac{\partial u^k_\alpha}{\partial \xi^j}\Big|_l\\
&[\hat{I}^i_{\Phi_\alpha}]^h_l = C^i_\alpha\big|_h \, \Phi_\alpha|_h - C^i_\alpha\big|_l \, \Phi_\alpha|_l - D^{ij}_{\Phi_\alpha}\Big|_h \, \frac{\partial \Phi_\alpha}{\partial \xi^j}\Big|_h + D^{ij}_{\Phi_\alpha}\Big|_l \, \frac{\partial \Phi_\alpha}{\partial \xi^j}\Big|_l,
\end{aligned}$$

where

$$i = \begin{cases} 1 & ;\ h = u,\ l = d \\ 2 & ;\ h = n,\ l = s \\ 3 & ;\ h = e,\ l = w \end{cases} \tag{2.24}$$

indicate the pair of faces in question. The phasic convection and diffusion coefficients C^i_α, D^{ij}_α and $D^{ij}_{\Phi_\alpha}$ are specified by the relations

$$C^i_\alpha\big|_c = \phi_\alpha|_c \, \rho_\alpha|_c \, \hat{u}^i_\alpha\big|_c \tag{2.25}$$

$$D^{ij}_\alpha\big|_c = \phi_\alpha|_c \, \mu_\alpha|_c \, G_{ij}|_c \tag{2.26}$$

$$D^{ij}_{\Phi_\alpha}\Big|_c = \phi_\alpha|_c \, \Gamma_\alpha|_c \, G_{ij}|_c, \tag{2.27}$$

where

$$i = \begin{cases} 1 & ;\ c = u, d \\ 2 & ;\ c = n, s \\ 3 & ;\ c = e, w \end{cases} \tag{2.28}$$

and

$$G_{ij} = \frac{A_m^i A_m^j}{|\mathbf{J}|}. \tag{2.29}$$

Values on cell faces

In order to calculate the flux terms $[\Phi]_d^u$, the material properties and the values of the dependent variables at the centers of the cell faces are needed. These values are found by a weighted linear interpolation scheme from the cell center values. The weight factors used in this context are based on the distances between cell centers and corresponding cell faces on the physical space (Fig. 2.3). The value on the cell face is then given by

$$\Phi|_c = \Phi_c = (1 - W_c)\Phi_P + W_c\Phi_C, \tag{2.30}$$

where

$$W_c = \frac{\Delta Pc}{\Delta Pc + \Delta Cc} \tag{2.31}$$

and where $c = (u, d, n, s, e, w)$ and $C = (U, D, N, S, E, W)$. This scheme is second order accurate in rectangular non-uniform meshes.

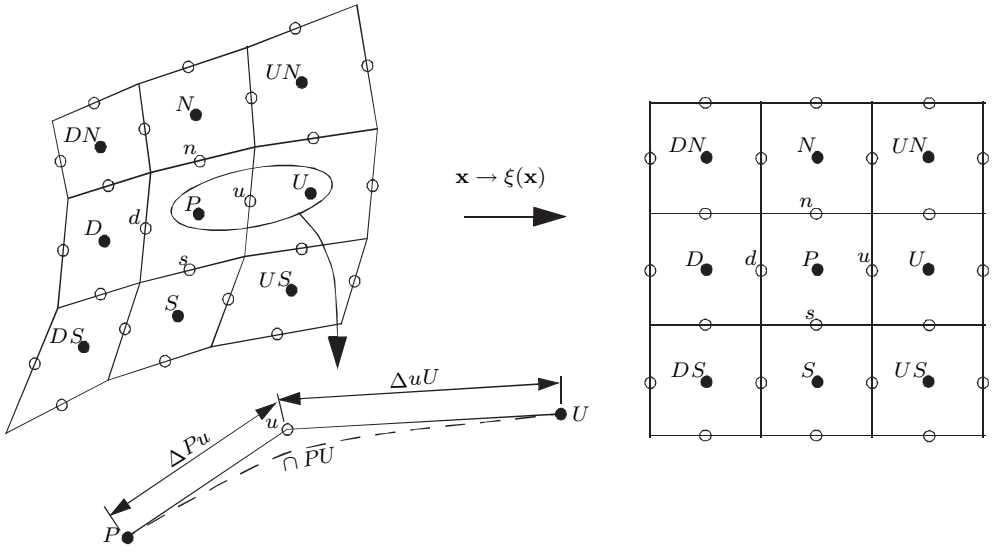

Figure 2.3: Illustration of the notations used in weighted interpolation.

Calculation of gradient at cell center

The source terms include the pressure gradients calculated at the cell centers. These gradients are approximated by the same type of weighted interpolation scheme like the one for values on the cell faces, but in order to enhance

the accuracy the weight factors are in this case based on the arc lengths between the cell centers (Fig. 2.3). Although the calculation of the arc lengths is computationally expensive, the Rhie-Chow interpolation method which is used to provide the normal flux velocity components $\hat{u}^i_\alpha$ on the cell faces requires second order accuracy also on the non-uniform curvilinear meshes. Thus the gradient at the cell center is obtained as

$$\left.\frac{\partial \Phi}{\partial x^i}\right|_P = W_L \Phi_H + (W_H - W_L)\Phi_P - W_H \Phi_L, \tag{2.32}$$

where the weight factors are defined to be

$$W_H = \frac{\cap HP}{\cap PL(\cap HP + \cap PL)} \tag{2.33}$$

$$W_L = \frac{\cap PL}{\cap HP(\cap HP + \cap PL)}. \tag{2.34}$$

Above the length of the arc for example from the point P to point L is denoted by $\cap PL$. According to the Eqn. (2.32), the pressure gradient source term in the discretized momentum equation is not calculated on the computational space but directly from the physical space gradient.

Calculation of gradient on cell faces

The total normal phasic fluxes include gradients of the dependent variable on the cell faces in their terms involved with diffusion fluxes. These gradients are all discretized using central differences on computational space. For the gradients normal to the cell faces the central difference method is applied as

$$\left.\frac{\partial \Phi}{\partial \xi^i}\right|_c = \Phi_C - \Phi_P \quad \text{with} \quad i = \begin{cases} 1; C = U, c = u \\ 2; C = N, c = n \\ 3; C = E, c = e. \end{cases} \tag{2.35}$$

In the case of cross-derivatives, i.e., derivatives on the plane of the cell face, the gradients are approximated as the mean of the two central differences calculated at the cell centers on the both sides of the face in question. As an example, the cross-derivatives on the cell face u are (Fig. 2.3)

$$\left.\frac{\partial \Phi}{\partial \xi^2}\right|_u = \tfrac{1}{4}(\Phi_N - \Phi_S + \Phi_{UN} - \Phi_{US}) \tag{2.36}$$

$$\left.\frac{\partial \Phi}{\partial \xi^3}\right|_u = \tfrac{1}{4}(\Phi_E - \Phi_W + \Phi_{UE} - \Phi_{UW}). \tag{2.37}$$

Approximation of the cross-derivatives connects eighteen neighboring cells to the treatment of every finite volume cell. To reduce the bandwidth of the coefficient matrix the treatment is reduced back to the usual one involving only the eight neighboring cells sharing a cell face with the cell under

consideration by the *deferred correction approach*, i.e., treating the cross-derivatives as source terms by using values from the previous iteration for the dependent variables in question. Thus in addition to the terms related to the gradients normal to the cell faces (the diagonal terms of the diffusion tensor), the deferred correction approach results to the following additional source terms expressing the effect of non-orthogonality

$$S^D_{\Phi_\alpha} = \left[D^{12}_{\Phi_\alpha} \frac{\partial^\star \Phi_\alpha}{\partial \xi^2} + D^{13}_{\Phi_\alpha} \frac{\partial^\star \Phi_\alpha}{\partial \xi^3} \right]_d^u + \left[D^{21}_{\Phi_\alpha} \frac{\partial^\star \Phi_\alpha}{\partial \xi^1} + D^{23}_{\Phi_\alpha} \frac{\partial^\star \Phi_\alpha}{\partial \xi^3} \right]_s^n + \left[D^{31}_{\Phi_\alpha} \frac{\partial^\star \Phi_\alpha}{\partial \xi^1} + D^{32}_{\Phi_\alpha} \frac{\partial^\star \Phi_\alpha}{\partial \xi^2} \right]_w^e, \quad (2.38)$$

where ${}^\star\Phi_\alpha$ denotes the value of the dependent variable from the previous iteration.

Following the details given above the formally discretized macroscopic balance equations (2.17), (2.18) and (2.19) can now be written in the final form. To enhance the readability and to keep more physical nature in the discretized equations they are next given in a partly discretized form retaining most of the terms in their previous form. Thus the macroscopic balance equations of mass, momentum and generic dependent scalar variables are

$$C^1_\alpha\big|_u - C^1_\alpha\big|_d + C^2_\alpha\big|_n - C^2_\alpha\big|_s + C^3_\alpha\big|_e - C^3_\alpha\big|_w = -\left[\frac{\phi_\alpha|_P \, \rho_\alpha|_P \, V_P}{\Delta t} \right]_t^{t+\Delta t} \quad (2.39)$$

$$\begin{aligned} \sum_c a_{u^k_\alpha}\Big|_c \, u^k_\alpha\Big|_P &= \sum_{c,C} a_{u^k_\alpha}\Big|_c \, u^k_\alpha\Big|_C - \phi_\alpha|_P \, \frac{\partial p}{\partial x^k}\bigg|_P V_P \\ &+ \left[\phi_\alpha \mu_\alpha \frac{A^1_m A^j_k}{|\mathbf{J}|} \frac{\partial u^m_\alpha}{\partial \xi^j} \right]_d^u + \left[\phi_\alpha \mu_\alpha \frac{A^2_m A^j_k}{|\mathbf{J}|} \frac{\partial u^m_\alpha}{\partial \xi^j} \right]_s^n + \left[\phi_\alpha \mu_\alpha \frac{A^3_m A^j_k}{|\mathbf{J}|} \frac{\partial u^m_\alpha}{\partial \xi^j} \right]_w^e \\ &+ \phi_\alpha|_P \, {}^0F^k_\alpha\Big|_P V_P + \sum_{\beta=1}^{N_p} B_{\alpha\beta}|_P \, (u^k_\beta\Big|_P - u^k_\alpha\Big|_P) V_P \\ &+ S^D_{u^k_\alpha} - \left[\frac{\phi_\alpha|_P \, \rho_\alpha|_P \, u^k_\alpha|_P \, V_P}{\Delta t} \right]_t \end{aligned} \quad (2.40)$$

$$\begin{aligned} \sum_c a_{\Phi_\alpha}|_c \, \Phi_\alpha|_P &= \sum_{c,C} a_{\Phi_\alpha}|_c \, \Phi_\alpha|_C + \sum_{\beta=1}^{N_p} B^I_{\alpha\beta}\Big|_P \, (\Phi_\beta|_P - \Phi_\alpha|_P) V_P \\ &+ {}^0S_\alpha\big|_P \, V_P \\ &+ S^D_{\Phi_\alpha} - \left[\frac{\phi_\alpha|_P \, \rho_\alpha|_P \, \Phi_\alpha|_P \, V_P}{\Delta t} \right]_t . \end{aligned} \quad (2.41)$$

In the Eqn. (2.41) ${}^0F^k_\alpha\big|_P$ and ${}^0S_\alpha\big|_P$ are the constant part of the linearized source terms. The summation symbols are defined as

$$\sum_c \Phi|_c = \Phi|_u + \Phi|_d + \Phi|_n + \Phi|_s + \Phi|_e + \Phi|_w \quad (2.42)$$

$$\sum_{c,C} a|_c \, \Phi|_C = a|_u \, \Phi|_U + a|_d \, \Phi|_D + a|_n \, \Phi|_N + a|_s \, \Phi|_S + a|_e \, \Phi|_E + a|_w \, \Phi|_W \, . \tag{2.43}$$

With hybrid differencing scheme the matrix coefficient from convective and diffusive transport above can be written as

$$\begin{aligned} a_{\Phi_\alpha}|_h &= \max\left(\tfrac{1}{2}\left|C^i_\alpha|_h\right|, D^{ii}_{\Phi_\alpha}|_h\right) - \tfrac{1}{2}\, C^i_\alpha|_h \quad i = \begin{cases} 1; h = u \\ 2; h = n \\ 3; h = e \end{cases} \\ a_{\Phi_\alpha}|_l &= \max\left(\tfrac{1}{2}\left|C^i_\alpha|_l\right|, D^{ii}_{\Phi_\alpha}|_l\right) + \tfrac{1}{2}\, C^i_\alpha|_l \quad i = \begin{cases} 1; l = d \\ 2; l = s \\ 3; l = w \end{cases} \end{aligned} \tag{2.44}$$

In the hybrid differencing scheme the central differencing is utilized when the cell Peclet number ($\mathrm{Pe}_\alpha = C_\alpha / D^{ii}_{\Phi_\alpha}$) is below two and the upwind differencing, ignoring diffusion, is performed when the Peclet number is greater than two. This scheme together with the deferred correction approach associated with the gradients on the cell faces guarantees the diagonal dominance of the resulting coefficient matrix. For that reason hybrid differencing scheme serves as the base method for which other more accurate schemes can be built upon by the deferred correction approach [Com, LL94].

2.2.3 Rhie-Chow algorithm

In calculating the convection fluxes across cell faces, velocities have to be inferred from those calculated at cell centers. A straightforward linear interpolation, i.e.,

$$u^i_\alpha\big|_e = \overline{u^i_\alpha|_e} = (1 - W_e)\; u^i_\alpha\big|_P + W_e \; u^i_\alpha\big|_E \tag{2.45}$$

would lead to the well known chequer-board oscillations in the pressure field, since the use of $2\delta\xi$-centered differences for the computation of pressure gradients at control cell centers effectively decouples the even and odd grids. This problem is overcome by the Rhie-Chow algorithm where the cell boundary velocities are obtained by interpolating the discrete momentum equations.

The Cartesian velocity components $u^k_\alpha\big|_P$, $u^k_\alpha\big|_E$ at control volume centered at P and at E correspondingly obey the discretized momentum equation (2.40) given in short hand form as

$$u^i_\alpha\big|_P + b_{\alpha i}{}^k\Big|_P \left.\frac{\partial p}{\partial x^k}\right|_P = S^i_\alpha\big|_P \tag{2.46}$$

$$u^i_\alpha\big|_E + b_{\alpha i}{}^k\Big|_E \left.\frac{\partial p}{\partial x^k}\right|_E = S^i_\alpha\big|_E, \tag{2.47}$$

where

$$b_{\alpha i}^{k}\Big|_C = \frac{\phi_\alpha|_C\, A_i^k}{\sum_c a_{u_\alpha^i}\big|_c} \tag{2.48}$$

$$S_\alpha^i\big|_C = \left(\left[\phi_\alpha \mu_\alpha \frac{A_m^1 A_i^j}{|\mathbf{J}|} \frac{\partial u_\alpha^m}{\partial \xi^j} \right]_d^u + \left[\phi_\alpha \mu_\alpha \frac{A_m^2 A_i^j}{|\mathbf{J}|} \frac{\partial u_\alpha^m}{\partial \xi^j} \right]_s^n + \left[\phi_\alpha \mu_\alpha \frac{A_m^3 A_i^j}{|\mathbf{J}|} \frac{\partial u_\alpha^m}{\partial \xi^j} \right]_w^e \right.$$
$$+ \phi_\alpha|_P\, {}^0F_\alpha^i\big|_P\, V_P + \sum_{\beta=1}^{N_p} B_{\alpha\beta}|_P\, (u_\beta^i\big|_P - u_\alpha^i\big|_P) V_P + S_{u_\alpha^i}^D$$
$$\left. - \left[\frac{\phi_\alpha|_P\, \rho_\alpha|_P\, u_\alpha^i\big|_P\, V_P}{\Delta t} \right]_t^{t+\Delta t} \right) \Big/ \left(\sum_c a_{u_\alpha^i}\big|_c \right). \tag{2.49}$$

In a staggered grid approach the pressure oscillation is avoided by discretizing the momentum equation on the grid whose centers are the faces of the original grid. In this case the face velocity component obeys the discretized momentum equation

$$u_\alpha^i\big|_e + b_{\alpha i}^{k}\Big|_e \left.\frac{\partial p}{\partial x^k}\right|_e = S_\alpha^i\big|_e, \tag{2.50}$$

where the pressure gradients are calculated using $1\delta\xi$-centered differences.

In the Rhie-Chow method the solution of Eqn. (2.50) is approximated interpolating linearly momentum equations (2.46) and (2.47). Approximating the right side term in Eqn. (2.50) by weighted linear interpolation of the corresponding terms in Eqns. (2.46) and (2.47) we get

$$u_\alpha^i\big|_e + b_{\alpha i}^{k}\Big|_e \left.\frac{\partial p}{\partial x^k}\right|_e = \overline{S_\alpha^i|_e} = \overline{u_\alpha^i|_e} + \overline{b_{\alpha i}^{k}\big|_e \left.\frac{\partial p}{\partial x^k}\right|_e}. \tag{2.51}$$

Assuming that $b_{\alpha i}^{k}\big|_e \approx \overline{b_{\alpha i}^{k}\big|_e}$, we obtain

$$u_\alpha^i\big|_e = \overline{u_\alpha^i|_e} + \overline{b_{\alpha i}^{k}\big|_e} \left(\overline{\left.\frac{\partial p}{\partial x^k}\right|_e} - \left.\frac{\partial p}{\partial x^k}\right|_e \right). \tag{2.52}$$

For the normal velocity components $\hat{u}_\alpha^i = A_k^i u_\alpha^k$ we get

$$\hat{u}_\alpha^i\big|_e = \overline{\hat{u}_\alpha^i|_e} + \overline{\hat{b}_\alpha^{ik}\big|_e} \left(\overline{\left.\frac{\partial p}{\partial x^k}\right|_e} - \left.\frac{\partial p}{\partial x^k}\right|_e \right), \tag{2.53}$$

where

$$\overline{\hat{b}_\alpha^{ik}\Big|_e} = A_j^i \overline{b_{\alpha j}^{k}\big|_e}. \tag{2.54}$$

Since all pressure gradients are computed using central differences, the cross-derivative terms in Eqn. (2.53) cancel leaving the formula

$$\hat{u}_\alpha^i\big|_e = \overline{\hat{u}_\alpha^i|_e} + \overline{\hat{b}_\alpha^{ii}\big|_e} \left(\overline{\left.\frac{\partial p}{\partial x^i}\right|_e} - \left.\frac{\partial p}{\partial x^i}\right|_e \right). \tag{2.55}$$

2.2.4 Inter-phase coupling algorithms

The macroscopic phasic balance equations (2.39), (2.40) and (2.41) are coupled to the corresponding balance equations of the other phases with the transport related to the change of phase and with the interfacial force density. In many cases these couplings are strong which results into a very slow convergence when iterative sequential solution methods are used. To solve this problem some degree of implicitness is required in the treatment of the interfacial coupling terms. The approaches are introduced here using the equation of the generic dependent variable (2.41).

Explicit treatment

The only necessary operation in this approach is to transfer all the terms depending on the variable to be solved, Φ_α, to the left side of Eqn. (2.41) (implicit handling of Φ_α) and leave the other terms on the right side (explicit handling of Φ_β). The resulting linear equation can be expressed in the following compact form

$$\mathcal{A}_{\Phi_\alpha}\, \Phi_\alpha|_P = \mathcal{C}_{\Phi_\alpha} \tag{2.56}$$

$$\mathcal{A}_{\Phi_\alpha} = \sum_c a_{\Phi_\alpha}|_c + \sum_{\beta=1}^{N_p} B^I_{\alpha\beta}\big|_P\, V_P - {}^1S_\alpha\big|_P\, V_P + \frac{\phi_\alpha|_P\, \rho_\alpha|_P\, V_P}{\Delta t} \tag{2.57}$$

$$\mathcal{C}_{\Phi_\alpha} = \sum_{c,C} a_{\Phi_\alpha}|_c\, \Phi_\alpha|_C + \sum_{\beta=1}^{N_p} B^I_{\alpha\beta}\big|_P\, \Phi_\beta|_P\, V_P + {}^0S_\alpha\big|_P\, V_P + S^D_{\Phi_\alpha} + \left.\frac{\phi_\alpha|_P\, \rho_\alpha|_P\, \Phi_\alpha|_P\, V_P}{\Delta t}\right|_t . \tag{2.58}$$

Partial Elimination Algorithm (PEA)

When there are only two phases to be considered simultaneously, the phasic balance equations of the dependent variables Φ_α and Φ_β can be written in the form where they can be mathematically eliminated from the balance equations of each other. The equations for the phases α and β are first written as

$$\mathcal{A}_{\Phi_\alpha}\, \Phi_\alpha|_P = \mathcal{B}^I_{\alpha\beta}(\,\Phi_\beta|_P - \Phi_\alpha|_P) + \mathcal{C}_{\Phi_\alpha} \tag{2.59}$$

$$\mathcal{A}_{\Phi_\beta}\, \Phi_\beta|_P = \mathcal{B}^I_{\alpha\beta}(\,\Phi_\alpha|_P - \Phi_\beta|_P) + \mathcal{C}_{\Phi_\beta}, \tag{2.60}$$

where the coefficient $\mathcal{A}_{\Phi_\alpha}$, $\mathcal{A}_{\Phi_\beta}$, $\mathcal{B}_{\alpha\beta}$, $\mathcal{C}_{\Phi_\alpha}$ and $\mathcal{C}_{\Phi_\beta}$ are defined by the equations

$$\mathcal{A}_{\Phi_\alpha} = \sum_c a_{\Phi_\alpha}|_c - {}^1S_\alpha\big|_P\, V_P + \frac{\phi_\alpha|_P\, \rho_\alpha|_P\, V_P}{\Delta t} \tag{2.61}$$

$$\mathcal{A}_{\Phi_\beta} = \sum_c a_{\Phi_\beta}\big|_c - {}^1S_\beta\big|_P V_P + \frac{\phi_\beta|_P\, \rho_\beta|_P\, V_P}{\Delta t} \tag{2.62}$$

$$\mathcal{B}^I_{\alpha\beta} = B^I_{\alpha\beta}\big|_P V_P \tag{2.63}$$

$$\mathcal{C}_{\Phi_\alpha} = \sum_{c,C} a_{\Phi_\alpha}\big|_c\, \Phi_\alpha|_C + {}^0S_\alpha\big|_P V_P + S^D_{\Phi_\alpha} + \frac{\phi_\alpha|_P\, \rho_\alpha|_P\, \Phi_\alpha|_P V_P}{\Delta t}\Big|_t \tag{2.64}$$

$$\mathcal{C}_{\Phi_\beta} = \sum_{c,C} a_{\Phi_\beta}\big|_c\, \Phi_\beta|_C + {}^0S_\beta\big|_P V_P + S^D_{\Phi_\beta} + \frac{\phi_\beta|_P\, \rho_\beta|_P\, \Phi_\beta|_P V_P}{\Delta t}\Big|_t. \tag{2.65}$$

Eqns. (2.59) and (2.60) can be rearranged to the form

$$(\mathcal{A}_{\Phi_\alpha} + \mathcal{B}^I_{\alpha\beta})\, \Phi_\alpha|_P = \mathcal{B}^I_{\alpha\beta}\, \Phi_\beta|_P + \mathcal{C}_{\Phi_\alpha} \tag{2.66}$$

$$(\mathcal{A}_{\Phi_\beta} + \mathcal{B}^I_{\alpha\beta})\, \Phi_\beta|_P = \mathcal{B}^I_{\alpha\beta}\, \Phi_\alpha|_P + \mathcal{C}_{\Phi_\beta}. \tag{2.67}$$

Now it is clearly seen that when the inter-phase transfer coefficient $\mathcal{B}^I_{\alpha\beta}$ is very large, the values of the the two phases are very close to each other. Furthermore, in the sequential iterative solution the variables would have changed very little from their starting values and thereby the rate of convergence is slow. PEA algorithm manipulates the above equations to eliminate Φ_α and Φ_β from the Eqns. (2.59) and (2.60) giving

$$\left(\mathcal{A}_{\Phi_\alpha} + \frac{\mathcal{B}^I_{\alpha\beta}}{\mathcal{A}_{\Phi_\beta}}(\mathcal{A}_{\Phi_\alpha} + \mathcal{A}_{\Phi_\beta})\right) \Phi_\alpha|_P = \frac{\mathcal{B}^I_{\alpha\beta}}{\mathcal{A}_{\Phi_\beta}}(\mathcal{C}_{\Phi_\alpha} + \mathcal{C}_{\Phi_\beta}) + \mathcal{C}_{\Phi_\alpha} \tag{2.68}$$

$$\left(\mathcal{A}_{\Phi_\beta} + \frac{\mathcal{B}^I_{\alpha\beta}}{\mathcal{A}_{\Phi_\alpha}}(\mathcal{A}_{\Phi_\alpha} + \mathcal{A}_{\Phi_\beta})\right) \Phi_\beta|_P = \frac{\mathcal{B}^I_{\alpha\beta}}{\mathcal{A}_{\Phi_\alpha}}(\mathcal{C}_{\Phi_\alpha} + \mathcal{C}_{\Phi_\beta}) + \mathcal{C}_{\Phi_\beta}. \tag{2.69}$$

Clearly the Eqns. (2.68) and (2.69) are now fully decoupled from each other and the problem of slow convergence related to the strong coupling of phases is eliminated. Though it should be noticed that in this approach only the interfacial force density can be incorporated implicitly in the algorithm but the transfer related to the change of phase would be treated as in the explicit method above.

Simultaneous solution of Non-linearly Coupled Equations (SINCE)

The PEA algorithm, developed for twophase flows above, can not be generalized for multifluid conditions. A straightforward method to include some implicitness in the treatment of the interfacial coupling terms also in multifluid flows has been developed by Lo [Lo89]. The generic macroscopic balance law for N_p phases can be arranged like Eqns. (2.66) and (2.67) in the twophase case to the following system of linear equations

$$\begin{aligned}
\mathcal{D}_{\Phi_1}\,\Phi_1|_P &= \mathcal{B}^I_{12}\,\Phi_2|_P + \mathcal{B}^I_{13}\,\Phi_3|_P + \ldots + \mathcal{B}^I_{1N_P}\,\Phi_{N_P}|_P + \mathcal{C}_{\Phi_1}\\
\mathcal{D}_{\Phi_2}\,\Phi_2|_P &= \mathcal{B}^I_{21}\,\Phi_1|_P + \mathcal{B}^I_{23}\,\Phi_3|_P + \ldots + \mathcal{B}^I_{2N_P}\,\Phi_{N_P}|_P + \mathcal{C}_{\Phi_2}\\
&\vdots \\
\mathcal{D}_{\Phi_{N_P}}\,\Phi_{N_P}|_P &= \mathcal{B}^I_{N_P1}\,\Phi_1|_P + \mathcal{B}^I_{N_P2}\,\Phi_2|_P + \ldots\\
&\qquad + \mathcal{B}^I_{N_P(N_P-1)}\,\Phi_{N_P-1}|_P + \mathcal{C}_{\Phi_{N_P}},
\end{aligned} \tag{2.70}$$

where

$$\mathcal{D}_{\Phi_\alpha} = \mathcal{A}_{\Phi_\alpha} + \sum_{\beta=1}^{N_P} \mathcal{B}^I_{\alpha\beta}. \tag{2.71}$$

This can be written in a matrix form as

$$\mathbf{E}_\Phi\,\Phi|^\star_P = \mathbf{C}_\Phi, \tag{2.72}$$

where $\Phi|^\star_P$ is the solution vector, $\mathbf{E}_\Phi$ is the coefficient matrix and $\mathbf{C}_\Phi$ is the right hand side vector. Solving this system cell by cell the new estimates are obtained. These are next substituted for the interfacial coupling terms on the right side of Eqns. (2.70) resulting to the following explicit balance equation

$$\mathcal{D}_{\Phi_\alpha}\,\Phi_\alpha|_P = \mathcal{C}_{\Phi_\alpha} + \sum_{\beta=1}^{N_P} \mathcal{B}^I_{\alpha\beta}\,\Phi_\beta|^\star_P. \tag{2.73}$$

2.2.5 Solution of volume fraction equations

In the simplified form the continuity equations (2.39) can be written for the solution of volume fractions as

$$\phi_\alpha|_P = \frac{N_\alpha}{D_\alpha} \tag{2.74}$$

where

$$D_\alpha = \sum_c a_{\phi_\alpha}|_c + \frac{\rho_\alpha|_P\,V_P}{\Delta t} \tag{2.75}$$

$$N_\alpha = \sum_{c,C} a_{\phi_\alpha}|_c\,\phi_\alpha|_C + \left.\frac{\phi_\alpha|_P\,\rho_\alpha|_P\,V_P}{\Delta t}\right|_t. \tag{2.76}$$

The coefficient $a_{\phi_\alpha}|_c$, $b_{\phi_\alpha}|_c$ above are defined as

$$a_{\phi_\alpha}|_h = \tfrac{1}{2}\,\rho_\alpha|_h \left(|\,\hat{u}^i_\alpha\big|_h\,| - \hat{u}^i_\alpha\big|_h\right), \quad i = \begin{cases} 1 & ;\ h = u \\ 2 & ;\ h = n \\ 3 & ;\ h = e \end{cases} \tag{2.77}$$

$$a_{\phi_\alpha}|_l = \tfrac{1}{2}\,\rho_\alpha|_l \left(|\,\hat{u}^i_\alpha\big|_l\,| + \hat{u}^i_\alpha\big|_l\right), \quad i = \begin{cases} 1 & ;\ l = d \\ 2 & ;\ l = s \\ 3 & ;\ l = w \end{cases} \tag{2.78}$$

To ensure that the volume fractions always sum to unity, i.e.,

$$\sum_{\alpha=1}^{N_P} \phi_\alpha|_P = 1 \tag{2.79}$$

we can solve instead of Eqn.(2.74) the equation

$$\phi_\alpha|_P = \frac{N_\alpha}{D_\alpha(1 + \sum_{\beta=1}^{N_P} \frac{N_\beta - \phi_\beta D_\beta}{D_\beta})}. \tag{2.80}$$

This equation is equivalent to the original equation when the constraint equation (2.79) is used. Furthermore, we can see that Eqn. (2.80) reduces to the form of Eqn. (2.74) when the residuals $N_\alpha - \phi_\alpha D_\alpha$ of all the phases α vanish.

2.2.6 Pressure-velocity coupling

Because of the iterative nature of the solution procedure, the velocities u^k_α obtained from the solution of the phasic momentum equations do not usually fulfill the phasic (2.39) and total mass balances when substituted into the corresponding continuity equations. Therefore a correction to the pressure δp is desired which produces new estimates of the phasic velocities $u^{k\star}_\alpha$ obeying the total mass balance. These new estimates are denoted as a sum of the current value and a correction

$$u^{k\star}_\alpha = u^k_\alpha + \delta u^k_\alpha \tag{2.81}$$

$$\hat{u}^{k\star}_\alpha = \hat{u}^k_\alpha + \delta \hat{u}^k_\alpha \tag{2.82}$$

$$p^\star = p + \delta p. \tag{2.83}$$

To limit the interdependency of the cells the velocity corrections to the neighbors of the cell under consideration are discarded. Accordingly, these velocities are approximated by

$$u^{k\star}_\alpha\Big|_C = u^k_\alpha\Big|_C + W_{pc}\left(u^{k\star}_\alpha\Big|_P - u^k_\alpha\Big|_P\right), \tag{2.84}$$

where the weight factor $W_{pc} = 0$ for the SIMPLE algorithm and $W_{pc} = 1$ for the SIMPLEC algorithm [VDR84]. Substituting the Eqns. (2.81), (2.82), (2.83) and (2.84) to the momentum equation (2.40) results in

$$\begin{aligned}\left(A_{u_\alpha^k}\Big|_P - W_{pc} \sum_c a_{u_\alpha^k}\Big|_c \right) u_\alpha^{k\star}\Big|_P &= \sum_{c,C} a_{u_\alpha^k}\Big|_c \, u_\alpha^k\Big|_C \\ &- \phi_\alpha|_P \, A_k^i|_P \, \frac{\partial p}{\partial \xi^i}\Big|_P + s_{u_\alpha^k}^R - W_{pc} \sum_c a_{u_\alpha^k}\Big|_c \, u_\alpha^k\Big|_P \\ &- \phi_\alpha|_P \, A_k^i|_P \, \frac{\partial \delta p}{\partial \xi^i}\Big|_P , \end{aligned} \tag{2.85}$$

where

$$A_{u_\alpha^k}\Big|_P = \sum_c a_{u_\alpha^k}\Big|_c + \sum_{\beta=1}^{N_p} B_{\alpha\beta}|_P \, V_P + \frac{\phi_\alpha|_P \, \rho_\alpha|_P \, V_P}{\Delta t} \tag{2.86}$$

$$\begin{aligned} s_{u_\alpha^k}^R = & \left[\phi_\alpha \mu_\alpha \frac{A_m^1 A_k^j}{|\mathbf{J}|} \frac{\partial u_\alpha^m}{\partial \xi^j} \right]_d^u + \left[\phi_\alpha \mu_\alpha \frac{A_m^2 A_k^j}{|\mathbf{J}|} \frac{\partial u_\alpha^m}{\partial \xi^j} \right]_s^n \\ & + \left[\phi_\alpha \mu_\alpha \frac{A_m^3 A_k^j}{|\mathbf{J}|} \frac{\partial u_\alpha^m}{\partial \xi^j} \right]_w^e + \phi_\alpha|_P \, F_\alpha^k\Big|_P V_P \\ & + \sum_{\beta=1}^{N_P} B_{\alpha\beta}|_P \, u_\beta^k\Big|_P V_P + S_{u_\alpha^k}^D + \left. \frac{\left(\phi_\alpha|_P \, \rho_\alpha|_P \, u_\alpha^k|_P \, V_P \right)}{\Delta t} \right|_t \end{aligned} \tag{2.87}$$

Using the original equation (2.40) some terms are canceled from the Eqn. (2.86) and the desired corrections to the phasic Cartesian velocity components can now be written in a compact form

$$\delta u_\alpha^k\Big|_P = - \, \mathcal{H}_{\alpha k}^{\;\; i}|_P \, \frac{\partial \delta p}{\partial \xi^i}\Big|_P , \tag{2.88}$$

where

$$\mathcal{H}_{\alpha k}^{\;\; i}\big|_P = \frac{\phi_\alpha|_P \, A_k^i|_P}{V_P} \, h_\alpha^k\Big|_P , \tag{2.89}$$

and

$$h_\alpha^k\Big|_P = \frac{V_P}{A_{u_\alpha^k}\Big|_P - W_{pc} \sum_c a_{u_\alpha^k}\Big|_c} . \tag{2.90}$$

The corresponding corrections to the phasic normal flux velocity components are according to the definition of phasic normal flux

$$\delta \hat{u}_\alpha^i\big|_P = \hat{\mathcal{H}}_\alpha^{ij}\Big|_P \, \frac{\partial \delta p}{\partial \xi^i}\Big|_P , \tag{2.91}$$

where

$$\hat{\mathcal{H}}_\alpha^{ij}\Big|_P = A_k^i\big|_P \, \mathcal{H}_{\alpha k}^{\ j}\Big|_P = \sum_{k=1}^{3} \frac{\phi_\alpha|_P \, A_k^i\big|_P \, A_k^j\Big|_P}{V_P} \, h_\alpha^k\Big|_P . \tag{2.92}$$

The corrections to the phasic normal flux velocity components produce also new estimates for the phasic convection coefficients (2.25), which can be expressed as

$$C_\alpha^{i\,\star}\Big|_c = C_\alpha^i\big|_c + \delta C_\alpha^i\big|_c = \phi_\alpha|_c \, \rho_\alpha|_c \, \hat{u}_\alpha^i\big|_c + \phi_\alpha|_c \, \rho_\alpha|_c \, \delta\hat{u}_\alpha^i\big|_c . \tag{2.93}$$

Finally to get the desired equation for the pressure correction the total mass balance is formed by adding all the phasic mass balances (2.39) together. Utilizing Eqn. (2.93) the joint continuity is given by

$$\begin{aligned} \sum_{\alpha=1}^{N_P} \Big[\big(& \delta C_\alpha^1\big|_u - \delta C_\alpha^1\big|_d + \delta C_\alpha^1\big|_n - \delta C_\alpha^1\big|_s \\ & + \delta C_\alpha^1\big|_e - \delta C_\alpha^1\big|_w + \mathcal{R}_{m_\alpha} \big) \,/\, \rho_\alpha|_P \Big] = 0, \end{aligned} \tag{2.94}$$

where $\mathcal{R}_{m_\alpha}$ denotes the phasic mass residual with the current convection coefficients C_α^i

$$\begin{aligned} \mathcal{R}_{m_\alpha} = \left[\frac{\phi_\alpha|_P \, \rho_\alpha|_P \, V_P}{\Delta t} \right]_t^{t+\Delta t} & + C_\alpha^1\big|_u - C_\alpha^1\big|_d + C_\alpha^2\big|_n - C_\alpha^2\big|_s + C_\alpha^3\big|_e \\ & - C_\alpha^3\big|_w . \end{aligned} \tag{2.95}$$

As shown by Eqn. (2.94), the mass balance of each phase is normalized by its phasic density before the summation in order to avoid bias of the correction procedure towards the heavier fluid. Evidently the total mass balance (2.94) can now be written for the corrections of the phasic normal flux velocity components as

$$\begin{aligned} \sum_{\alpha=1}^{N_P} \Big[\big(& \phi_\alpha|_u \, \rho_\alpha|_u \, \delta\hat{u}_\alpha^1\big|_u - \phi_\alpha|_d \, \rho_\alpha|_d \, \delta\hat{u}_\alpha^1\big|_d + \phi_\alpha|_n \, \rho_\alpha|_n \, \delta\hat{u}_\alpha^2\big|_n \\ & - \phi_\alpha|_s \, \rho_\alpha|_s \, \delta\hat{u}_\alpha^2\big|_s + \phi_\alpha|_e \, \rho_\alpha|_e \, \delta\hat{u}_\alpha^3\big|_e - \phi_\alpha|_w \, \rho_\alpha|_w \, \delta\hat{u}_\alpha^3\big|_w \\ & + \mathcal{R}_{m_\alpha} \big) \,/\, \rho_\alpha|_P \Big] = 0. \end{aligned} \tag{2.96}$$

In Eqn. (2.96) the corrections of the phasic normal flux velocity components are introduced on the cell faces. This necessitates interpolation of these values from the cell centers where they are originally determined (see Eqn. (2.91). The adjugate Jacobian matrix A_k^i is naturally defined on the cell face but the coefficient h_α^k has to be interpolated following the weighted linear interpolation procedure introduced by Eqn. (2.30). If the pressure correction

gradients on the cell faces are approximated using central differences on the computational space (2.35)–(2.37), Eqn. (2.91) can be substituted in the joint continuity equation (2.96) to give the desired pressure correction, namely

$$A_p|_P \, \delta p|_P = \sum_{c,C} a_p|_c \, \delta p|_C + S_p^D - \sum_{\alpha=1}^{N_P} \frac{\mathcal{R}_{m_\alpha}}{\rho_\alpha|_P}, \tag{2.97}$$

where

$$A_p|_P = \sum_c a_p|_c \tag{2.98}$$

$$a_p|_c = \sum_{\alpha=1}^{N_P} \frac{\phi_\alpha|_c \, \rho_\alpha|_c \, \hat{\mathcal{H}}_\alpha^{ij}\Big|_c}{\rho_\alpha|_P}. \tag{2.99}$$

The term S_p^D in Eqn.(2.97) denotes the cross-derivatives of the shared pressure corrections treated according to the deferred correction approach. Using the formal discretization notation it can be written as

$$\begin{aligned} S_p^D \;=\; & \left[E_p^{12} \frac{\partial^\star \delta p}{\partial \xi^2} + E_p^{13} \frac{\partial^\star \delta p}{\partial \xi^3} \right]_d^u + \left[E_p^{21} \frac{\partial^\star \delta p}{\partial \xi^1} + E_p^{23} \frac{\partial^\star \delta p}{\partial \xi^3} \right]_s^n \\ & + \left[E_p^{31} \frac{\partial^\star \delta p}{\partial \xi^1} + E_p^{32} \frac{\partial^\star \delta p}{\partial \xi^2} \right]_w^e, \end{aligned} \tag{2.100}$$

where the pressure correction coefficients are defined as

$$E_p^{ij} = \sum_{\alpha=1}^{N_P} \frac{\phi_\alpha|_c \, \rho_\alpha|_c \, \hat{\mathcal{H}}_\alpha^{ij}\Big|_c}{\rho_\alpha|_P}. \tag{2.101}$$

2.2.7 Solution algorithm

The discretized macroscopic balance equations of mass, momentum and generic scalar dependent variable (2.39), (2.40) and (2.41) are solved iteratively in a sequential manner. The solution methods studied are extensions of the well known single phase solution algorithm SIMPLE (Semi-Implicit Method for Pressure-Linked Equations) of Patankar & Spalding [PS72].

Inter Phase Slip Algorithm (IPSA)

The IPSA method [Spa77, Spa80, Spa83] is based on the following sequential solution steps repeated until the convergence is achieved:

Algorithm 1

1. Solve momentum equations for all the phases using values for the dependent variables obtained from the initial guess or from the previous iteration cycle.

2. Solve the pressure correction equation (2.97) based on the joint continuity equation (2.94).

3. Update the pressure (2.83).

4. Correct the phasic Cartesian velocity components (2.88).

5. Correct the normal flux velocities at cell centers (2.91).

6. Calculate the normal flux velocity components at cell faces with the Rhie-Chow interpolation method (2.55).

7. Calculate the phasic convection (2.25) coefficients.

8. Solve the phasic continuity equations for the phasic volume fractions from Eqn.(2.80).

9. Solve the conservation equations for the other scalar dependent variables.

As shown by Eqn. (2.85), in the IPSA method the interphase coupling terms are treated as in the explicit algorithm (2.56)– (2.58). In the IPSA-C method [KL99] the performance of the pressure correction step has been improved by incorporating the interphase coupling terms into this step following the idea of the SINCE method. In cases where the coupling of the phases is strong this improves convergence.

2.3 Multifluid Finite Element Method

In finite element methods the development of multifluid flow algorithms must also be based on the one phase algorithms. For one phase flow it is well known that the standard Galerkin methods may suffer from spurious oscillations when applied directly to Navier-Stokes equations. This is due to two main reasons. The first reason is the advection-diffusion character of the equations, when oscillations contaminate the dominating advection. The second reason is the mixed formulation character which, with unsuitable choice of pressure-velocity interpolations, may lead to pressure oscillations, similarly to FVM. These shortcomings can be dealt with proper choice of interpolation pair fulfilling the 'inf-sup' condition and modifying the advective operator to include some 'upwinding' effect. Recently, great interest have been taken in the so-called stabilized finite element methods [FFH92, FF92, FHS92], where these two problems can be handled by adding extra stabilizing terms into the system of variational equations. The consistency is preserved within these methods since the stabilizing terms will vanish with the residual of the governing equations. This stabilizing algorithm can be extended to cover twofluid flows [Hil97]. When applied a

strongly coupled system arises. Besides the inter-phase coupling we have an extra coupling, although not so tight, appearing through the stabilizing terms. The use of PEA like algorithms reducing the inter-phase coupling is not possible because of the nonlocal character of elementwise equations. To be able to solve this system properly all equations must be solved simultaneously. This amounts to need of more memory and computation time for a single iteration step but on the other hand when Newton based linearisation is used gives an optimal convergence rate and therefore less iteration steps are needed.

In this Section we will represent a stabilized finite element algorithm for the solution of isothermal steady-state twofluid continuum equations. Let $\Omega \in \mathbb{R}^{\mathrm{N}}$, $\mathrm{N} = 2, 3$ be the flow domain and let the carrier fluid be denoted by subscript f and the dispersed phase be denoted by subscript A. Let the phases be intrinsically incompressible, *i.e.*, $\tilde{\rho}_{\mathrm{A}} = \text{constant}, \tilde{\rho}_{\mathrm{f}} = \text{constant}$. Assuming stationary flow we get from Eqns. (2.1) and (2.3)

$$\begin{aligned}
\nabla \cdot (\phi_{\mathrm{A}} \bar{\mathbf{u}}_{\mathrm{A}}) &= 0 \qquad (2.102)\\
\nabla \cdot (\phi_{\mathrm{f}} \bar{\mathbf{u}}_{\mathrm{f}}) &= 0\\
-2\mu_{\mathrm{A}} \nabla \cdot (\phi_{\mathrm{A}} \boldsymbol{\Pi}(\bar{\mathbf{u}}_{\mathrm{A}})) + \tilde{\rho}_{\mathrm{A}} \phi_{\mathrm{A}} (\bar{\mathbf{u}}_{\mathrm{A}} \cdot \nabla) \bar{\mathbf{u}}_{\mathrm{A}} &= -\phi_{\mathrm{A}} \nabla \tilde{p} + B(\bar{\mathbf{u}}_{\mathrm{A}} - \bar{\mathbf{u}}_{\mathrm{f}})\\
&\quad + \phi_{\mathrm{A}} \tilde{\mathbf{F}}_{\mathrm{A}}\\
-2\mu_{\mathrm{f}} \nabla \cdot (\phi_{\mathrm{f}} \boldsymbol{\Pi}(\bar{\mathbf{u}}_{\mathrm{f}})) + \tilde{\rho}_{\mathrm{f}} \phi_{\mathrm{f}} (\bar{\mathbf{u}}_{\mathrm{f}} \cdot \nabla) \bar{\mathbf{u}}_{\mathrm{f}} &= -\phi_{\mathrm{f}} \nabla \tilde{p} + B(\bar{\mathbf{u}}_{\mathrm{f}} - \bar{\mathbf{u}}_{\mathrm{A}})\\
&\quad + \phi_{\mathrm{f}} \tilde{\mathbf{F}}_{\mathrm{f}},
\end{aligned}$$

where $\boldsymbol{\Pi}(\bar{\mathbf{u}}) = \frac{1}{2}(\nabla \bar{\mathbf{u}} + (\nabla \bar{\mathbf{u}})^t)$ is the rate of deformation tensor. For simplicity, viscosities μ_α are assumed to be constant. For the inter-phase momentum transfer coefficient we have $B = B_{\mathrm{Af}} = B_{\mathrm{fA}}$. Next we will write Eqns. (2.102) in dimensionless form. To this end we introduce the dimensionless coordinates and independent variables. Let U be some characteristic velocity and L some characteristic length of the system. We define $\mathbf{x}^\star = \mathbf{x}/\mathrm{L}$ to be the dimensionless coordinate, $\mathbf{u}_\alpha^\star = \bar{\mathbf{u}}_\alpha/\mathrm{U}$ to be the dimensionless velocity and $p^\star = \tilde{p}/(\tilde{\rho}_{\mathrm{f}} \mathrm{U}^2)$ to be the dimensionless pressure. With these notations Eqns. (2.102) can be written in a dimensionless form as

$$\begin{aligned}
\nabla^\star \cdot (\phi_{\mathrm{A}} \mathbf{u}_{\mathrm{A}}^\star) &= 0 \qquad (2.103)\\
\nabla^\star \cdot (\phi_{\mathrm{f}} \mathbf{u}_{\mathrm{f}}^\star) &= 0\\
-(2/\mathrm{R}e_{\mathrm{A}}) \nabla^\star \cdot (\phi_{\mathrm{A}} \boldsymbol{\Pi}(\mathbf{u}_{\mathrm{A}}^\star)) + \phi_{\mathrm{A}} (\mathbf{u}_{\mathrm{A}}^\star \cdot \nabla^\star) \mathbf{u}_{\mathrm{A}}^\star &= \beta[-\phi_{\mathrm{A}} \nabla^\star p^\star + B^\star(\mathbf{u}_{\mathrm{f}}^\star - \mathbf{u}_{\mathrm{A}}^\star)\\
&\quad + \phi_{\mathrm{A}} \mathbf{F}_{\mathrm{A}}^\star]\\
-(2/\mathrm{R}e_{\mathrm{f}}) \nabla^\star \cdot (\phi_{\mathrm{f}} \boldsymbol{\Pi}(\mathbf{u}_{\mathrm{f}}^\star)) + \phi_{\mathrm{f}} (\mathbf{u}_{\mathrm{f}}^\star \cdot \nabla^\star) \mathbf{u}_{\mathrm{f}}^\star &= -\phi_{\mathrm{f}} \nabla^\star p^\star - B^\star(\mathbf{u}_{\mathrm{f}}^\star - \mathbf{u}_{\mathrm{A}}^\star)\\
&\quad + \phi_{\mathrm{f}} \mathbf{F}_\gamma^\star,
\end{aligned}$$

where $\mathrm{R}e_\alpha = \tilde{\rho}_\alpha \mathrm{UL}/\mu_\alpha$ is the Reynolds number for phase α, $\beta = \tilde{\rho}_{\mathrm{f}}/\tilde{\rho}_{\mathrm{A}}$ is the density ratio, $\nabla^\star$ is the dimensionless gradient operator, $B^\star = \mathrm{L}/(\bar{\rho}_{\mathrm{f}} \mathrm{U}) B$ is the dimensionless momentum transfer coefficient and $\mathbf{F}_\alpha^\star = \mathrm{L}/(\mathrm{U}^2 \tilde{\rho}_{\mathrm{f}}) \tilde{\mathbf{F}}_\alpha$ is the dimensionless body force.

2.3.1 Stabilized Finite Element Method

The traditional sequential methods, which are frequently used with the finite volume methods suffer from poor convergence when the inter-phase coupling is significant enough. In order to attain better convergence in such cases fully coupled equations must be solved. Although this will lead to a large algebraic system of equations and therefore will demand more memory and computation time, the achieved gain in convergence, especially when Newton-type linearization is used, will yield lower total cost in computing time. This is even more plausible in cases where efficient iterative solvers and especially matrix free algorithms are used. About the algorithmic procedures for effective solution strategies see the paper by Hughes and Jansen [HJ95]. Another advantage of the full coupling is the increased stability of the method. For Eqns. (2.103) stabilization must be applied at two levels, namely the stabilization of velocity pressure pair and the stabilization of phase volume fractions.

In what follows a stabilized finite element method for solving the system of Eqns. (2.103) is introduced [Hil97]. Within the method the above mentioned problems of coupling and stabilization of the equations are resolved. To understand the following presentation of the method the reader needs some basic knowledge of the functional spaces. One can study these things from the standard FEM text book, for example [KN90]. In the sequel $\mathrm{L}^2(\Omega)$ is the space of square integrable functions in Ω and $\mathrm{L}^2_0(\Omega)$ the space of functions in $\mathrm{L}^2(\Omega)$ with zero mean value in Ω. Furthermore $(\cdot,\cdot)$ stands for the L^2-inner product in Ω, *e.g.*, for functions $\mathbf{u},\mathbf{v}\in\mathbf{V}_h$ the L^2-inner product is defined as

$$(\mathbf{u},\mathbf{v}) = \sum_{i=1}^{N}\int_{\Omega} u_i v_i \mathrm{d}x. \tag{2.104}$$

Also, $\mathcal{C}^0(\Omega)$ is the space of continuous functions in Ω and $\mathrm{H}^1_0(\Omega)$ is the Sobolev space of functions with square integrable value and derivatives in Ω with zero value on the boundary of Ω.

In order to formulate the stabilized finite element method we first specify the required functional spaces as follows

$$\begin{aligned}\mathbf{V}_\mathrm{h} &= \{\mathbf{v}\in \mathrm{H}^1_0(\Omega)^\mathrm{N} \,:\, \mathbf{v}|_\mathrm{K}\in \mathrm{P}_\mathrm{k}(\mathrm{K})^\mathrm{N}, \mathrm{K}\in\Pi_\mathrm{h}\},\\ P_\mathrm{h} &= \{p\in \mathcal{C}^0(\Omega)\cap \mathrm{L}^2_0(\Omega) \,:\, p|_\mathrm{K}\in \mathrm{P}_\mathrm{l}(\mathrm{K}), \mathrm{K}\in\Pi_\mathrm{h}\},\end{aligned}$$

where N is the dimension of the problem and $\mathrm{k},\mathrm{l}\geq 1$ are integers. The symbol Π_h denotes the partition of $\bar{\Omega}$ into elements and h is the size of that partition. The symbol $\mathrm{P}_\mathrm{k}(\mathrm{K})$ denotes the space of polynomial functions of degree k or less defined on element K. Furthermore for volume fractions we introduce the space

$$\Phi_\mathrm{h} = \{\phi\in \mathrm{H}^1(\Omega) \,:\, \phi|_\mathrm{K}\in \mathrm{P}_\mathrm{m}(\mathrm{K}), \mathrm{K}\in\Pi_\mathrm{h}\},$$

where the integer m ≥ 1. In what follows, we drop the superscript $\star$ in Eqns. (2.103). The stabilized method considered for Eqns. (2.103) can now be stated formally as:

Method 2.3.1 *Find* $(\mathbf{u}_{\mathrm{A}_h}, \mathbf{u}_{\mathrm{f}_h}, \phi_{\mathrm{A}_h}, p_{\mathrm{h}}) \in \mathbf{V}_{\mathrm{h}} \times \mathbf{V}_{\mathrm{h}} \times \Phi_{\mathrm{h}} \times P_{\mathrm{h}}$ *such that*

$$\begin{aligned} A(\mathbf{u}_{\mathrm{A}_h}, \mathbf{u}_{\mathrm{f}_h}, \phi_{\mathrm{A}_h}, p_{\mathrm{h}}; \mathbf{v}_{\mathrm{A}}, \mathbf{v}_{\mathrm{f}}, q_{\mathrm{f}}, q_{\mathrm{A}}) &= F(\mathbf{v}_{\mathrm{A}}, \mathbf{v}_{\mathrm{f}}, q_{\mathrm{A}}, q_{\mathrm{f}}), \qquad (2.105) \\ & \quad (\mathbf{v}_{\mathrm{A}}, \mathbf{v}_{\mathrm{f}}, q_{\mathrm{A}}, q_{\mathrm{f}}) \in \mathbf{V}_{\mathrm{h}} \times \mathbf{V}_{\mathrm{h}} \times \Phi_{\mathrm{h}} \times P_{\mathrm{h}}, \end{aligned}$$

with

$$\begin{aligned} A(\mathbf{u}_{\mathrm{A}}, \mathbf{u}_{\mathrm{f}}, \phi_{\mathrm{A}}, p; \mathbf{v}_{\mathrm{A}}, \mathbf{v}_{\mathrm{f}}, q_{\mathrm{A}}, q_{\mathrm{f}}) &= \sum_{\alpha=\mathrm{A},f} \{ \underbrace{C_\alpha(\mathbf{u}_\alpha; \mathbf{v}_\alpha)}_{convection} + \underbrace{D_\alpha(\mathbf{u}_\alpha; \mathbf{v}_\alpha)}_{viscous\ stress} \\ & \quad - \underbrace{P_\alpha(\mathbf{v}_\alpha; p)}_{pressure} - \underbrace{P_\alpha(\mathbf{u}_\alpha; q_\alpha)}_{continuity} - \underbrace{I_\alpha(\mathbf{u}_\beta - \mathbf{u}_\alpha; \mathbf{v}_\alpha)}_{interaction} \\ & \quad + \underbrace{S_\alpha(\mathbf{u}_\alpha, p, \mathbf{u}_\beta - \mathbf{u}_\alpha; \mathbf{v}_\alpha, q_\alpha)}_{momentum\ stabilization} \\ & \quad + \underbrace{S^M_\alpha(\mathbf{u}_\alpha, \phi_\alpha; \mathbf{u}_\alpha, q_\alpha)}_{continuity\ stabilization} \} + \underbrace{\bar{D}_{\mathrm{A}}(\phi_{\mathrm{A}}; q_{\mathrm{A}})}_{discont.\ capturing} \ \} \\ F(\mathbf{v}_{\mathrm{A}}, \mathbf{v}_{\mathrm{f}}, q_{\mathrm{A}}, q_{\mathrm{f}}) &= \sum_{\alpha=\mathrm{A},f} B_\alpha(\mathbf{v}_\alpha, q_\alpha) \end{aligned}$$

where

$$\begin{aligned} C_\alpha(\mathbf{u}; \mathbf{v}) &= (\phi_\alpha \mathbf{u} \cdot \nabla \mathbf{u}, \mathbf{v}) \\ D_\alpha(\mathbf{u}; \mathbf{v}) &= ((2/\mathrm{R}e_\alpha)\phi_\alpha \boldsymbol{\Pi}(\mathbf{u}), \boldsymbol{\Pi}(\mathbf{v})) \\ \bar{D}_{\mathrm{A}}(\phi; q) &= (\kappa \nabla \phi, \nabla q) \\ P_\alpha(\mathbf{v}; q) &= (\nabla \cdot (\beta_\alpha \phi_\alpha \mathbf{v}), q) \\ I_\alpha(\mathbf{w}; \mathbf{v}) &= (B \beta_\alpha \mathbf{w}, \mathbf{v}) \\ S_\alpha(\mathbf{u}, p, \mathbf{w}; \mathbf{v}, q) &= (Res_\alpha(\mathbf{u}, p, \mathbf{w}), \tau_\alpha(\phi_\alpha \mathbf{u}_\alpha \cdot \nabla \mathbf{v} - \phi_\alpha \beta_\alpha \nabla q)) \\ Res_\alpha(\mathbf{u}, p, \mathbf{w}) &= -(2/\mathrm{R}e_\alpha) \nabla \cdot (\phi_\alpha \boldsymbol{\Pi}(\mathbf{u})) + \phi_\alpha \mathbf{u} \cdot \nabla \mathbf{u} + \phi_\alpha \beta_\alpha \nabla p - \beta_\alpha B \mathbf{w} \\ S^M_\alpha(\mathbf{u}, \phi; \mathbf{v}, q) &= (Res^M_\alpha(\phi, \mathbf{u}), \delta_\alpha \nabla \cdot (\beta_\alpha q \mathbf{v})) \\ Res^M_\alpha(\phi, \mathbf{u}) &= \nabla \cdot (\beta_\alpha \phi \mathbf{u}) \\ G_\alpha(\mathbf{v}, q) &= (\phi_\alpha \beta_\alpha \tilde{\mathbf{F}}_\alpha, \mathbf{v} + \tau_\alpha(\phi_\alpha \mathbf{u}_\alpha \cdot \nabla \mathbf{v} - \phi_\alpha \beta_\alpha \nabla q)) \\ \beta_\alpha &= \tilde{\rho}_{\mathrm{f}} / \tilde{\rho}_\alpha. \end{aligned}$$

The coefficient κ for discontinuity capturing operator and the stability parameters $\tau_\alpha, \delta_\alpha$ are defined as

$$\begin{aligned} \kappa &= c_{\mathrm{dif}} \mathrm{h}_{\mathrm{K}} Res_{\mathrm{TOT}} / (|\nabla U|_{\mathrm{p}} + \mathrm{h}_{\mathrm{K}}) \\ Res_{\mathrm{TOT}} &= |Res_{\mathrm{A}}|_1 + |Res_{\mathrm{f}}|_1 + |Res^{\mathrm{M}}_{\mathrm{A}}| + |Res^{\mathrm{M}}_{\mathrm{f}}| \end{aligned}$$

$$
\begin{aligned}
|\nabla U|_{\mathrm{p}} &= \sum_{i=1}^{\mathrm{N}}(|\nabla u_{\mathrm{A}_i}|_{\mathrm{p}} + |\nabla u_{\mathrm{f}_i}|_{\mathrm{p}}) + |\nabla \phi_{\mathrm{A}}|_{\mathrm{p}} + |\nabla p|_{\mathrm{p}} \\
\delta_{\mathrm{f}} &= \lambda_{\mathrm{f}} |\mathbf{u}_{\mathrm{f}}|_{\mathrm{p}} \mathrm{h_K} \xi(\mathrm{R}e_{\mathrm{f}}^{\mathrm{K}}(\mathbf{x})) \\
\delta_{\mathrm{A}} &= \lambda_{\mathrm{A}} |\phi_{\mathrm{A}}|_{\mathrm{p}} \mathrm{h_K} \xi(\mathrm{P}e_{\mathrm{A}}^{\mathrm{K}}(\mathbf{x})) \\
\tau_\alpha &= \tfrac{\mathrm{h_K}}{2|\mathbf{u}_\alpha|_{\mathrm{p}}} \xi(\mathrm{R}e_\alpha^{\mathrm{K}}(\mathbf{x})) \\
\mathrm{R}e_\alpha^{\mathrm{K}}(\mathbf{x}) &= \tfrac{1}{4} \mathrm{m_K} |\mathbf{u}_\alpha|_{\mathrm{p}} \mathrm{h_K} \mathrm{R}e_\alpha \\
\mathrm{P}e_{\mathrm{A}}^{\mathrm{K}}(\mathbf{x}) &= \tfrac{1}{2} \mathrm{m_K} |\mathbf{u}_{\mathrm{A}}|_{\mathrm{p}} \mathrm{h_K} / \kappa \\
\xi(\gamma) &= \begin{cases} \gamma, & 0 \le \gamma < 1 \\ 1, & \gamma \ge 1 \end{cases} \\
|\mathbf{u}_\alpha|_{\mathrm{p}} &= \begin{cases} \left(\sum_{\mathrm{i}=1}^{\mathrm{N}} |u_{\alpha_{\mathrm{i}}}|^{\mathrm{p}} \right)^{1/\mathrm{p}}, & 1 \le \mathrm{p} < \infty \\ \max_{\mathrm{i}=1,\mathrm{N}} |u_{\alpha_{\mathrm{i}}}|, & \mathrm{p} = \infty, \end{cases}
\end{aligned}
$$

where λ_α, $\mathrm{c_{dif}}$ and $\mathrm{m_K}$ are positive constants.

Notice that the variational system (2.105) is nonlinear due to the convection and interaction terms and due to the discontinuity capturing terms and the stabilization terms. The stabilization terms S_α for momentum equations are similar to those used for incompressible Navier-Stokes equations (see, *e.g.*, [FF92]). The only difference is that here the volume fractions are involved. The contribution arising from the lower order terms in stabilization, *i.e.*, the interaction terms in the momentum equations, is neglected. The inclusion of interaction terms would lead to different stability parameters. Such a case is studied for diffusion-convection type scalar equation for example in ref. [LFF95]. Since we shall restrict ourselves to linear approximations here, the terms including second order derivatives are neglected. The stabilization terms S_α^{M} arising from the continuity equations are different for each phase. For the carrier phase it affects directly the momentum equation while for dispersed phase it affects the continuity equation. That is also reason for the different normalization of the stabilization parameters δ_α. Since steep gradients can be expected in many applications of the method, we have introduced the discontinuity capturing operator $\bar{D}(\phi_{\mathrm{A}}, q_{\mathrm{A}})$ to the equations. In the above method this term is added only for continuity equation of the dispersed phase. The corresponding diffusivity coefficient κ depends on the discrete residual of the system. The form of the coefficient equals to the one introduced by Hansbo and Johnson [HJ91]. The value of the coefficient is largest near steep gradients and vanishes when the solution is smooth.

Stability analysis can be carried out for the linearized form of Eqns. (2.105) following the same guidelines as for incompressible Navier-Stokes equations (see, *e.g.*, [FF92]), except of additional complications which arise from the interaction terms and from the compressible nature of the flow.

The analysis is nevertheless nontrivial and is skipped here.

In Galerkin Finite Element Method the solution functions $(\mathbf{u}_{\mathrm{A}_h}, \mathbf{u}_{\mathrm{f}_h}, \phi_{\mathrm{A}_h}, p_{\mathrm{h}})$ are approximated as a linear combination of basis functions $(\tilde{\mathbf{v}}_{\mathrm{A}}, \tilde{\mathbf{v}}_{\mathrm{f}}, \tilde{q}_{\mathrm{A}}, \tilde{q}_{\mathrm{f}})$ in a finite-dimensional product space $\mathbf{V}_{\mathrm{h}} \times \mathbf{V}_{\mathrm{h}} \times \Phi_{\mathrm{h}} \times P_{\mathrm{h}}$. In other words, the phase velocities $u^k_{\alpha\mathrm{h}} \in V_h$, $\mathbf{V}_h = (V_h)^{\mathrm{N}}$ (componentwise) are approximated as

$$u^k_{\alpha h}(\mathbf{x}) = \sum_{j=1}^{\dim V_h} u^k_{\alpha j} \tilde{v}_j(\mathbf{x}),\ k = 1, \ldots, N \tag{2.106}$$

where $u^k_{\alpha j} \in \mathbb{R}$ are the unknowns in discretization points x_j, $j = 1, \ldots, \dim V_h$. In a same way the dispersed phase volume fraction ϕ_{A_h} and pressure p_{h} are approximated as

$$\phi_{\mathrm{A}_h}(\mathbf{x}) = \sum_{j=1}^{\dim \Phi_h} \phi_{\mathrm{A}\,j} \tilde{q_{\mathrm{A}}}_j(\mathbf{x}) \tag{2.107}$$

$$p_{\mathrm{h}}(\mathbf{x}) = \sum_{j=1}^{\dim P_h} p_j \tilde{q}_{\mathrm{f}\,j}(\mathbf{x}), \tag{2.108}$$

where $\phi_{\mathrm{A}\,j}$ and p_j are the nodal values of the dispersed phase volume fraction and pressure respectively. In the following we will assume that the unknowns are approximated using equal order elements and therefore the nodal values are collocated and if boundary effects (elimination of degrees of freedoms) are neglected the dimensions of the spaces equals, *i.e.*, we can denote $\dim V_h = \dim \Phi_h = \dim P \equiv n_{dofs}$.

In Galerkin approximation, the test functions $(\mathbf{v}_{\mathrm{A}}, \mathbf{v}_{\mathrm{f}}, q_{\mathrm{A}}, q_{\mathrm{f}})$ and basis functions $(\tilde{\mathbf{v}}_{\mathrm{A}}, \tilde{\mathbf{v}}_{\mathrm{f}}, \tilde{q}_{\mathrm{A}}, \tilde{q}_{\mathrm{f}})$ are taken from the same space. Let us then denote $\varphi_j \equiv \tilde{v}_j = \tilde{q_{\mathrm{A}}}_j = \tilde{q}_{\mathrm{f}\,j}$. Using definitions (2.106)–(2.108) the variational system of equations (2.105) can be written in semi-discretized matrix form

$$\mathbf{AU} = \mathbf{F}, \tag{2.109}$$

where $\mathbf{A}$ is an $(2 \times (\mathrm{N}+1) \times n_{dofs}) \times (2 \times (\mathrm{N}+1) \times n_{dofs})$ matrix and $\mathbf{F} = (F_1(k), F_2(k), \ldots, F_{2\times(\mathrm{N}+1)}(k))^t$ is the right hand side vector, where $F_i(k)$ are n_{dofs} dimensional subvectors. The vector $\mathbf{U} = (\mathbf{u}^1_{\mathrm{f}}, \ldots, \mathbf{u}^{\mathrm{N}}_{\mathrm{f}}, \mathbf{p}, \mathbf{u}^1_{\mathrm{A}}, \ldots, \mathbf{u}^{\mathrm{N}}_{\mathrm{A}}, \phi_{\mathrm{A}})^t$ is the nodal unknown, where the subvectors are defined by

$$\mathbf{u}^i_\alpha = (u^i_{\alpha 1}, \ldots, u^i_{\alpha n_{dofs}}) \tag{2.110}$$

$$\mathbf{p} = (p_1, p_2, \ldots, p_{n_{dofs}}) \tag{2.111}$$

$$\phi_{\mathrm{A}} = (\phi_{\mathrm{A}1}, \phi_{\mathrm{A}2}, \ldots, \phi_{\mathrm{A}n_{dofs}}). \tag{2.112}$$

Note that the above system of equations is nonlinear in the sense that the coefficient matrix $\mathbf{A}$ and the right hand side vector $\mathbf{F}$ depend on the solution $\mathbf{U}$.

2.3.2 Integration and isoparametric mapping

The construction of the coefficient matrix **A** and right hand side vector **F** requires the computation of integrals over interpolation functions φ_j. Instead of the global integration and global equations and global interpolation functions we can integrate in a single element with local equations and local interpolation functions. These local equations can then be assembled to a global system using special assembling algorithm. Details concerning these standard finite element procedures one can find in any textbook concerning finite element methods. One further standard procedure in finite element methods is the use of isoparametric mapping converting the physical coordinates into computational coordinates (compare with BFC in FVM). In finite element method the relationship between the physical coordinates (x^1, x^2, x^3) and the computational coordinates (ξ^1, ξ^2, ξ^3) for any element K in the partitioning Π_h is obtained using parametric concept, *i.e.*, a coordinate transformation defined by

$$x^i(\xi^j) = \sum_{k=1}^{n^{\mathrm{K}}_{nodes}} \lambda_k(\xi^j) x^i_k, \tag{2.113}$$

where λ_k are the interpolation functions over the element K and x^i_k the nodal coordinate values of that element. The symbol n^{K}_{nodes} denotes the number of the nodes in element K. The above defined transformation is quite general. When the interpolation functions defining the dependent variables are of the same order as the functions defining the element geometry, *i.e.*, $\varphi_i = \lambda_i$, the element is called isoparametric. If the order of λ_i is greater or less than that of φ_i the element is superparametric or subparametric correspondingly. For example the four node quadrilateral element in 2 dimension is isoparametric and we get

$$x^1(\xi^1, \xi^2) = \sum_{k=1}^{4} \tilde{\varphi}_k(\xi^1, \xi^2) x^1_k$$
$$x^2(\xi^1, \xi^2) = \sum_{k=1}^{4} \tilde{\varphi}_k(\xi^1, \xi^2) x^2_k$$

Note that the interpolation functions $\tilde{\varphi}_k(\xi^1, \xi^2)$ above are local functions in reference element, *i.e.*, they are the same for every physical element (see Fig. 2.4).

The derivatives are transferred according to the chain rule. In a matrix form we get

$$\begin{bmatrix} \frac{\partial \tilde{\varphi}_i}{\partial \xi^1} \\ \frac{\partial \tilde{\varphi}_i}{\partial \xi^2} \\ \frac{\partial \tilde{\varphi}_i}{\partial \xi^3} \end{bmatrix} = \mathbf{J} \begin{bmatrix} \frac{\partial \varphi_i}{\partial x^1} \\ \frac{\partial \varphi_i}{\partial x^2} \\ \frac{\partial \varphi_i}{\partial x^3} \end{bmatrix}, \tag{2.114}$$

where $\mathbf{J}$ is the Jacobian matrix of the mapping $\xi^j \rightarrow x^i(\xi^j)$. From this we get

$$\begin{bmatrix} \frac{\partial \varphi_i}{\partial x^1} \\ \frac{\partial \varphi_i}{\partial x^2} \\ \frac{\partial \varphi_i}{\partial x^3} \end{bmatrix} = \mathbf{J}^{-1} \begin{bmatrix} \frac{\partial \tilde{\varphi}_i}{\partial \xi^1} \\ \frac{\partial \tilde{\varphi}_i}{\partial \xi^2} \\ \frac{\partial \tilde{\varphi}_i}{\partial \xi^3} \end{bmatrix}, \tag{2.115}$$

where $\mathbf{J}^{-1}$ is the inverse of the Jacobian.

When isoparametric elements are used, integration can be done over the reference element. Let us denote the reference element by E. Now we have for example for the local convection coefficient

$$\begin{aligned} C_\alpha^{(\mathrm{K})}(k,l) &= (\phi_\alpha \mathbf{u}_\alpha \cdot \nabla \varphi_l, \varphi_k)_\mathrm{K} \\ &= \int_\mathrm{K} \phi_\alpha(\mathbf{x}) \mathbf{u}_\alpha(\mathbf{x}) \cdot \nabla \varphi_l(\mathbf{x}) \varphi_k(\mathbf{x}) \mathrm{d}\mathbf{x} \\ &= \int_\mathrm{E} \phi_\alpha(\xi) \mathbf{u}_\alpha(\xi) \cdot \nabla \varphi_l(\xi) \varphi_k(\xi) |\mathbf{J}| \mathrm{d}\xi \\ &= \int_\mathrm{E} \phi_\alpha(\xi) u_\alpha^i(\xi) (\mathbf{J}^{-1})^{im} \frac{\partial \tilde{\varphi}_l(\xi)}{\partial \xi^m} \tilde{\varphi}_k(\xi) |\mathbf{J}| \mathrm{d}\xi. \end{aligned}$$

In practise this integration must be done numerically. Gauss numerical integration formulae are used. The order of the integration is naturally kept the same as the interpolation order of the unknowns.

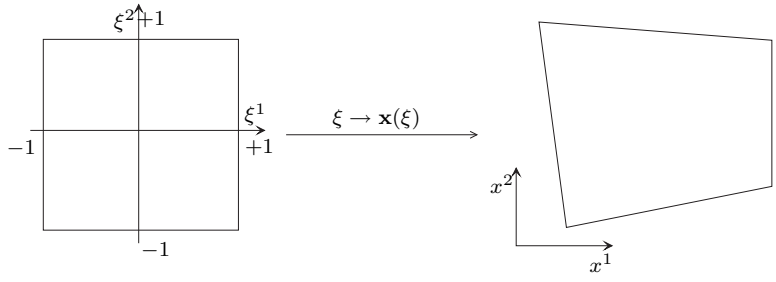

Figure 2.4: Mapping of the local reference element in ξ -coordinates to global element in physical $\mathbf{x}$ -coordinates for four point quadrilateral element

2.3.3 Solution of the discretized system

The system of nonlinear equations (2.109) is transferred to algebraic system using the integration formula given above. To solve this resulting nonlinear system of algebraic equations a variety of methods exists. Nonlinearity results to iterative methods. The most naive approach would be to use fixed point iteration (Picard iteration), where the nonlinearity is eliminated taking the coefficient values from the previous iteration step. Unfortunately this method results to slow convergence. More effective way is to

use Newton-type methods, where the system is expanded using Taylor series in the neigborhood of the solution. This results to method with asymptotically quadratic convergence. Unfortunately the radius of convergence of this method can sometimes be quite small and care must be exercised in the choice of the initial solution vector. Convergence radius can be expanded using for example the so called incremental method where the right side load is incremented step by step. Another way is to take a few Picard iteration steps before proceeding to the Newton steps. We might also have to control the magnitude of the Newton step. This is needed when the Jacobian is not calculated exactly like in the Modified Newton-Raphson method, where the Jacobian is calulated only once in the beginning of the iterations or like in the Quasi-Newton method where the Jacobian is updated in a more simple manner than calculating it exactly or like in the inexact Newton methods where the Jacobian is evaluated from the residual vector using difference approximations. An effective way is to use line-search backtracking.

For every nonlinear step we have to solve a linear system. When large systems are considered, like the system (2.109) mostly is, we have to use iterative solvers. Iterative solvers start with an initial guess and compute a sequence of approximate solutions that converge to the exact solution. The accuracy of the solutions depend on the number of iterations performed. When the linear equation solver is part of the nonlinear iteration loop, like we have, exact convergence is not required. The amount of work used with iterative solvers depends on the convergence rate and the desired accuracy. Depending on the system to be solved the convergence of the iterative methods can be slow and irregular. The rate of the convergence depends on the spectrum of the coefficient matrix and hence the condition number of the matrix. The rate of the convergence can often be increased by the technique of preconditioning. When the system of linear equations is nonsymmetric, like system (2.109), special methods must be used. Methods like Conjugate Gradient Squared (CGS) [SWd85] and the Generalized Minimum Residual Method (GMRES) [SS83] are succesively used. For the solution of the (2.109) the GMRES method is succesfully used [Hil97].

In the following the Newton-GMRES algorithm with the linesearch backtracking is introduced. Let the nonlinear system of equations be $\mathbf{R}(\mathbf{U}) = \mathbf{A}(\mathbf{U})\mathbf{U} - \mathbf{F}(\mathbf{U}) = \mathbf{0}$. Then the method as expressed in algorithmic form is as follows,

Algorithm 2

$\mathbf{U}_0$ given, $\mathrm{n} = -1$
REPEAT
  $\mathrm{n} = \mathrm{n} + 1$
  Solve $\mathbf{J}(\mathbf{U}^{\mathrm{n}})\delta(\mathrm{n}) = -\mathbf{R}(\mathbf{U}^{\mathrm{n}})$ by GMRES
  $\mathbf{U}^{\mathrm{n}+1} = \mathbf{U}^{\mathrm{n}} + \omega^{\mathrm{n}}\delta(\mathrm{n})$

UNTIL convergence
Above ω_{n} is computed by line-search backtracking to decrease residual norm $r(\mathbf{U}) = \frac{1}{2}\mathbf{R}(\mathbf{U})^t\mathbf{R}(\mathbf{U})$.

Above the superscript n denotes the n^{th} iteration step, *i.e.*, previous iteration step. Matrix $\mathbf{J}(\mathbf{U}^{\mathrm{n}})$ is the Jacobian associated with $\mathbf{R}(\mathbf{U}^{\mathrm{n}})$, *i.e.*,

$$J^{ij}(n) = A^{ij} + \frac{\partial A^{ik}(\mathbf{U}^n)}{\partial U_j} U_k^n + \frac{\partial F^i}{\partial U_j}, \tag{2.116}$$

where U_j is the j^{th} component of the vector $\mathbf{U}$ in (2.109). Furthermore $\delta(\mathrm{n})$ is the desired search direction, ω_{n} is the length of the step and $R(\mathbf{U}_{\mathrm{n}})$ is the residual from the previous step. As a preconditioner for the GMRES the ILU preconditioning is preferred, which seems to work fairly well in the present problem of twofluid flow. For detailed analysis of Newton-GMRES algorithms (including also inexact Newton algorithms), see Ref. [CE93].

2.4 Particle tracking

From the algorithmic point of view the particle tracking is a considerably simple method as compared to multifluid algorithms. For the solution of the carrier fluid with low particle volume fractions standard one-phase algorithms can be used with extra source terms emanating from the appearance of the particulate phase. Particle trajectories are given by the kinematic equation. The treatment of this equation involves only technical difficulties. Equations of motion are reduced to ordinary differential equations and are therefore easy to solve. The coupling between the carrier phase and the particulate phase is taken into account through source terms. These terms can be obtained elementwise (or cellwise) keeping track of trajectories passing through the considered element.

The solution strategy used in the particle tracking is an iterative one. First the solution of the carrier phase is obtained. Next the ordinary differential equations for the dispersed phase are solved for a number of particles using the continuum phase solution. The computed trajectories (and also other scalar quantities such as temperature and masses of particles) are combined into source terms of momentum equations (and of energy and continuity equations). These source terms are then used in the next solution of the continuum equations. The process is iterated until convergence is attained. In this procedure, *two-way coupling* is said to prevail since information is transfered from the carrier phase to dispersed phase and vice versa. When the particles are not affecting to the carrier phase and the tracking is such a postprocessing after the flow field of the carrier phase is solved one speaks of *one-way coupling*. The principle of numerical solution

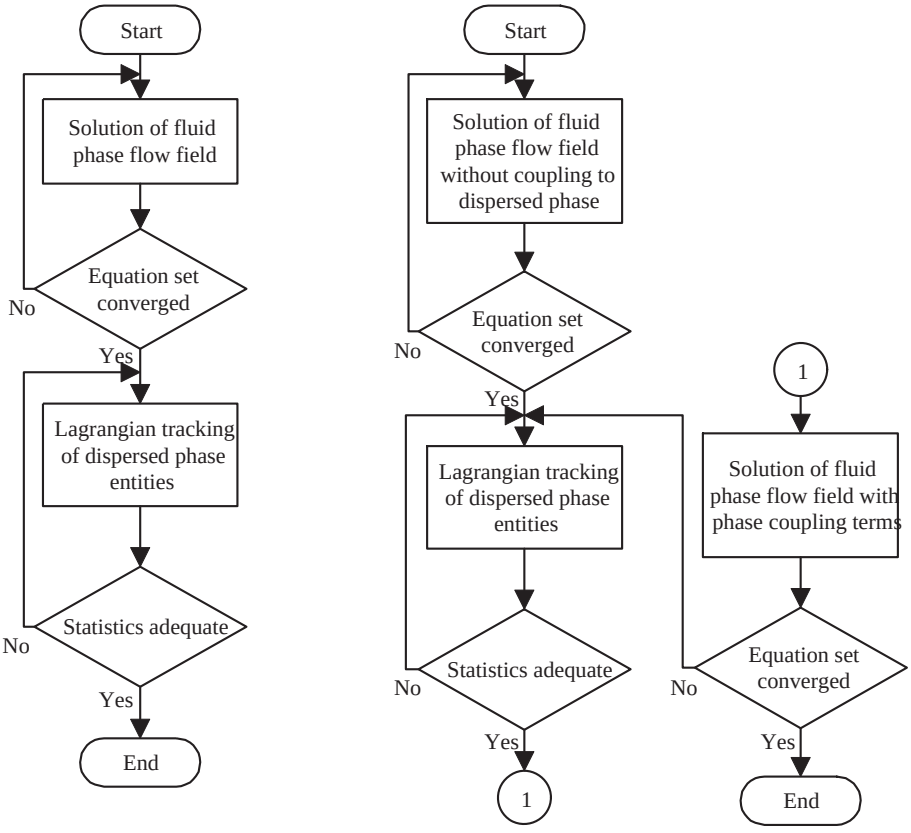

Figure 2.5: Solution schemes for problems corresponding to one-way and two-way coupling.

for one-way coupled systems and for two-way coupled systems is illustrated in Fig. 2.5.

In this section the numerical realization of the particle tracking is shortly reviewed. All numerous technical details are excluded as well as special considerations for turbulent flows. In turbulent tracking we refer here to the widely used work by Gosman and Ioannides [GI81b], where $k-\varepsilon$ turbulence model for the carrier fluid and a one-step-per-eddy, Monte-Carlo simulation for the particles were used.

2.4.1 Solution of the system of equation of motion

To solve the momentum equation (1.109) several numerical methods for ODE can be used. Let us write equation (1.109) in a form

$$\frac{d}{dt}\mathbf{V} = \mathbf{F}(\mathbf{V}, t). \tag{2.117}$$

In order to solve this system, an explicit second-order predictor-corrector method could be used, *i.e.*,

$$\begin{aligned} \mathbf{V}^{n+1} &= \mathbf{V}^n + \Delta t\, \mathbf{F}(\mathbf{V}^{n+\frac{1}{2}}, t^{n+\frac{1}{2}}) \\ \mathbf{V}^{n+\frac{1}{2}} &= \mathbf{V}^n + \tfrac{1}{2}\Delta t\, \mathbf{F}(\mathbf{V}^n, t^n). \end{aligned} \tag{2.118}$$

It is well known however that explicit methods perform poorly when system of equations becomes stiff, *i.e.*, when relaxation times becomes small. In such cases unconditionally stable implicit methods are preferred. An example is the following Crank-Nicholson second order scheme

$$\mathbf{V}^{n+1} = V^n + \Delta t\, \frac{\mathbf{F}(\mathbf{V}^n, t^n) + \mathbf{F}(\mathbf{V}^{n+1}, t^{n+1})}{2}. \tag{2.119}$$

2.4.2 Solution of particle trajectories

Particle trajectories are given by the kinematic equation

$$\frac{d}{dt}\mathbf{Y} = \mathbf{V}, \tag{2.120}$$

where $\mathbf{Y}(t)$ is the position of the particle at time t and $\mathbf{V}(t)$ the corresponding velocity.

Using the finite element method for the equation (2.120) we get componentwise

$$\frac{d}{dt}Y^i = \sum_k V_k^i(t)\phi_k(\xi^j). \tag{2.121}$$

The relationship between local coordinates ξ^j and the global coordinates Y^i is given by the isoparametric mapping (2.113). Now we get for the reference element

$$\frac{d}{dt}Y^i = \frac{\partial Y^i}{\partial \xi^j}\frac{d}{dt}\xi^j = V^i, \tag{2.122}$$

or in matrix form

$$\frac{d}{dt}\mathbf{Y} = \mathbf{J}\frac{d}{dt}\xi = \mathbf{V}, \tag{2.123}$$

where $\mathbf{J}$ is the Jacobian of the parametric transformation. So we can transform the original problem to a problem in reference element,

$$\frac{d}{dt}\xi = \mathbf{J}^{-1}\mathbf{V}. \tag{2.124}$$

Furthermore using second order Crank-Nicholson scheme for time derivative we get

$$\xi^j(t_{n+1}) = \xi^j(t_n) + \Delta t\, \frac{(J^{-1})^{jk}V^k(t_n) + (J^{-1})^{jk}V^k(t_{n+1})}{2}. \tag{2.125}$$

For finite volume methods the calculation of the trajectories is performed more or less the same way as within finite element method. Like in FEM, instead of dealing with physical coordinates computational coordinates are used.

2.4.3 Source term calculation

In the PSIC approach [CSS77], the source terms are calulated from the residence time of the each individual particle on each cell or element.

Let n_p^j be the number of particles per unit time traversing the jth trajectory and δt_E^j be the residence time of a particle on trajectory j with respect to element E. Then the contribution to the ith momentum transfer source to element E is

$$S^i(E) = \frac{1}{V_E} \sum_{j=1}^{n_E} n_p^j \Big[(m_p^j V^i)_{out} - (m_p^j V^i)_{in} \Big], \tag{2.126}$$

where n_E is the number of trajectories passing through element E and V_E is the volume of that element and $(m_p^j V^i)_{out}$ is the momentum of the particle leaving the element and $(m_p^j V^i)_{in}$ the momentum of the particle entering the element E with respect to the trajectory j.

2.4.4 Boundary condition

When a particle reaches the domain boundary, the distribution of source terms between the carrier phase and the boundary depends on whether the particle penetrates, rebounds or attaches the boundary. A penetrating particle exchanges momentum (and, in general, energy and mass) with the carrier phase up to the boundary and then exits the domain carrying a residual of momentum (and of energy and mass). If the particle rebounds from the boundary, it exchanges momentum with the carrier phase and with the boundary face. If the particle attaches the boundary, it simply loses all its momemtum to the boundary.

2.5 Mesoscopic simulation methods

Numerical solution of flow has traditionally been based on finding a solution for partial differential continuum equations such as continuity and Navier-Stokes equations that govern the fluid flow. In principle, it would be possible to solve any fluid flow problem on microscopic level with direct molecular-dynamical simulations. It is quite clear that practical fluid flow problems cannot be solved with this approach at the present due to the large number of particles, and thus large amount of computer resources that would be needed for such a simulation. Another possibility for direct microscopic simulation of flow would be using the standard kinetic theory. Here the basic object is the particle distribution function $f(\mathbf{r}, \mathbf{v})$ which gives the probability of finding at position $\mathbf{r}$ a particle with velocity $\mathbf{v}$. The time evolution of this function is given by the Boltzmann equation

$$(\partial_t + \mathbf{v}_1 \cdot \nabla_{\mathbf{r}} + \frac{\mathbf{F}}{m} \cdot \nabla_{\mathbf{v}_1}) f_1 = \int d\Omega \int d^3\mathbf{v}_2 \delta(\Omega) |\mathbf{v}_1 - \mathbf{v}_2| (f_2' f_1' - f_1 f_2). \tag{2.127}$$

This approach is also far too complicated in most practical problems even for gaseous fluids. Many dynamical systems can however be modeled with radically simplified microscopic or mesosocopic models. This has been utilized, *e.g.*, in the famous Ising models for magnetic materials, and since 1950's in various cellular-automaton models for biological and physical systems. Encouraged by these models, similar models (*i.e.* models that were not based on continuum mechanics) for fluid flows were also developed, first with a limited success, though. In 1986 it was realised that fluid flow could be successfully simulated with very simple discrete models provided that the simulation lattice was carefully chosen. This discovery was the starting point of the lattice-gas methods [FdH$^+$87, RZ97, Kop98] and later of the lattice-Boltzmann methods [RZ97, Kop98, QdL92, BSV92]. We refer these methods as 'mesoscopic' indicating that the size scale of the basic constituents ('particles') or variables of the model is large as compared to molecular scale of the fluid, but small as compared to the typical size scale of macroscopic flow, and the local hydrodynamical quantities are defined as suitable averages of the basic variables.

In the lattice-gas method fluid is modeled with identical particles which move in a discrete lattice interacting with each other only at the lattice nodes. A 'particle' is not considered here as a physical molecule, but rather as a 'fluid particle' that contains a large number of molecules. The space, the time and the velocity of particles are all discrete. Notice that the method is not based on explicitly solving any governing equation of particle motion. It is simply an algorithm of moving particles in the lattice with a set of collision rules that conserve mass (number of particles) and momentum. The basic hydrodynamic quantities such as local flow velocity can be defined as the velocity of particles averaged over a specified volume, time or both. Provided that the simulation lattice fulfills certain symmetry requirements, the lattice-gas automaton indeed develops macroscopic flow field that is close to the solution of the Navier-Stokes equations for incompressible flow in the same macroscopic conditions. The number of particles needed for a realistic simulation of many practical systems is well in the limits of present computational capabilities.

The boolean and local nature of the lattice-gas model gives several technical advantages in computing. Perhaps the most important advantage is the ease of introducing complex flow geometries, which follows from the regular lattice and from the extremely simple and strictly local updating rules of the method. Since particles can be represented by single bits in computer, the method does not require very large memory as compared to other methods. Furthermore, rounding errors are not involved in bit manipulations, and unconditional numerical stability is guaranteed. The computations are also inherently parallel thus being ideal for massive parallel computers. In recent years many sophistications have helped to get rid of most of the early problems [RZ97, BSV92], and the lattice-gas method is now a viable tool

for computational fluid dynamics.

The early deficiencies of the lattice-gas models inspired the formulation of the more advanced lattice-Boltzmann models. The idea behind this model was to track a population of (fluid) particles instead of a single particle, a reasonable modification justified by the Boltzmann molecular-chaos assumption from kinetic theory of gases. This mean-value representation of particles eliminates much of the statistical noise present in lattice-gas methods. The basic variable to be solved within lattice-Boltzmann methods is the discrete distribution function that fulfils a discretised version of the Boltzmann equation (see eqn. (2.128) below). The hydrodynamic variables are defined in terms of the distribution function as averaged quantities analogously with the manner in which those variables are defined in the usual kinetic theory of gases. In the next section we discuss in more detail one of the simplest versions of the lattice-Boltzmann models that is regularly used in practical simulations, namely the lattice-BGK (Bhatnagar-Gross-Krook) model [QdL92].

Recently a third mesoscopic method, dissipative particle dynamics (DPD), has been developed [MBE97]. This method is a combination of molecular dynamics, Brownian dynamics and lattice-gas automata. The DPD algorithm models a fluid with fluid particles out of equilibrium and conserves mass and momentum. The fluid particles interact with each other through conservative and dissipative forces. In contrast to the lattice-gas and lattice-Boltzmann methods, the position and velocity of these fluid particles are continuous, as in molecular dynamics, but time is discrete. This method is very suitable *e.g.* for simulating rheological properties of complex fluids on hydrodynamic time scales.

2.5.1 The lattice-BGK model

In the lattice-Boltzmann method a simplified version of the Boltzmann equation, eqn. (2.127), is solved on a discrete, regular lattice. Fluid particles, described by the discrete distribution function, move synchronously along the bonds of this lattice, and interact locally according to a given set of rules. A single iteration step (time step) within this method consists of the following two phases:

1. Propagation; particles move along lattice bonds to the neighboring lattice nodes.

2. Collision; particles on the same lattice node shuffle their velocities locally conserving mass and momentum.

In the lattice-BGK (Bhatnagar-Gross-Krook) model the collision operator is based on a single time relaxation to the local equilibrium distribution [QdL92]. The lattice structure can be chosen in several ways (see Fig. 2.6

for two possible realizations). In the $D3Q19$ lattice-BGK model, each lattice point is linked in three dimensional space with its six nearest neighbors at a unit distance and with twelve diagonal neighbors at a distance of $\sqrt{2}$. Including the rest state, the particles can thus have 19 different velocity states. The dynamics of the $D3Q19$ model is given by the equation [RZ97, QdL92],

$$f_i(\mathbf{r}+\mathbf{c}_i, t+1) = f_i(\mathbf{r},t) + \frac{1}{\tau}(f_i^{(0)}(\mathbf{r},t) - f_i(\mathbf{r},t)) \quad , \tag{2.128}$$

where $\mathbf{c}_i$ is the i-th link, $f_i(\mathbf{r},t)$ is the density of particles moving in the $\mathbf{c}_i$-direction, τ is the BGK relaxation parameter, and $f_i^{(0)}(\mathbf{r},t)$ is the equilibrium distribution function towards which the particle populations are relaxed. The hydrodynamic fields such as the density ρ, the velocity $\mathbf{v}$ and the momentum tensor Π are obtained from moments of the discrete velocity distribution $f_i(\mathbf{r},t)$ as

$$\rho(\mathbf{r},t) = \sum_{i=0}^{18} f_i(\mathbf{r},t), \qquad \mathbf{v}(\mathbf{r},t) = \frac{\sum_{i=0}^{18} f_i(\mathbf{r},t)\mathbf{c}_i}{\rho(\mathbf{r},t)},$$

$$\Pi_{\alpha\beta}(\mathbf{r},t) = \sum_{i=0}^{18} c_{i\alpha}c_{i\beta}f_i(\mathbf{r},t).$$

The equilibrium distribution function can be chosen in several ways. A common choice is

$$f_i^{(0)} = t_i\rho(1 + \frac{1}{c_s^2}(\mathbf{c}_i\cdot\mathbf{v}) + \frac{1}{2c_s^4}(\mathbf{c}_i\cdot\mathbf{v})^2 - \frac{1}{2c_s^2}v^2),$$

where t_i is a weight factor depending on the length of the link vector and c_s is the speed of sound. The weight factors can be chosen as $\frac{1}{3}$, $\frac{1}{18}$ and $\frac{1}{36}$ for the rest particle, nearest neighboring and diagonal neighboring links, respectively. These values yield to a correct hydrodynamic behavior for an incompressible fluid in the limit of low Mach and Knudsen numbers. The speed of sound and the kinematic viscosity of the simulated fluid in lattice units are given by $c_s = \frac{1}{\sqrt{3}}$ and $\nu = \frac{2\tau-1}{6}$, respectively [QdL92].

2.5.2 Boundary conditions

In lattice-gas and lattice-Boltzmann simulations the no-slip boundary condition is usually realized using the bounce-back condition [RZ97, Kop98]. In this approach the momenta of particles that meet wall points are simply reversed. The bounce-back boundary may generate errors which in some cases violate the second-order spatial convergence of these methods and more sophisticated boundaries have been proposed [FH97]. For practical simulations the bounce-back boundary is however very attractive, because it is a simple

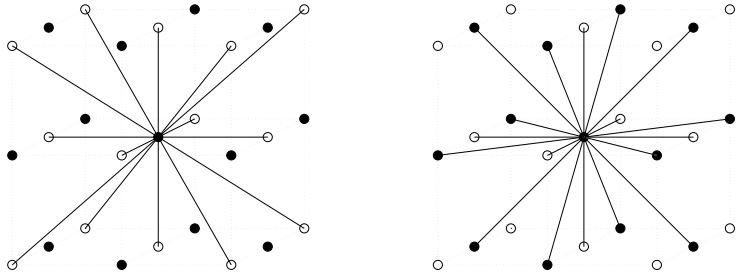

Figure 2.6: Two possible realizations of lattice structures.

and computationally efficient method for imposing no-slip walls in irregular geometries. Also, the bounce-back method can easily be generalized to allow moving boundaries [Lad94a, Lad94b].

Successful numerical simulation of practical fluid flow problems requires that the velocity and pressure boundary conditions of the system have been imposed in a consistent way. So far most of the practical simulations have used a body force [Kop98] instead of pressure or velocity boundaries. When a body force is used, a pressure gradient acting on the fluid is replaced by a uniform external force. (Usually periodic boundaries are imposed at least in the direction of the flow.) The use of a body force is based on the assumption that the effect of an external pressure gradient is approximately constant all over the system, and that it can be replaced by a constant force that adds at every time step a fixed amount of momentum to fluid particles. In a simple tube flow the body-force approach is exact. In more complicated geometries this approach is supposed to work best with small Reynolds numbers where nonlinear effects on the flow are small.

2.5.3 Liquid-particle suspensions

The bounce-back condition can easily be modified [Lad94a] to allow moving boundaries with no-slip boundary condition. We assume that a boundary moving with velocity $\mathbf{u}_w$ is located in the halfway of links between the last fluid points and the first solid points. The distribution function for particles moving along such a link towards the solid point is given by

$$f_i(\mathbf{r} + \mathbf{c}_i, t + 1) = f_{i'}(\mathbf{r} + \mathbf{c}_i, t_+) + 2\rho_f B_i(\mathbf{u}_w \cdot \mathbf{c}_i). \tag{2.129}$$

Here t_+ is used to indicate the post-collision distribution, i' denotes the bounce-back link, and $B_i = \frac{1}{3}, \frac{1}{12}$ for the diagonal and non-diagonal links, respectively. The last term in Eqn. 2.129 is added in order to account for the momentum transfer between the fluid and the moving solid boundary. For computational convenience the fluid is usually made to fill also the suspended solid particles. This trick removes the need for creating and destroying fluid when particles move. Models without interior fluid have also been used.

The lattice-Boltzmann method for suspensions is based upon Newtonian dynamics of solid particles that move in a continuous space. The discretized images of these particles interact with the lattice-Boltzmann fluid at their boundary nodes. The technique takes advantage of the fact that the hydrodynamic interactions are time dependent and develop from purely local interactions at the solid-liquid interfaces. Thus it is not necessary to consider the global system, but one can update one particle at a time. The method scales linearly with the number of suspended particles and, therefore, allows far larger simulations than the conventional methods. The hydrodynamic interactions between solid particles are fully accounted for, both at zero and finite Reynolds numbers [Lad94a]. Furthermore, there is no need for solution of the linear systems. Therefore, lattice-Boltzmann method can be efficiently implemented on parallel processors. The electrostatic interactions, the flow geometry, the Peclet number, the shear and particle Reynolds numbers, as well as the size and shape of the suspended particles can easily be varied.

2.5.4 Applicability of mesoscopic methods

The most important property of the mesoscopic methods discussed above is the simplicity with which models for many complex flows such as multiphase flows and flows in porous media can be implemented. Numerical simulation is based on a simple algorithm, or on numerical solution of a single transport equation instead of a system of coupled partial differential equations of conventional methods. Another important property of the lattice-gas and lattice-Boltzmann methods is the inherent spatial locality of their updating rules, which makes these methods ideal for parallel processing. Both methods are also numerically relatively stable. In the lattice-gas and lattice-Boltzmann methods a uniform lattice is usually used, and they can thus be easily and quickly applied to new geometries. Also, time-dependent simulations can be carried out relatively easily, as no time is lost for remeshing. Moreover, these methods spontaneously generate hydrodynamic instabilities which make them useful for simulating fluid flow at moderately large Reynolds numbers. At very large Reynolds numbers mesoscopic methods encounter the problem of turbulence like the more conventional methods: in a fully turbulent flow wave lengths of all scales are present, and the solution would require a very large lattice or additional turbulence modelling. Furthermore, some features of the methods such as use of irregular lattice for improved accuracy, implementation of velocity and pressure boundary conditions and models for finite-temperature systems are still under development.

So far, successful implementations of mesoscopic methods have included *e.g.* multiphase flows [RZ97, MC96], suspension flows [Lad94a] and flows in complex geometries [KKHA98, Kop98, MC96]. In Ref. [KVH$^+$99] a

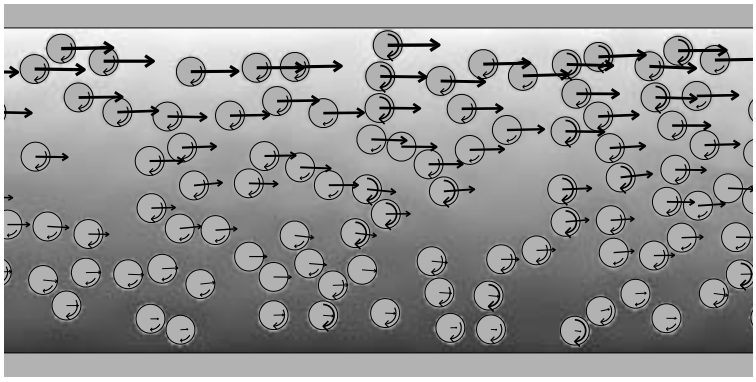

Figure 2.7: Couette flow of liquid-particle suspension as solved using the lattice-BGK-method in two dimensions. The upper wall is moving to right and the lower wall is fixed. The velocity of the liquid is indicated by gray scale (light colour indicating high velocity) and the motion and rotation of particles by arrows.

detailed comparison between conventional methods and lattice-Boltzmann methods was given for 3D fluid flow in an industrial static mixer. In addition to basic flow simulation, these methods are convenient in finding numerical correlations for closure relations and constitutive relations necessary in conventional methods for solving multiphase flows, as discussed in chapter 1. The essential property of the mesoscopic methods in this respect is the simplicity of constructing complicated geometries and implementing moving boundaries. Due to this feature it is straightforward, *e.g.*, to generate a large ensemble of macroscopically identical systems of particles suspended in a liquid, solve the flow and the motion of the particles for each system (possibly with a given interaction between the suspended particles), and finally compute the properly averaged quantities and transfer integrals as defined in chapter 1. The results can then be used to correlate the unknown terms such as Γ_α and $\mathbf{M}_\alpha$ in averaged flow equations (see eqns. (1.27)–(1.28) or eqns. (1.79)–(1.80)) with basic averaged flow quantities. Similarly, these methods could be helpful in finding rheological properties and boundary conditions of multiphase fluids to be used in conventional non-Newtonian simulation of such flows.

As an example of a typical solution obtained by the lattice-Boltzmann method, we show in Figure 2.7 the instantaneous flow pattern of a two-dimensional liquid-particle suspension in a shear flow [RSMK$^+$00]. Here, the flow of the carrier fluid is calculated using the lattice-BGK -model while the motion of the suspended spherical particles is given by Newtonian mechanics including the impulsive forces due to direct collisions between particles, and the hydrodynamic forces due to fluid flow. The numerical solution can be

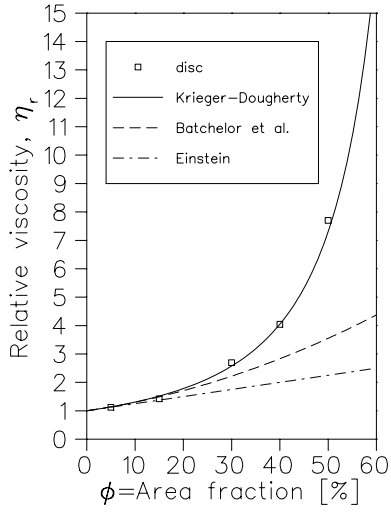

Figure 2.8: Viscosity of two-dimensional liquid-particle suspension as a function of consistency (area fraction) calculated by lattice-Boltzmann simulations (see Fig. 2.7). The open squares are the calculated values. The semiempirical result by Krieger and Dougherty [KD59], and the analytical results by Batchelor [BG72, Bat77] and Einstein [Ein06, Ein11] valid for low consistencies are given by lines as indicated.

used to compute, *e.g.*, the time averaged total shear force acting on the walls, and thereby to find the dependence of the nominal viscosity on the mean shear velocity and on the properties of the suspension. Figure 2.8 shows the viscosity of the two dimensional liquid-particle suspension as a function of consistency of particles as calculated using lattice-Boltzmann simulations. The result is also compared with previous analytical results by Einstein [Ein06, Ein11] and Batchelor [BG72, Bat77], and with the semiempirical results by Krieger and Dougherty [KD59].

Bibliography

[Aut83] Auton, T.R. *The dynamics of bubbles, drops and particles in motion in liquids.* PhD thesis, University of Cambridge, 1983.

[Bas88] Basset, A.B. *Treatise on hydrodynamics.* Pp. 285–297. Deighton Bell, London, 1888.

[Bat53] Batchelor, G.K. *The theory of homogeneous turbulence.* Cambridge University Press, London, 1953.

[Bat77] Batchelor, G.K. The effect of brownian motion on the bulk stress in a suspension of spherical particles. *Journal of Fluid Mechanics*, 83:97–117, 1977.

[BB93] Burry, D. and Bergeles, G. Dispersion of particles in anisotropic turbulent flows. *Int. J. Multiphase Flow*, 19:651–664, 1993.

[BBS95] Boëlle, A., Balzer, G., and Simonin, O. Second order prediction of the particle phase stress tensor of inelastic spheres in simple shear dense suspensions. *Gas-Solid Flows, ASME FED*, 228:9–18, 1995.

[BDG90] Berlemont, A., Desjonqueres, P., and Gousbet, G. Particle lagrangian simulation in turbulent flows. *Int. J. Multiphase Flow*, 16:19–34, 1990.

[Bea72] Bear, J. *Dynamics of Fluids in Porous Media.* American Elsevier, New York, 1972.

[BG72] Batchelor, G.K. and Green, J.T. The determination of the bulk stress in a suspension of spherical particles to order c^2. *Journal of Fluid Mechanics*, 56:401–427, 1972.

[BH79] Brown, D.J. and Hutchinson, P. The interaction of solid or liquid particles and turbulent fluid flow fields — a numerical simulation. *Journal of Fluids Engineering*, 101:265–269, 1979.

[BM90] Burnage, H. and Moon, S. Predetermination de la dispersion de particules materielles dans un ecoulement turbulent. *C. R. Acad. Sci. Paris*, 310:1595–1600, 1990.

[Boe97] Boemer, A. *Euler/Euler-Simulation der Fluiddynamik Blasenbildender Wirbelschichten*. PhD thesis, Aachen, 1997.

[Bou03] Boussinesq, J. Theorie analytique de la chaleur. L'École Polytechnique, Paris, 1903.

[BP80] Baliga, B.R. and Patankar, S.V. A new finite-element formulation for convection-diffusion problems. *Numerical Heat Transfer*, 3:393–409, 1980.

[BS78] Buyevich, Y.A. and Shchelchkova, I.N. Flow of dense suspensions. *Prog. Aerospace Sci.*, 18:121–150, 1978.

[BSV92] Benzi, R., Succi, S., and Vergassola, M. *Phys. Rap.*, 222:145, 1992.

[Bur38] Burgers, J.M. 2nd report on viscosity and plasticity. Kön. Ned. Akad. Wet., Verhand, 1938.

[Buy66] Buyevich, Y.A. Motion resistance of a particle suspended in a turbulent medium. *Izv. AN SSSR. Mechanika Zhidkosti i Gaza*, 1:182–183, 1966. English translation in Fluid Dynamics.

[Buy71] Buyevich, Y.A. Statistical hydromechanics of disperse systems. Part 1. Physical background and general equations. *J. Fluid Mech.*, 49(3):489–507, 1971.

[Buy92a] Buyevich, Y.A. Heat and mass transfer in disperse media - I. Averaged field equations. *Int. J. Heat Mass Transfer*, 35(10):2445–2452, 1992.

[Buy92b] Buyevich, Y.A. Heat and mass transfer in disperse media - II. Constitutive equations. *Int. J. Heat Mass Transfer*, 35(10):2453–2463, 1992.

[BW87] Burns, A.D. and Wilkes, N.S. A finite difference method for the computation of fluid flows in complex three dimensional geometries. Technical Report AERE-R 12342, Harwell Laboratory, 1987.

[CC70] Chapman, S. and Cowling, T.G. *The mathematical theory of non-uniform gases*. Cambridge Mathematical Library, Cambridge, 1970.

[CE93] Choquet, R. and Erhel, J. Some convergence results for the Newton-GMRES algorithm. Internal publication 755, IRISA, September 1993.

[Cha64] Chao, B.T. Turbulent transport behavior of small particles in dilute suspension. *Österreichisches Ingenieur Archiev*, 18(7):7–21, 1964.

[Com] Computational fluid dynamics services, Oxfordshire. *CFDS-FLOW3D; User Manual, Release 3.3*.

[Cro93] Crowe, C.T. Modeling turbulence in multiphase flows. In W., Rodi and F., Martelli (editors), *Engineering Turbulence Modelling and Experiments 2*. Pp. 899–913. 1993.

[Csa63a] Csanady, G.T. An atmospheric dust fall experiment. *J. Atm. Sci.*, 21:222–225, 1963.

[Csa63b] Csanady, G.T. Turbulent diffusion of heavy particles in the atmosphere. *J. Atm. Sci.*, 20:201–208, 1963.

[CSS77] Crowe, C.T., Sharma, M.P., and Stock, D.E. The particle Source-in-Cell Method for gas-droplet flows. *J. Fluid Eng.*, 99:325–332, 1977.

[CTC96] Crowe, C.T., Troutt, T.R., and Chung, J.N. Numerical models for two-phase turbulent flows. *Annu. Rev. Fluid. Mech.*, 28:11–43, 1996.

[DALJ90] Drew, D.A., Arnold, G.S., and Lahey Jr., R.T. Relation of microstructure to constitutive equations. In Joseph, D.D. and Schaeffer, D.G. (editors), *Two phase flows and waves*. Pp. 45–56, 1990.

[DG90] Ding, J. and Gidaspow, D. A bubbling fluidization model using kinetic theory of granular flow. *AIChE Journal*, 36(4):523–538, 1990.

[DLJ79] Drew, D.A. and Lahey Jr., R.T. Application of general constitutive principles to the derivation of multidimensional two-phase flow equations. *Int. J. Multiphase Flow*, 5:243–264, 1979.

[DLJ92] Drew, D.A. and Lahey Jr., R.T. Chapter 16: Analytical modeling of multiphase flow. In Roco, M. (editor), *Particulate Two-Phase Flows*. Butterworth-Heinemann, 1992.

[Dre71] Drew, D.A. Averaged field equations for two-phase media. *Studies in Applied Mathematics*, 50:133–166, 1971.

[Dre76] Drew, D.A. Two-phase flows: Constitutive equations for lift and Brownian motion and some basic flows. *Arch. Rat. Mech. Anal.*, 62(117), 1976.

[Dre83] Drew, D.A. Mathematical modeling of two-phase flow. *Ann. Rev. Fluid Mech.*, 15:261–291, 1983.

[DS71] Drew, D.A. and Segel, L.A. Averaged equations for two-phase flows. *Studies in Applied Mathematics*, 50(3):205–231, 1971.

[EF94] Eaton, J.K. and Fessler, J.R. Preferential concentration of particles by turbulence. *Int. J. Multiphase Flow*, 20 Suppl.:169–209, 1994.

[Ein06] Einstein, A. *Ann. Phys.*, 19:289, 1906.

[Ein11] Einstein, A. *Ann. Phys.*, 34:591, 1911.

[Erg52] Ergun, S. Fluid flow through packed columns. *Chemical Engineering Progress*, 48(2):89–94, 1952.

[Fae83] Faeth, G.M. Recent advances in modeling particle transport properties and dispersion in turbulent flow. In *Proc. ASME-JSME Thermal Engineering Conference, Vol. 2.* Pp. 517–534, 1983.

[Fax22] Faxen, H. Die Bewegung einer starren Kugel lïgs der Achse eines mit zäher Flüssigkeit gefüllten Rohres. *Ark. Mat., Astron. Fys.*, 17:1–28, 1922.

[FdH+87] Frisch, U., d'Humiéres, D., Hasslacher, B., Lallemand, P., Pomeau, Y., and Rivet, J.-P. *Complex Syst.*, 1:649, 1987.

[FF92] Franca, L.P. and Frey, S.L. Stabilized finite element methods: II. The incompressible Navier-Stokes equations. *Computer Methods in Applied Mechanics and Engineering*, 99:209–233, 1992.

[FFH92] Franca, L.P., Frey, S.L., and Hughes, T.J.R. Stabilized finite element methods: I. Application to the advective-diffusive model. *Computer Methods in Applied Mechanics and Engineering*, 95:253–276, 1992.

[FH97] Filippova, O. and Haenel, D. *Computers in Fluids*, 26:697, 1997.

[FHS92] Franca, L.P., Hughes, T.J.R., and Stenberg, R. Stabilized finite element methods. In Gunzburger, M. D. and Nicolaides,

R. A. (editors), *Incompressible Computational Fluid Dynamics Trends and Advances*. Pp. 87–107. Cambridge University Press, 1992.

[GBD92] Gidaspow, D., Bezburual, R., and Ding, J. Hydrodynamics of circulating fluidized beds, kinetic theory approach. In *Fluidization VII, Proceedings of the 7th Engineering foundation conference on fluidization*. Pp. 75–82, 1992.

[GHN89] Govan, A.H., Hewitt, G.F., and Ngan, C.F. Particle motion in a turbulent pipe flow. *Int. J. Multiphase Flow*, 15:471–481, 1989.

[GI81a] Gosman, A.D. and Ioannides, E. Aspects of computer simulation of liquid-fuelled combustors. In *AIAA 19th Aerospace Sciences Meeting, Paper AIAA-81-0323*. 1981.

[GI81b] Gosman, A.D. and Ioannides, E. Aspects of computer simulation of liquid-fuelled combustors. *Paper AIAA-81-0323, presented at AIAA 19th Aerospace Science Meeting, St Louis, MO*, 1981.

[Gid94] Gidaspow, D. *Multiphase flow and fluidization. Continuum and kinetic theory descriptions*. Academic Press, San Diego, 1994.

[GJ96] Graham, D.I. and James, P.W. Turbulent dispersion of particles using eddy interaction models. *Int. J. Multiphase Flow*, 22(1):157–175, 1996.

[HHD71] Hutchinson, P., Hewitt, G.F., and Dukler, A.E. Deposition of liquid or solid dispersions from turbulent gas streams: a stochastic model. *Chem. Engineering Sci.*, 26:419–439, 1971.

[Hil97] Hiltunen, K. A stabilized finite element method for particulate two-phase flow equations: Laminar isothermal flow. *Computer Methods in Applied Mechanics and Engineering*, 147:387–399, 1997.

[Hin75] Hinze, J.O. *Turbulence*. McGraw-Hill, New York, 1975.

[HJ91] Hansbo, P. and Johnson, C. Adaptive streamline diffusion methods for compressible flow using conservation variables. *Computer Methods in Applied Mechanics and Engineering*, 87:267–280, 1991.

[HJ95] Hughes, T.J.R. and Jansen, K. A stabilized finite element formulation for the Reynolds-averaged Navier-Stokes equations. *Surveys on Mathematics for Industry*, 4(4):279–317, 1995.

[HS89] Hwang, G.-J. and Shen, H.H. Modeling the solid phase stress in a fluid-solid mixture. *Int. J. Multiphase Flow*, 15(2):257–268, 1989.

[HS91] Hwang, G.-J. and Shen, H.H. Modeling the phase interaction in the momentum equations of a fluid-solid mixture. *Int. J. Multiphase Flow*, 17(1):45–57, 1991.

[Hwa89] Hwang, G.-J. *Modeling two-phase flows of a fluid and solid mixture*. PhD thesis, Clarkson University, 1989.

[IM84] Ishii, M. and Mishima, K. Two-fluid model and hydrodynamic constitutive relations. *Nucl. Eng. & Des.*, 82:107–126, 1984.

[Ish75] Ishii, M. *Thermo-fluid dynamic theory of two-phase flow*. Eyrolles, 1975.

[IZ79] Ishii, M. and Zuber, N. Drag coefficient and relative velocity in bubbly, droplet or particulate flows. *AIChE Journal*, 25(5):843–855, September 1979.

[JHW80] James, P.W., Hewitt, G.F, and Whalley, P.B. Droplet motion in two-phase flow. In *Proc. ANS/ASME/NRC International Topical Meeting on Nuclear Reactor Thermal-Hydraulics*. Pp. 1484–1503, 1980.

[JL90] Joseph, D.D. and Lundgren, T.S. Ensemble averaged and mixture theory equations for incompressible fluid-particle suspensions. *Int. J. Multiphase Flow*, 16:35–42, 1990.

[JR85] Jenkins, J.T. and Richman, M.W. Grad's 13 moment system for a dense gas of inelastic spheres. *Arch. Ratio. Mech. Anal.*, 87:355–377, 1985.

[JS83] Jenkins, J.T. and Savage, S.B. A theory for the rapid flow of identical, smooth, nearly elastic, spherical particles. *J. Fluid Mech.*, 130:187–202, 1983.

[Kar02] Karema, H. *Application of pressure correction method to multi-pressure systems of dispersed flows*. PhD thesis, Tampere University of Technology, 2002.

[KD59] Krieger, I.M. and Dougherty, T.J. *Trans. Soc. Rheol.*, 3:2817, 1959.

[KKHA98] Koponen, A., Kandhai, D., Hellén, E., and Alava, M. *Phys. Rev. Lett.*, 80:716, 1998.

[KL99] Karema, H. and Lo, S. Efficiency of interphase coupling algorithms in fluidized bed conditions. *Computers & Fluids*, 28:323–360, 1999.

[KN90] Krizek, M. and Neittaanmäki, P. *Finite Element Approximation of Variational Problems and Applications.* Longman Scientific & Technical, 1990.

[Kop98] Koponen, A. *Simulations of fluid flow in porous media by lattice gas and lattice-Boltzmann methods.* PhD thesis, University of Jyväskylä, 1998.

[KR89] Kalio, G.A. and Reeks, M.W. A numerical simulation of particle deposition in turbulent boundary layers. *Int. J. Multiphase Flow*, 15:433–446, 1989.

[KVH+99] Kandhai, D., Vidal, D., Hoekstra, A., Hoefsloot, H., Iedema, P., and Sloot, P. *Int. J. Num. Meth. Fluids*, 31:1019, 1999.

[Lad94a] Ladd, A.J.C. *J. Fluid. Mech.*, 271:285, 1994.

[Lad94b] Ladd, A.J.C. *J. Fluid. Mech.*, 271:311, 1994.

[LFA93] Lu, Q.Q., Fontaine, J.R., and Aubertin, G. A lagrangian model for solid particles in turbulent flows. *Int. J. Multiphase Flow*, 19:347–367, 1993.

[LFF95] Lesoinne, M., Farhat, C., and Franca, L.P. Unusual stabilized finite element methods for second order linear differential equations. In Cecchi, M. M., Morgan, K., Periaux, J., Schrefler, B. A., and Zienkiewicz, O. C. (editors), *Finite elements in fluids, New trends and applications.* Pp. 377–386. IACM, October 1995.

[LL94] Lien, F.S. and Leschziner, M.A. A general non-orthogonal collocated finite volume algorithm for turbulent flow at all speeds incorporating second-moment turbulence-transport closure, part 1: Computational implementation. *Computer Methods in Applied Mechanics and Engineering*, 114:149–167, 1994.

[Lo89] Lo, S.M. Mathematical basis of a multi-phase flow model. Technical Report AERE R 13432, Harwell Laboratory, Oxfordshire, 1989.

[Lo90] Lo, S.M. Multiphase flow model in the Harwell-Flow3D computer code. unclassified AEA-InTec-0062, Harwell Laboratory, Computational fluid dynamics section, Thermal hydraulics division, Oxfordshire, June 1990.

[LSJC84] Lun, C.K.K., Savage, F.B., Jeffrey, D.J., and Chepurniy, N. Kinetic theories for granular flow: Inelastic particles in couette flow and slightly inelastic particles in a general flowfield. *Journal of Fluid Mechanics*, 140(4):223–256, 1984.

[Lum57] Lumley, J.L. *Some problems connected with the motion of small particles suspended in turbulent fluid*. PhD thesis, the Johns Hopkins University, 1957.

[MB94] Masson, C. and Baliga, B.R. A control-volume finite-element method for dilute gas-solid particle flows. *Computers & Fluids*, 23(8):1073–1096, 1994.

[MBE97] Marsh, C., Backs, G., and Ernst, M. *Phys. Rev. E*, 56:1676, 1997.

[MC96] Martys, N. and Chen, H. *Phys. Rev. E*, 53:743, 1996.

[MM97] Mathur, S.R. and Murthy, J.Y. A pressure-based method for unstructured meshes. *Numerical Heat Transfer, part B*, 31:195–215, 1997.

[MR83] Maxey, M.R. and Riley, J.J. Equation of motion for a small rigid sphere in a nonuniform flow. *Phys. Fluids*, 26:883–889, 1983.

[MTK96] Manninen, M., Taivassalo, V., and Kallio, S. On the mixture model for multiphase flow. Research report 288, VTT Technical Research Centre of Finland, Espoo, 1996.

[Nig79] Nigmatulin, R.I. Spatial averaging in the mechanics of heterogeneous and dispersed systems. *Int. J. Multiphase Flow*, 5:353–385, 1979.

[Ose27] Oseen, C.W. *Hydrodynamik*. Akademische Verlagsgesellschaft M.B.H., Leipzig, 1927.

[PBG86] Picart, A., Berlemont, A., and Gouesbet, G. Modelling and predicting turbulence fields and the dispersion of discrete particles transported by turbulent flows. *Int. J. Multiphase Flow*, 12:237–261, 1986.

[Pei98] Peirano, E. *Modelling and simulation of turbulent gas-solid flows applied to fluidization*. PhD thesis, Chalmers University of Technology, 1998.

[PS72] Patankar, S.V. and Spalding, D.B. A calculation procedure for heat, mass and momentum transfer in parabolic flows. *Int. J. Heat Mass Transfer*, 15:1787–1806, 1972.

[QdL92] Qian, Y.H., d'Humiéres, D., and Lallemand, P. *Europhys. Lett.*, 17:479, 1992.

[RC83] Rhie, C.M. and Chow, W.L. Numerical study of the turbulent flow past an airfoil with trailing edge separation. *AIAA Journal*, 21(11):1525–1532, 1983.

[Ril71] Riley, J.J. PhD thesis, The Johns Hopkins University, 1971.

[RSMK+00] Raiskinmäki, P., Shakib-Manesh, A., Koponen, A., Jäsberg, A., Kataja, M., and Timonen, J. Simulations of non-spherical particles suspended in a shear flow, to be published in. *Comput. Phys. Comm.*, 2000.

[Rut62] Rutgers, I.R. Relative viscosity and concentration. *Rheologica Acta, Band 2*, Heft 4:305–348, 1962.

[RZ54] Richardson, J.F. and Zaki, W.N. Sedimentation and Fluidisation: Part I. *Transactions of the Institution of Chemical Engineers*, 32(1):35–53, 1954.

[RZ97] Rothman, D.H. and Zaleski, S. *Lattice-gas cellular automata*. Cambridge University Press, Cambridge, 1997.

[SAW92] Sommerfeld, M., Ando, A., and Wennerberg, D. Swirling, particle-laden flows through a pipe expansion. *ASME J. Fluids Engineering*, 114:648–655, 1992.

[SCQM96] Shirolkar, J.S., Coimbra, C.F.M., and Queiroz McQuay, M. Fundamental aspects of modeling turbulent particle dispersion in dilute flows. *Progr. Energy Combust. Sci.*, 22:363–399, 1996.

[Soo90] Soo, S.L. *Multiphase Fluid Dynamics*. Science Press, Beijing, 1990.

[Spa77] Spalding, B.D. The calculation of free-convection phenomena in gas-liquid mixtures. In Spalding B. D., Afgan N. (editor), *Heat transfer and turbulent buoyant convection studies and application*. Pp. 569–586. Hemisphere, 1977.

[Spa80] Spalding, D.B. Numerical computation of multi-phase fluid flow and heat transfer. In Taylor, C. and Morgan, K. (editors), *Recent Advances In Numerical Methods In Fluids*. Pp. 139–168. Pineridge Press, Swansea U.K., 1980.

[Spa83] Spalding, D.B. Developments in the IPSA procedure for numerical computation of multiphase-flow phenomena with interphase slip, unequal temperatures, etc. In Shih, T. M. (editor),

Numerical Methodologies in Heat Transfer. Pp. 421–436. Second National Symposium, Hemisphere, 1983.

[SRO93] Syamlal, M., Rogers, W., and O'Brien, T.J. *MFIX Documentation, Theory Guide, Technical Note DOE/METC-94/1004*. DOE, Morgatown, 1993.

[SS83] Saad, Y. and Schultz, M.H. GMRES: A generalized minimum residual algorithm for solving nonsymmetric linear systems. Technical Report Research report 254, Department of computer science, Yale University, 1983.

[SWd85] Sonneveld, P., Wesseling, P., and de Zeeuw, P.M. Multigrid and conjugate gradient methods as convergence acceleration techniques. In Paddon, D.J. and Holstein, H. (editors), *Multigrid methods for integral and differential equations*. Clarendon Press, Oxford, 1985.

[Tay21] Taylor, G.I. Diffusion by continuous movements. *Proceedings of the London Mathematical Society, Series 2*, 20:196, 1921.

[Tch47] Tchen, C.M. *Mean value and correlation problems connected with the motion of small particles suspended in a Turbulent fluid*. Martinus Nijhoff, The Hague, 1947.

[TL72] Tennekes, H. and Lumley, J.L. *A first course in turbulence*. The MIT Press, Cambridge, 1972.

[Ung93] Ungarish, M. *Hydrodynamics of suspensions: Fundamentals of centrifugal and gravity separation*. Springer-Verlag, Berlin, 1993.

[VDR84] Van Doormal, J.P. and Raithby, G.D. Enhancements of the SIMPLE method for predicting incompressible fluid flows. *Numerical Heat Transfer*, 7:147–163, 1984.

[WAW82] Wilkes, N.S., Azzopardi, B.J., and Willets, I. Drop motion and deposition in annular two-phase flow. Research report HTFS RS425 AERE R10571, AERE Engineering Sciences Division, Harwell, 1982.

[WBAS84] Weber, R., Boysan, F., Ayers, W.H., and Swithenbank, J. Simulation of dispersion of heavy particles in confined turbulent flows. *AICHE J.*, 30:490–493, 1984.

[WS92] Wang, L-P. and Stck, D.E. Stochastic trajectory models for turbulent diffusion: Monte carlo process versus markov chains. *Atmospher. Envir.*, 26A:1599–1607, 1992.

Appendix 1

Submatrices and vectors for the finite-element matrix system (2.109):

$$
\begin{aligned}
A_{kl}^{11} &= 2K_{\mathrm{f}}^{11}(k,l) + K_{\mathrm{f}}^{22}(k,l) + K_{\mathrm{f}}^{33}(k,l) + C_{\mathrm{f}}(k,l) + I_{\mathrm{f}}(k,l) \\
&\quad + S_{\mathrm{f}}^{c}(k,l) + S_{\mathrm{f}}^{I}(k,l) + S_{\mathrm{f}}^{M^{11}}(k,l) \\
A_{kl}^{12} &= K_{\mathrm{f}}^{12}(k,l) + S_{\mathrm{f}}^{M^{12}}(k,l) \\
A_{kl}^{13} &= K_{\mathrm{f}}^{13}(k,l) + S_{\mathrm{f}}^{M^{13}}(k,l) \\
A_{kl}^{14} &= -P_{\mathrm{f}}^{1}(k,l) + S_{\mathrm{f}}^{p^{1}}(k,l) \\
A_{kl}^{15} &= -I_{\mathrm{f}}(k,l) - S_{\mathrm{f}}^{I}(k,l) \\
A_{kl}^{1i} &= 0,\ i = 6,7,8 \\
A_{kl}^{21} &= K_{\mathrm{f}}^{21}(k,l) + S_{\mathrm{f}}^{M^{21}}(k,l) \\
A_{kl}^{22} &= K_{\mathrm{f}}^{11}(k,l) + 2K_{\mathrm{f}}^{22}(k,l) + K_{\mathrm{f}}^{33}(k,l) + C_{\mathrm{f}}(k,l) + I_{\mathrm{f}}(k,l) \\
&\quad + S_{\mathrm{f}}^{c}(k,l) + S_{\mathrm{f}}^{I}(k,l) + S_{\mathrm{f}}^{M^{22}}(k,l) \\
A_{kl}^{23} &= K_{\mathrm{f}}^{23}(k,l) + S_{\mathrm{f}}^{M^{23}}(k,l) \\
A_{kl}^{24} &= -P_{\mathrm{f}}^{2}(k,l) + S_{\mathrm{f}}^{p^{2}}(k,l) \\
A_{kl}^{25} &= 0 \\
A_{kl}^{26} &= -I_{\mathrm{f}}(k,l) - S_{\mathrm{f}}^{I}(k,l) \\
A_{kl}^{2i} &= 0,\ i = 7,8 \\
A_{kl}^{31} &= K_{\mathrm{f}}^{31}(k,l) + S_{\mathrm{f}}^{M^{31}}(k,l) \\
A_{kl}^{32} &= K_{\mathrm{f}}^{32}(k,l) + S_{\mathrm{f}}^{M^{32}}(k,l) \\
A_{kl}^{33} &= K_{\mathrm{f}}^{11}(k,l) + K_{\mathrm{f}}^{22}(k,l) + 2K_{\mathrm{f}}^{33}(k,l) + C_{\mathrm{f}}(k,l) + I_{\mathrm{f}}(k,l) \\
&\quad + S_{\mathrm{f}}^{c}(k,l) + S_{\mathrm{f}}^{I}(k,l) + S_{\mathrm{f}}^{M^{33}}(k,l) \\
A_{kl}^{34} &= -P_{\mathrm{f}}^{3}(k,l) + S_{\mathrm{f}}^{p^{3}}(k,l) \\
A_{kl}^{3i} &= 0,\ i = 5,6 \\
A_{kl}^{37} &= -I_{\mathrm{f}}(k,l) - S_{\mathrm{f}}^{I}(k,l) \\
A_{kl}^{38} &= 0 \\
A_{kl}^{41} &= -P_{\mathrm{f}}^{1}(l,k) - S_{\mathrm{f}}^{q_c{}^{1}}(k,l) - S_{\mathrm{f}}^{q_I{}^{1}}
\end{aligned}
$$

$$
\begin{aligned}
A_{kl}^{42} &= -P_{\mathrm{f}}^{2}(l,k) - S_{\mathrm{f}}^{q_c{}^2}(k,l) - S_{\mathrm{f}}^{q_I{}^2}(k,l)\\
A_{kl}^{43} &= -P_{\mathrm{f}}^{3}(l,k) - S_{\mathrm{f}}^{q_c{}^3}(k,l) - S_{\mathrm{f}}^{q_I{}^3}(k,l)\\
A_{kl}^{44} &= -S_{\mathrm{f}}^{q_p}(k,l)\\
A_{kl}^{45} &= S_{\mathrm{f}}^{q_I{}^1}(k,l)\\
A_{kl}^{46} &= S_{\mathrm{f}}^{q_I{}^2}(k,l)\\
A_{kl}^{47} &= S_{\mathrm{f}}^{q_I{}^3}(k,l)\\
A_{kl}^{48} &= 0\\
A_{kl}^{51} &= -I_{\mathrm{A}}(k,l) - S_{\mathrm{A}}^{I}(k,l)\\
A_{kl}^{5i} &= 0,\ i = 2,3\\
A_{kl}^{54} &= -P_{\mathrm{A}}^{1}(k,l) + S_{\mathrm{A}}^{p^1}(k,l)\\
A_{kl}^{55} &= 2K_{\mathrm{A}}^{11}(k,l) + K_{\mathrm{A}}^{22}(k,l) + K_{\mathrm{A}}^{33}(k,l) + C_{\mathrm{A}}(k,l) + I_{\mathrm{A}}(k,l)\\
&\quad + S_{\mathrm{A}}^{c}(k,l) + S_{\mathrm{A}}^{I}(k,l)\\
A_{kl}^{56} &= K_{\mathrm{A}}^{12}(k,l)\\
A_{kl}^{57} &= K_{\mathrm{A}}^{13}(k,l)\\
A_{kl}^{58} &= 0\\
A_{kl}^{61} &= 0\\
A_{kl}^{62} &= -I_{\mathrm{A}}(k,l) - S_{\mathrm{A}}^{I}(k,l)\\
A_{kl}^{63} &= 0\\
A_{kl}^{64} &= -P_{\mathrm{A}}^{2}(k,l) + S_{\mathrm{A}}^{p^2}(k,l)\\
A_{kl}^{65} &= K_{\mathrm{A}}^{21}(k,l)\\
A_{kl}^{66} &= K_{\mathrm{A}}^{11}(k,l) + 2K_{\mathrm{A}}^{22}(k,l) + K_{\mathrm{A}}^{33}(k,l) + C_{\mathrm{A}}(k,l) + I_{\mathrm{A}}(k,l)\\
&\quad + S_{\mathrm{A}}^{c}(k,l) + S_{\mathrm{A}}^{I}(k,l)\\
A_{kl}^{67} &= K_{\mathrm{A}}^{23}(k,l)\\
A_{kl}^{68} &= 0\\
A_{kl}^{71} &= 0\\
A_{kl}^{72} &= 0\\
A_{kl}^{73} &= -I_{\mathrm{A}}(k,l) - S_{\mathrm{A}}^{I}(k,l)\\
A_{kl}^{74} &= -P_{\mathrm{A}}^{3}(k,l) + S_{\mathrm{A}}^{p^3}(k,l)\\
A_{kl}^{75} &= K_{\mathrm{A}}^{31}(k,l)\\
A_{kl}^{76} &= K_{\mathrm{A}}^{32}(k,l)\\
A_{kl}^{77} &= K_{\mathrm{A}}^{11}(k,l) + K_{\mathrm{A}}^{22}(k,l) + 2K_{\mathrm{A}}^{33}(k,l) + C_{\mathrm{A}}(k,l) + I_{\mathrm{A}}(k,l)\\
&\quad + S_{\mathrm{A}}^{c}(k,l) + S_{\mathrm{A}}^{I}(k,l)\\
A_{kl}^{78} &= 0\\
A_{kl}^{81} &= S_{\mathrm{A}}^{q_I{}^1}(k,l)
\end{aligned}
$$

$$
\begin{aligned}
A^{82}_{kl} &= S^{q_I{}^2}_{\mathrm{A}}(k,l)\\
A^{83}_{kl} &= S^{q_I{}^3}_{\mathrm{A}}(k,l)\\
A^{84}_{kl} &= -S^{q_p}_{\mathrm{A}}(k,l)\\
A^{85}_{kl} &= -S^{q_c{}^1}_{\mathrm{A}}(k,l) - S^{q_I{}^1}_{\mathrm{A}}(k,l)\\
A^{86}_{kl} &= -S^{q_c{}^2}_{\mathrm{A}}(k,l) - S^{q_I{}^2}_{\mathrm{A}}(k,l)\\
A^{87}_{kl} &= -S^{q_c{}^3}_{\mathrm{A}}(k,l) - S^{q_I{}^3}_{\mathrm{A}}(k,l)\\
A^{88}_{kl} &= -D^{M}(k,l) - \bar{P}^{1}_{\mathrm{A}}(l,k) - \bar{P}^{2}_{\mathrm{A}}(l,k) - \bar{P}^{3}_{\mathrm{A}}(l,k)\\
&\quad +\bar{S}^{M^{11}}_{\mathrm{A}}(k,l) + \bar{S}^{M^{12}}_{\mathrm{A}}(k,l) + \bar{S}^{M^{13}}_{\mathrm{A}}(k,l)\\
&\quad +\bar{S}^{M^{21}}_{\mathrm{A}}(k,l) + \bar{S}^{M^{22}}_{\mathrm{A}}(k,l) + \bar{S}^{M^{23}}_{\mathrm{A}}(k,l)\\
&\quad +\bar{S}^{M^{31}}_{\mathrm{A}}(k,l) + \bar{S}^{M^{32}}_{\mathrm{A}}(k,l) + \bar{S}^{M^{33}}_{\mathrm{A}}(k,l),
\end{aligned}
$$

where the indices get values $k, l = 1, \ldots, n_{dofs}$. The integral forms above are defined as

$$
\begin{aligned}
D^{ij}_{\alpha}(k,l) &= (1/Re_{\alpha})(\phi_{\alpha}\frac{\partial\varphi_l}{\partial x_i}, \frac{\partial\varphi_k}{\partial x_j})\\
C_{\alpha}(k,l) &= (\phi_{\alpha}\mathbf{u}_{\alpha}\cdot\nabla\varphi_l, \varphi_k)\\
P^{i}_{\alpha}(k,l) &= (\varphi_l, \beta_{\alpha}(\phi_{\alpha}\frac{\partial\varphi_k}{\partial x_i} + \varphi_k\frac{\partial\phi_{\alpha}}{\partial x_i}))\\
\bar{P}^{i}_{\alpha}(k,l) &= (\varphi_l, \beta_{\alpha}(\varphi_k\frac{\partial u_{\alpha i}}{\partial x_i} + u_{\alpha i}\frac{\partial\varphi_k}{\partial x_i}))\\
I_{\alpha}(k,l) &= (g\beta_{\alpha}\varphi_l, \varphi_k)\\
S^{c}_{\alpha}(k,l) &= (\phi_{\alpha}\mathbf{u}_{\alpha}\cdot\nabla\varphi_l, \tau_{\alpha}\mathbf{u}_{\alpha}\cdot\nabla\varphi_k)\\
S^{p^i}_{\alpha}(k,l) &= (\beta_{\alpha}\phi_{\alpha}\frac{\partial\varphi_l}{\partial x_i}, \tau_{\alpha}\mathbf{u}_{\alpha}\cdot\nabla\varphi_k)\\
S^{I}_{\alpha}(k,l) &= (g\beta_{\alpha}\varphi_l, \tau_{\alpha}\mathbf{u}_{\alpha}\cdot\nabla\varphi_k)\\
S^{q_c{}^i}_{\alpha}(k,l) &= (\phi_{\alpha}\mathbf{u}_{\alpha}\cdot\nabla\varphi_l, \tau_{\alpha}\beta_{\alpha}\frac{\partial\varphi_k}{\partial x_i})\\
S^{q_p}_{\alpha}(k,l) &= (\beta_{\alpha}\phi_{\alpha}\nabla\varphi_l, \tau_{\alpha}\beta_{\alpha}\nabla\varphi_k)\\
S^{q_I{}^i}_{\alpha}(k,l) &= (g\beta_{\alpha}\varphi_l, \tau_{\alpha}\beta_{\alpha}\frac{\partial\varphi_k}{\partial x_i})\\
S^{M^{ij}}_{\alpha}(k,l) &= (\beta_{\alpha}(\phi_{\alpha}\frac{\partial\varphi_l}{\partial x_j} + \varphi_l\frac{\partial\phi_{\alpha}}{\partial x_j}), \delta_{\alpha}\beta_{\alpha}(\phi_{\alpha}\frac{\partial\varphi_k}{\partial x_i} + \varphi_k\frac{\partial\phi_{\alpha}}{\partial x_i}))\\
\bar{S}^{M^{ij}}_{\alpha}(k,l) &= (\beta_{\alpha}(\varphi_l\frac{\partial u_{\alpha j}}{\partial x_j} + u_{\alpha j}\frac{\partial\varphi_l}{\partial x_j}), \delta_{\alpha}\beta_{\alpha}(\varphi_k\frac{\partial u_{\alpha i}}{\partial x_i} + u_{\alpha i}\frac{\partial\varphi_k}{\partial x_i}))\\
D^{M}(k,l) &= (\beta_{\mathrm{A}}\kappa\nabla\varphi_l, \nabla\varphi_k).
\end{aligned}
$$

Appendix 1

The subvectors of the right hand side vector $\mathbf{F}$ are defined as

$$
\begin{aligned}
F_i(k) &= (\phi_{\mathrm{f}}\beta_{\mathrm{f}}\tilde{F}^i_{\mathrm{f}}, \varphi_k + \tau_{\mathrm{f}}(\phi_{\mathrm{f}}\mathbf{u}_{\mathrm{f}} \cdot \nabla\varphi_k)),\ i = 1,2,3 \\
F_4(k) &= (\phi_{\mathrm{f}}\beta_{\mathrm{f}}\tilde{\mathbf{F}}_{\mathrm{f}}, -\tau_{\mathrm{f}}\phi_{\mathrm{f}}\beta_{\mathrm{f}}\nabla\varphi_k) \\
F_i(k) &= (\phi_{\mathrm{A}}\beta_{\mathrm{A}}\tilde{F}^{i-4}_{\mathrm{A}}, \varphi_k + \tau_{\mathrm{A}}(\phi_{\mathrm{A}}\mathbf{u}_{\mathrm{A}} \cdot \nabla\varphi_k)),\ i = 5,6,7 \\
F_8(k) &= (\phi_{\mathrm{A}}\beta_{\mathrm{A}}\tilde{\mathbf{F}}_{\mathrm{A}}, -\tau_{\mathrm{A}}\phi_{\mathrm{A}}\beta_{\mathrm{A}}\nabla\varphi_k),
\end{aligned}
$$

where $k = 1, \ldots, n_{dofs}$.

Series title, number and
report code of publication

VTT Publications 722
VTT-PUBS-722

Author(s)
Kai Hiltunen, Ari Jäsberg, Sirpa Kallio, Hannu Karema, Markku Kataja,
Antti Koponen, Mikko Manninen & Veikko Taivassalo

Title

Multiphase Flow Dynamics
Theory and Numerics

Abstract

The purpose of this work is to review the present status of both theoretical and numerical research of multiphase flow dynamics and to make the results of that fundamental research more readily available for students and for those working with practical problems involving multiphase flow.

Flows that appear in many of the common industrial processes are intrinsically multiphase flows. The advanced technology associated with these flows has great economical value. Nevertheless, our basic knowledge and understanding of these processes is often quite limited as, in general, is our capability of solving these flows. In the first part of this publication we give a comprehensive review of the theory of multiphase flows accounting for several alternative approaches. We also give general guidelines for solving the 'closure problem', which involves, *e.g.*, characterising the interactions between different phases and thereby deriving the final closed set of equations for the particular multiphase flow under consideration. The second part is devoted to numerical methods for solving those equations.

ISBN
978-951-38-7365-3 (soft back ed.)
978-951-38-7366-0 (URL: http://www.vtt.fi/publications/index.jsp)

Series title and ISSN	Project number
VTT Publications 1235-0621 (soft back ed.) 1455-0849 (URL: http://www.vtt.fi/publications/index.jsp)	33861

Date	Language	Pages
December 2009	English, Finnish abstr.	113 p. + app. 4 p.

Name of project	Commissioned by
Dynamics of Multiphase Flows, Finnish national Computational Fluid Dynamics Technology Programme 1995–1999	

Keywords	Publisher
Multiphase flows, volume averaging, ensemble averaging, mixture models, multifluid finite volume method, multifluid finite element method, particle tracking, the lattice-BGK model	VTT Technical Research Centre of Finland P.O. Box 1000, FI-02044 VTT, Finland Phone internat. +358 20 722 4520 Fax +358 20 722 4374

Julkaisun sarja, numero ja raporttikoodi

VTT Publications 722
VTT-PUBS-722

Tekijä(t)
Kai Hiltunen, Ari Jäsberg, Sirpa Kallio, Hannu Karema, Markku Kataja, Antti Koponen, Mikko Manninen & Veikko Taivassalo

Nimeke

Monifaasivirtausten dynamiikka
Teoriaa ja numeriikkaa

Tiivistelmä

Työssä tarkastellaan monifaasivirtausten teoreettisen ja numeerisen tutkimuksen nykytilaa, ja muodostetaan tuon perustutkimuksen tuloksista selkeä kokonaisuus opiskelijoiden ja käytännön virtausongelmien kanssa työskentelevien käyttöön. Monissa teollisissa prosesseissa esiintyvät virtaukset ovat olennaisesti monifaasivirtauksia – esimerkiksi kaasu-partikkeli-, neste-partikkeli- ja neste-kuitususpensioiden virtaukset, sekä kuplavirtaukset, neste-neste-virtaukset ja virtaus huokoisen aineen läpi. Julkaisun ensimmäisessä osassa tarkastellaan kattavasti monifaasivirtausten teoriaa ja esitetään useita vaihtoehtoisia lähestymistapoja. Toisessa osassa käydään läpi monifaasivirtauksia kuvaavien yhtälöiden numeerisia ratkaisumenetelmiä.

ISBN
978-951-38-7365-3 (nid.)
978-951-38-7366-0 (URL: http://www.vtt.fi/publications/index.jsp)

Avainnimeke ja ISSN	Projektinumero
VTT Publications 1235-0621 (nid.) 1455-0849 (URL: http://www.vtt.fi/publications/index.jsp)	33861

Julkaisuaika	Kieli	Sivuja
Joulukuu 2009	Englanti, suom. tiiv.	113 s. + liitt. 4 s.

Projektin nimi	Toimeksiantaja(t)
Dynamics of Multiphase Flows, Finnish national Computational Fluid Dynamics Technology Programme 1995–1999	

Avainsanat	Julkaisija
Multiphase flows, volume averaging, ensemble averaging, mixture models, multifluid finite volume method, multifluid finite element method, particle tracking, the lattice-BGK model	VTT PL 1000, 02044 VTT Puh. 020 722 4520 Faksi 020 722 4374

The purpose of this work is to review the present status of both theoretical and numerical research of multiphase flow dynamics and to make the results of that fundamental research more readily available for students and for those working with practical problems involving multiphase flow.

Flows that appear in many of the common industrial processes are intrinsically multiphase flows. The advanced technology associated with these flows has great economical value. Nevertheless, our basic knowledge and understanding of these processes is often quite limited as, in general, is our capability of solving these flows. In the first part of this publication we give a comprehensive review of the theory of multiphase flows accounting for several alternative approaches. We also give general guidelines for solving the 'closure problem', which involves, e.g., characterising the interactions between different phases and thereby deriving the final closed set of equations for the particular multiphase flow under consideration. The second part is devoted to numerical methods for solving those equations.

ISBN 978-951-38-7365-3 (soft back ed.)
ISSN 1235-0621 (soft back ed.)

ISBN 978-951-38-7366-0 (URL: http://www.vtt.fi/publications/index.jsp)
ISSN 1455-0849 (URL: http://www.vtt.fi/publications/index.jsp)